



universität
wien

MASTERARBEIT

Titel der Masterarbeit

„PARP inhibition potentiates the cytotoxic activity of
camptothecin, a topoisomerase I inhibitor in human
BRCA1-positive breast cancer cells“

verfasst von

Marlene Chladek BSc

angestrebter akademischer Grad

Master of Science (MSc)

Wien, 2013

Studienkennzahl lt.
Studienblatt:

A 066 834

Studienrichtung lt.
Studienblatt:

Molekulare Biologie

Betreut von:

Ao.Univ.-Prof. Mag. Dr. Johann Rotheneder

Table of contents

1.	Introduction	7
1.1	BIOLOGICAL FUNCTIONS OF TOPOISOMERASES	7
1.2	REPAIR MECHANISMS OF DNA DAMAGE	11
1.3	DEFECTIVE DNA REPAIR MECHANISMS IN HUMAN CANCERS	16
1.4	CONCEPT OF SYNTHETIC LETHALITY	26
2.	Aims of the master thesis	34
3.	Material and methods	35
3.1	MATERIAL	35
3.2	METHODS	43
4.	Results	53
4.1	EFFECT OF TOPO1 INHIBITION ON THE NUMBER OF LIVING HUMAN BREAST CANCER CELLS	53
4.2	IMPACT OF THE INHIBITION OF PARP-1 ACTIVITY IN BREAST CANCER CELLS	56
4.3	INHIBITION OF PARP-1 POTENTIATES THE ANTI-PROLIFERATIVE ACTION OF CPT IN BT-20 CELLS	59
4.4	INTERFERENCE WITH THE PARP-1 ACTIVITY POTENTIATES THE DISTRIBUTION CHANGES IN THE CELL CYCLE PHASES OF BT-20 CELLS	61
4.5	SIMULTANEOUS INHIBITION OF TOPO1 AND PARP-1 SHOWED SYNERGISTIC EFFECTS EXCLUSIVELY IN BT-20 CELLS	62
4.6	INHIBITION OF PARP-1 INDUCES APOPTOSIS AND MITOTIC ABERRATIONS IN BT-20 CELLS	65
4.7	PARP-1 INHIBITION INDUCES CASPASE-3 ACTIVITY IN BT-20 CELLS	66
4.8	INACTIVATION OF PARP-1 LEADS TO ACCUMULATION OF DNA DAMAGE IN BT-20 CELLS	70
5.	Discussion	72
6.	Appendix	76
6.1	ABBREVIATIONS	76
6.2	LIST OF FIGURES	80
6.3	LIST OF TABLES	81
7.	Acknowledgement	82
8.	References	83
9.	Curriculum vitae	90

Abstract

The tumour suppressor genes *BRCA1* and *BRCA2* are major key players in the repair of DNA double strand breaks by homologous recombination. Their functionality is essential for maintaining genomic stability; mutations in these genes are associated with an increased predisposition for the development of breast, ovarian and prostate cancer, respectively. Cancer therapies based on the concept of synthetic lethality take advantage of these inherited mutations and additionally target another DNA repair pathway and disturb it. This further generates lethal DNA damage and triggers the selective killing of tumour cells. Involvement of PARP in DNA repair pathways, especially in DNA base excision repair, was shown to be crucial for the repair of DNA single strand breaks. The positive effects of PARP inhibition in DNA repair-deficient cells as seen in carriers of *BRCA* mutations have already been demonstrated in several studies. During the last years DNA topoisomerase inhibitors became promising therapeutic agents in anti-cancer therapy. Their mode of action implies the interference with the enzyme activity, essential in the basal gene expression processes thereby generating DNA lesions and promoting apoptosis. Cells that exhibit an impaired DNA repair either due to inherited mutations or synthetically induced using pharmacological agents, display an increased sensitivity to the inhibition of DNA topoisomerases.

In the course of the master thesis the impact of PARP-1 inhibitor NU1025 and topoisomerase I inhibitor camptothecin (CPT) on *BRCA1*-positive BT-20 and T47D and *BRCA1*-negative SKBr-3 cells was examined. Interestingly, among the tested cell lines *BRCA1*-positive BT-20 cells displayed the highest sensitivity towards PARP-1 inhibition. We further showed that simultaneous inhibition of PARP-1 and topoisomerase I activity significantly reduced the number of living BT-20 cells compared to untreated controls and single treatment by CPT. Chromatin changes that are characteristic for apoptosis, including chromatin condensation and nuclear fragmentation were both found to be increased upon PARP-1 inhibition and was attributable to the strong stimulation of caspase 3 activity in treated cells. Co-treatment of CPT with NU1025 was shown to enhance the observed effects. These results demonstrated that inhibition of PARP-1 activity potentiates cytotoxic effects of CPT at already low doses. Surprisingly, *BRCA1*-deficient SKBr-3 cells were resistant to PARP inhibition and the interference with PARP-1 activity did not synergize the action of CPT in these cells.

The observed effects may be the result of a still unidentified deficiency in DNA repair pathways present in BT-20 cells that sensitise these cells to PARP-1 inhibition despite their positive *BRCA1* status. These findings lead to the assumption that treatment with PARP inhibitors is not exclusively determined to patients carrying mutations in *BRCA1* and *BRCA2*.

Kurzzusammenfassung

Die menschliche DNA ist laufend strukturverändernden exogenen und endogenen Prozessen ausgesetzt, die Mutationen begünstigen. Die beiden Tumorsuppressorgene *BRCA1* und *BRCA2* spielen eine wesentliche Rolle bei der Reparatur von DNA-Doppelstrangbrüchen und sind damit essentiell für die Aufrechterhaltung der genomischen Stabilität. Mutationen welche die Funktionalität von *BRCA1* und *BRCA2* beeinträchtigen begünstigen die Entstehung von malignen Neoplasien und werden mit einem erhöhten Risiko an Brust-, Eierstock- oder Prostatakrebs zu erkranken, assoziiert. Das Konzept der synthetischen Letalität basiert auf der synthetisch induzierten Blockade eines DNA- Reparatur-Pathways die in gesunden Zellen ohne Konsequenzen bleibt, in Zellen mit einem bereits beeinträchtigten DNA-Reparaturmechanismus jedoch zu schweren Schäden führt. Diese Zellen sind nicht in der Lage die generierten Schäden zu kompensieren, DNA Läsionen akkumulieren und führen in weiterer Folge zur Apoptose.

Das Enzym Poly (ADP-ribose)-Polymerase 1 (PARP-1) spielt bei der Reparatur von DNA Schäden insbesondere bei der Beseitigung von DNA Einzelstrangbrüchen durch Base excision repair (BER) eine tragende Rolle. Die gezielte Zerstörung von Zellen mit fehlerhaften DNA-Reparaturmechanismen durch PARP-1 Inhibitoren wurde bereits in mehreren Studien demonstriert. In den vergangenen Jahren rückten DNA-Topoisomerase Inhibitoren zunehmend in das Interesse der Anti-Krebsforschung. DNA-Topoisomerase Inhibitoren hemmen die Enzymaktivität durch die Bildung eines DNA-Enzym-Intermediats. Dieses DNA-Enzym-Intermediat führt sowohl zu DNA-Einzelstrang- als auch zu DNA-Doppelstrangbrüchen, wodurch in weiterer Folge Apoptose eingeleitet wird. Verschiedene Studien konnten bereits zeigen, dass Zellen mit einem fehlerhaften DNA-Reparatursystem, ob durch Mutationen entstanden oder synthetisch induziert, eine erhöhte Sensitivität gegenüber Inhibitoren von DNA-Topoisomerasen aufweisen.

Im Zuge der Masterarbeit wurden die Wirkungen des PARP-1 Inhibitors NU1025 und des Topoisomerase I Inhibitors Camptothecin (CPT) sowohl als Mono- als auch als Kombinationstherapie auf Brustkrebszellen untersucht. Bei den verwendeten Zelllinien handelte es sich um die *BRCA1*-positiven Brustkrebszellen BT-20 und T47D und um die *BRCA1*-negative Brustkrebszelllinie SKBr-3. Erstaunlicherweise war der antiproliferative Effekt als Reaktion auf die Hemmung der PARP-1 Aktivität in den *BRCA1* positiven BT-20 Zellen am stärksten ausgeprägt. Desweiteren zeigten unsere Untersuchungen, dass die Kombinationstherapie mit CPT und NU1025 zu einer signifikanten Reduktion der Anzahl der lebend Zellen im Vergleich zur unbehandelten Kontrolle und Einzeltherapie mit CPT führte. Die Behandlung mit NU1025 steigerte darüber hinaus die Aktivität der Caspase 3, welche durch spezifische Änderungen in der Chromatinstruktur, die für die Einleitung der Apoptose charakteristisch sind, detektiert wurde. Die Ergebnisse der Kombinationstherapie von CPT und NU1025 verdeutlichten, dass die Hemmung der PARP-1 Aktivität durch NU1025, die zytotoxischen Effekte der Behandlung mit CPT in *BRCA1*-positiven BT-20 Zellen synergistisch

verstärken und ein signifikanter Rückgang der Zellzahl bereits bei geringen Dosen CPT verzeichnet werden kann. Interessanterweise zeigte die BRCA1-negative Brustkrebszelllinie SKBr-3 eine Resistenz gegenüber der Hemmung der PARP-1 Aktivität. In dieser Zelllinie konnten keine synergistischen Effekte bei der simultanen Behandlung mit NU1025 und CPT beobachtet werden. Unsere Ergebnisse lassen vermuten, dass die in den BRCA1-positiven BT-20 Zellen beobachteten Effekte, auf noch unbeschriebene Defekte in den DNA Reparaturmechanismen zurückzuführen sind, die diese Zellen für die Behandlung mit einem PARP-Inhibitor sensibilisieren.

Diese Entdeckungen sind von medizinischer Relevanz, da sie zeigen, dass sich das Anwendungsfeld von PARP Inhibitoren in der Anti-Krebstherapie nicht nur auf Patienten beschränkt, welche Träger einer angeborenen *BRCA1/2* Mutation sind. Therapieansätze basierend auf dem Konzept der synthetischen Letalität sind somit nicht nur auf *BRCA1/2* Mutationsträger limitiert, wodurch mehr Patienten erreicht werden, die von dieser Therapie profitieren können.

1. Introduction

1.1. Biological functions of topoisomerases

The double helical structure of DNA generates topological problems during cellular processes such as replication transcription and chromatin condensation. DNA gets under- or overwound leading to problematic DNA structures like negative and positive supercoils or catenates.

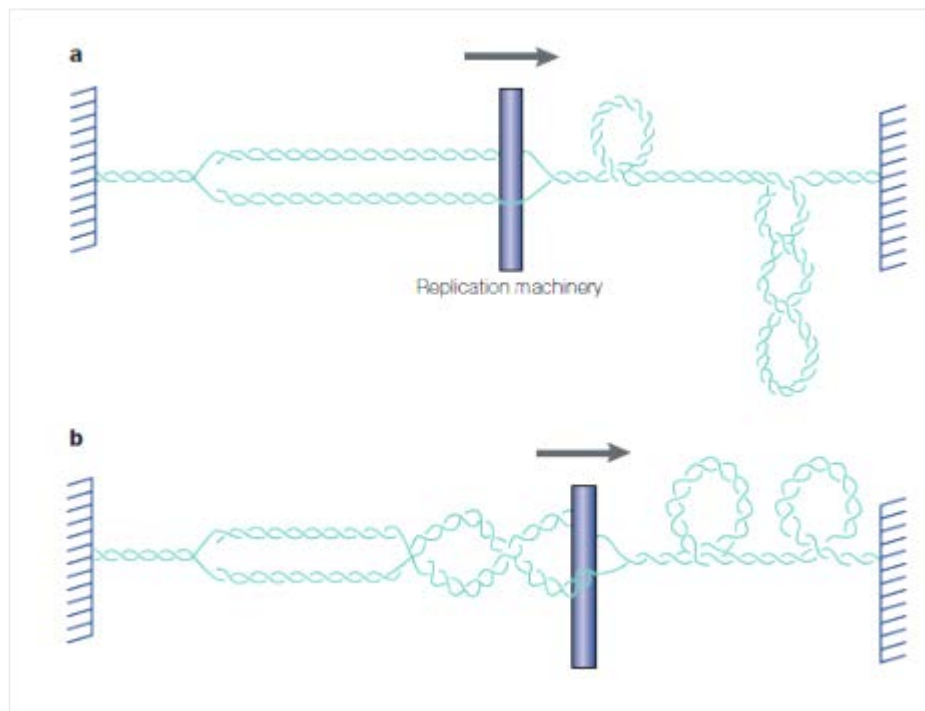


Figure 1. Problems in DNA topology arising during replication (picture reproduced from Wang, J. C et al. (2002)^[1])

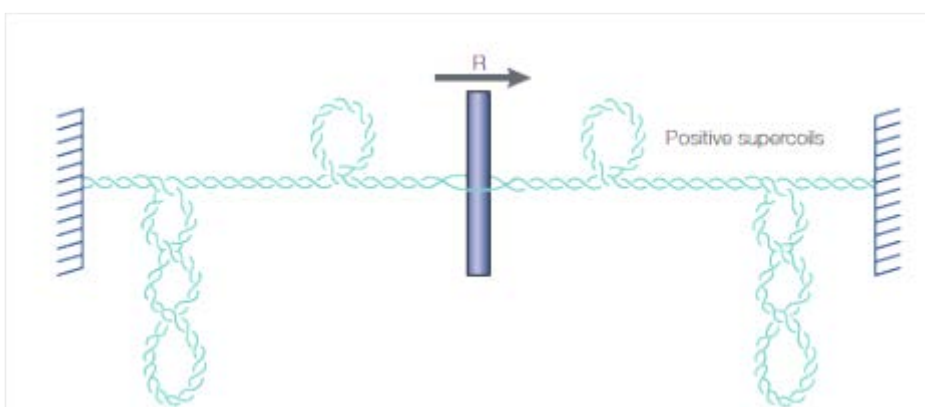


Figure 2. Problems in DNA topology arising during transcription (picture reproduced from Wang, J. C et al. (2002)^[1])

Topoisomerases are enzymes required for managing DNA topology by removing topological changes arising during physiological processes (e.g. DNA replication or transcription), introducing either DNA single or double strand breaks. These enzymes are divided into two

groups, those which cleave only one strand are defined as type I topoisomerases whereas those which cleave both strands are defined as type II topoisomerases^{2,1}.

DNA cleavage is executed by topoisomerases binding to DNA and breaking its backbone. This results in the formation of a transient enzyme-DNA intermediate called the cleavable complex. In this complex topoisomerase I is covalently bound to the DNA through a phosphotyrosine bond. The induced break allows the topoisomerase to change DNA topology by unwinding the DNA to restore its original formation. In the final step of this catalytic cycle the DNA strand gets resealed again^{1,3}.

Table 1. Human topoisomerases data summarized from ^{1,2,3,4}

Enzyme	Type	Attachment side to cleaved DNA	ATP dependent	Single strand break (SSB) or double strand break (DSB)
Topoisomerase I	IB	3'	no	SSB
Mitochondrial Topoisomerase I	IB	3'	no	SSB
Topoisomerase II α	IIA	5'	yes	DSB
Topoisomerase II β	IIA	5'	yes	DSB
Topoisomerase III α	IA	5'	no	SSB
Topoisomerase III β	IA	5'	no	SSB

1.1.1 Action of pharmacological inhibitors of topoisomerases

By their role in managing DNA topology and making DNA accessible for different cellular processes, topoisomerases became a promising target in cancer therapy. For this purpose topoisomerases inhibitors were developed. Compounds targeting topoisomerases are either categorised as agents that trap the DNA enzyme intermediate, so called topoisomerase poisons or as agents which interfere with the enzymes' catalytic activity, so called topoisomerase inhibitors².

Topoisomerase poisons form a stable enzyme-DNA intermediate and therefore block cellular processes such as transcription and replication by generating physical barriers. Topoisomerase introduced DNA strand breaks cannot get resealed and lead, if remain unrepaired, to cell death^{1,4}.

Topoisomerase inhibitors target any other step in the enzymes' catalytic cycle and therefore repress its catalytic activity. The enzymes' activity is either blocked by preventing their binding to the DNA or interfering with ATP binding/hydrolysis which is necessary for type II topoisomerases. Topoisomerase poisons in contrast to topoisomerase inhibitors are regarded as DNA damaging agents because their mode of action includes induction of DNA strand breaks⁵.

Inhibitors of topoisomerase I (e.g. Camptothecin)

Camptothecin is an only topoisomerase I targeting cytotoxic plant alkaloid which was discovered in 1966 by M. E. Wall and M. C. Wani in the bark of the Chinese tree *Camptotheca acuminata*⁶. This alkaloid was shown to be a potent anti-tumour drug, its two derivatives topotecan for ovarian and lung cancers and irinotecan for colorectal cancer has been approved by the US Food and Drug Administration^{7,8}.

Intercalating to the topoisomerase I-DNA complex, also known as the cleavable complex, camptothecin traps the enzyme by forming a ternary complex *via* hydrogen bonding^{9,10}.

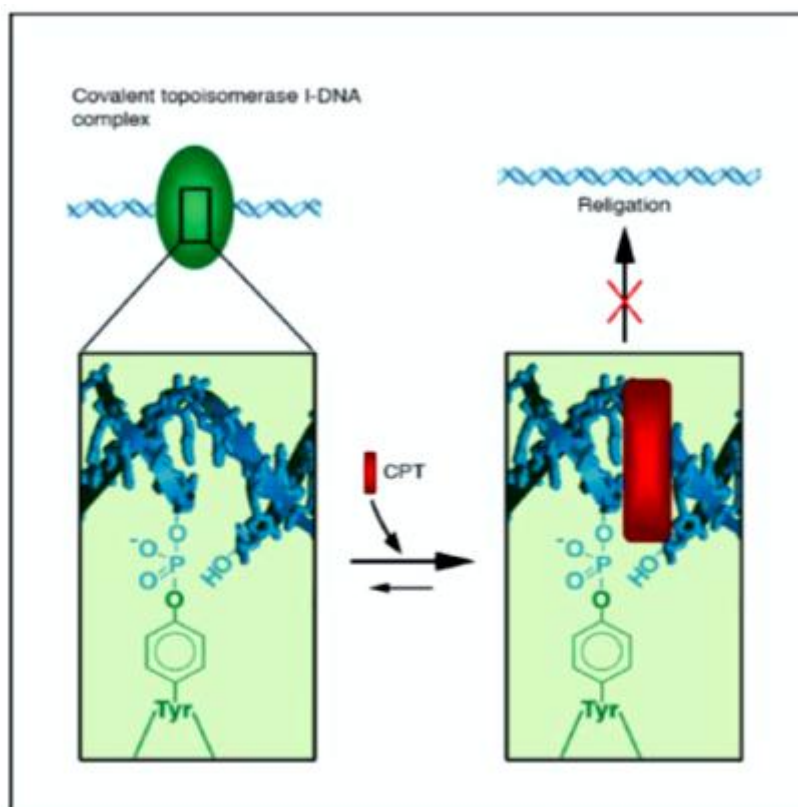


Figure 3. Binding of camptothecin to the cleavable complex (picture reproduced from Leppard, J. B et al. (2005)[³])

This ternary complex generates a physical barrier to the replication machinery, leading to collisions between the replication fork and the complex during S-phase. Single strand breaks originally induced by topoisomerase I convert into double strand breaks in the presence of camptothecin during replication. Camptothecin therefore targets primarily cells during S-phase leading to S-phase specific cell death and induces S- and G₂ arrest. Cells which fail to repair these lesions as a result of an impaired DNA repair pathway or DNA damage response undergo apoptosis^{3,8,10,11,12}.

Inhibitors of topoisomerase II (e.g. etoposide and C-1305)

Etoposide

Podophyllotoxin, derived from the plant *Podophyllum peltatum* was already used as medication by different cultures in the past. After further investigations in the 1950s a series of podophyllotoxin derivatives was synthesized. 1966 one of these derivatives, etoposide (VP-16) was recognized as a topoisomerase II inhibitor, exhibiting broad anti-tumour activity and became approved by the US Food and Drug Administration in the late 1970s¹³.

Etoposide targets topoisomerase II and acts by trapping the enzyme-DNA intermediate, thus preventing relegation of the by topoisomerase II induced double strand break. Effectiveness of etoposide depends on the ATP/ADP ratio in cells, since ATP is necessary to generate the DNA double strand breaks^{11,13,14}. However, clinical studies indicated that medication with etoposide can lead to secondary malignancies^{11,13,14,15,16}. Targeting specific binding sites at translocation breakpoints etoposide medication leads to chromosomal rearrangements causing acute myeloid leukemias^{11,14,16}.

C-1305

Triazoloacridones were developed and synthesized at the Gdansk University of Technology. C-1305 represents the most effective derivative of this group of compounds inhibiting the catalytic activity of DNA topoisomerase II and stabilizing the cleavable enzyme DNA complex^{17,18}. Potency of C-1305 as a topoisomerase II inhibitor was evaluated by a comparison study *in vitro* and in human tumour cells. Including the triazoloacridone derivative C-1305, the triazoloacridone derivative C-1311 which is structurally similar to C-1305 but does not show anti-tumour effects and the well-known topoisomerase II inhibitor *m*-amsacrine. This study demonstrated the influence of C-1305 on topoisomerase II by stabilizing the cleavable enzyme DNA complex *in vitro* and in living cells¹⁷.

The details of the operating mode of triazoloacridones are under investigation. Lemke, K. et al. demonstrated that binding of C-1305 to DNA leads to unusual structural changes compared to other analysed topoisomerase inhibitors. These perturbations were found especially in DNA regions containing guanine triplets and are unique for treatment with C-1305^{17,19}. The human genome contains many guanine triplets or guanine-rich sequences many of them are in functional regions like telomeres, centromeres and promoter regions. Structural changes in these regions due to C-1305 might disrupt the functionality of these regions and therefore be from high importance in cancer therapy¹⁹.

1.1.2 Interference with the activity of topoisomerases as therapeutic option for treatment of human cancers

Although topoisomerase inhibitors showed great success as anti-cancer agents, also negative consequences as a result of medication with these agents were observed. Patient survival rates indicated a connection between treatment with agents targeting DNA topoisomerase II and the appearance of secondary malignancies in those patients^{9,11}.

One of the first observed adverse drugs reactions was found in patients who developed acute myeloid leukaemia after medication with topoisomerase II inhibitors etoposide and teniposide. These arising secondary malignancies were linked to topoisomerase II inhibitor-induced double strand breaks within the breakpoint cluster region (BCR), thereby inducing oncogenic translocations. These findings suggest that future research should be directed towards maximising cytotoxic effects of DNA topoisomerase inhibitors but simultaneously reducing arising adverse effects^{9,11}.

1.1.3 Inhibition of topoisomerases induces DNA lesions

Topoisomerases are enzymes essential for maintaining DNA structure during cellular processes such as replication and transcription. Their mode of action comprises binding to DNA, formation of a transient enzyme-DNA intermediate, induction of either DNA single strand or DNA double strand breaks, unwinding of DNA and religation of the strands. These strand breaks occurring during removal of structural perturbations are a part of normal cellular processes and under a certain level do not induce apoptosis. If these cleavable DNA-topoisomerase complexes are stabilized, relegation of the strands is prevented and the enzyme- DNA intermediate persists. Agents that inhibit topoisomerase I and topoisomerase II therefore became interesting targets in anti-cancer therapy. Stabilisation of the under normal conditions harmless enzyme- DNA intermediate induces DNA double strand breaks during replication. These DNA double strand breaks are a result of collision of the DNA replication fork with the artificial stabilized enzyme-DNA intermediate. Inhibition of DNA topoisomerase additionally leads to arrest of the replication machinery at the replication fork and induces the formation of an enzyme-DNA adduct. These topoisomerase inhibitor induced DNA lesions further trigger activation of the DNA damage response and lead if unrepaired to cell cycle arrest and cell death^{11,12,20}.

1.2.Repair mechanisms of DNA damage

The human genome is constantly exposed to DNA damaging events and agents introducing DNA lesions. These lesions can occur spontaneously during normal cellular processes or can be derived exogenously by UV light, radiation, viruses or chemical agents. Maintenance of these lesions can lead to genomic rearrangements which can promote carcinogenesis. To

maintain genomic integrity and stability the cell has evolved different DNA repair mechanisms to deal with arising DNA damage. DNA repair mechanisms can be classified in those involved in the repair of DNA single strand breaks (NER, BER, and MMR) and those which deal with DNA double strand breaks (NHEJ, MMEJ and HR). Defects in repair pathways are a main issue in medicine their impairment increase sensitivity to carcinogens, cancer risk and promote tumourigenesis^{21,22,23}.

1.2.1 Repair mechanisms of DNA single strand breaks

Nucleotide excision repair (NER)

The nucleotide excision repair system (NER) is a DNA repair pathway which detects and removes bulky DNA adducts induced as a result of exposure to UV light, chemicals or protein addition to DNA. This repair mechanism starts with DNA damage recognition and assembly of the incision complex. Dual incision on the target strand is performed by the incision complex followed by removal of the damaged bases. The excised oligomer carrying the bulky DNA adducts is released and DNA synthesis is performed using the other undamaged strand as a template. After ligation of the newly synthesised fragment to the strand, the gap is filled and DNA repair is completed^{22,24}.

The hereditary autosomal recessive disease Xeroderma pigmentosum is an example of a disease with a defect in this repair mechanism. Patients who suffer from Xeroderma pigmentosum are extremely sun sensitive and have an increased predisposition for sunlight induced skin cancer and multiple neoplasms due to an impaired DNA repair²⁵.

Base excision repair (BER)

Mammalian cells possess different mechanism to repair arising DNA damage. One important mechanism is the base excision repair pathway. This repair mechanism has two forms based on the number of replaced nucleotides on the damaged strand. Replacement of only one nucleotide in the case of single-nucleotide BER and two or more nucleotides in the case of long patch BER^{22,26,27,28}. The first step in base excision repair is the removal of the damaged base by a specific DNA glycosylase. This enzyme catalysis the excision of the damaged nucleotide resulting in generation of apurinic/apyrimidinic (AP) sites in DNA. The developed AP site is recognised by APE1 endonuclease which cleaves the DNA backbone thereby creating a gap with a 3' hydroxyl on the one side and a 5' deoxyribose-phosphate moiety on the other side^{22,26,27,28}. In the case of single base excision repair, DNA polymerase removes the deoxyribose-phosphate moiety with its intrinsic lyase activity and fills the one nucleotide gap. If long patch base excision repair takes place, a short oligonucleotide containing the problematic AP site is removed. After removal of the damaged base and gap filling by DNA polymerase, strand integrity is then restored by DNA ligase^{22,26,27,28}.

Mismatch repair (MMR)

Mismatch repair is a highly conserved DNA repair mechanism which corrects errors arising during DNA replication. It recognises incorrect base pairing and insertion/deletion loops the major key player in mismatch repair are the proteins MutS, MutL and MutH. MutS is essential for mismatch recognition, MutH has endonuclease activity and MutL mediates the interaction between MutS and MutH. The three proteins involved in this repair pathway are conserved in prokaryotes as well as in eukaryotes^{29,30,31,32}. In human the two heterodimer MutS α (MSH2/MSH6) and MutS β (MSH2/MSH3) are responsible for DNA damage recognition. The heterodimer MutL α (MLH1/ PMS2) mediates the incision of the DNA strand containing the mismatch. PCNA and replication factor C (RFC) also are involved in single strand incision, replication protein A (RPA) binds the single stranded DNA and thereby prevents generation of secondary structures. Strand excision is performed by exonuclease 1 (EXO1), DNA polymerase δ synthesis the new strand. In contrast to *E.coli*, strand incision in human mismatch repair is performed by MutL and not by MutH^{29,30,31,32}.

Loss of this repair system promotes spontaneous mutations leading to a susceptibility to cancer^{29,30,31,32}.

1.2.2 Repair mechanisms of DNA double strand breaks

Non homologous end joining (NHEJ)

Non homologous end joining is a DNA repair mechanism in cells to cope with DNA double strand breaks. In contrast to homologous recombination this pathway does not require an intact DNA strand as a template and broken strands are directly religated with minimal processing of the ends^{21,22,23,33}.

After DNA damage a heterodimer of Ku70 and Ku80 binds to the broken strand ends and facilitates binding of DNA- PKcs. Physical juxtaposition of the two strands is mediated *via* protein-protein interactions. Proteins bound to the Ku heterodimer act as end-bridging-factors also involving the components of the MRN complex (RAD50, MRE11 and NBS1). The final step in the non homologous end joining pathway involves ligation of the two aligned double strands *via* the DNA IV ligase/XRCC4 heterodimer^{21,22,23,33}.

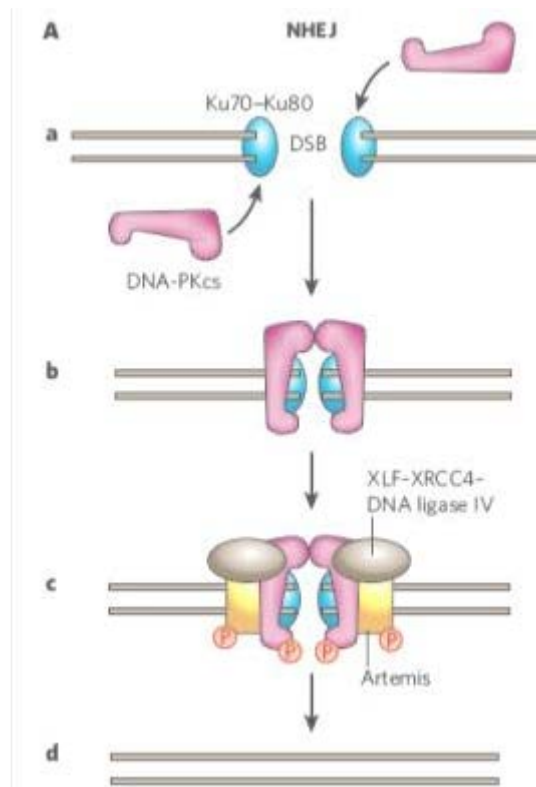


Figure 4. Non homologous end joining in mammalian cells (reproduced from Downs, J. et al. (2007) ^[33])

NHEJ plays a major role in mammalian cells during V(D)J recombination and in DNA double strand break repair. Defects in this pathway enhance genomic instability and increase cancer risk^{21,34}.

Microhomology-mediated end joining (MMEJ)

Microhomology-mediated end joining is a repair pathway of DNA double strand breaks using short homologous sequences of approximately 5-25 base pairs. The first step in this repair mechanism is the nucleotide restriction at the ends of the double strand breaks to monitor exposure of homologous sequences. After finding a suitable sequence, strand annealing occurs forming a MMEJ intermediate and thereby creating non homologous 3' end tails. These generated tails are further removed by the XPF/ERCC1 protein complex before ligation *via* DNA ligase I takes place³⁵.

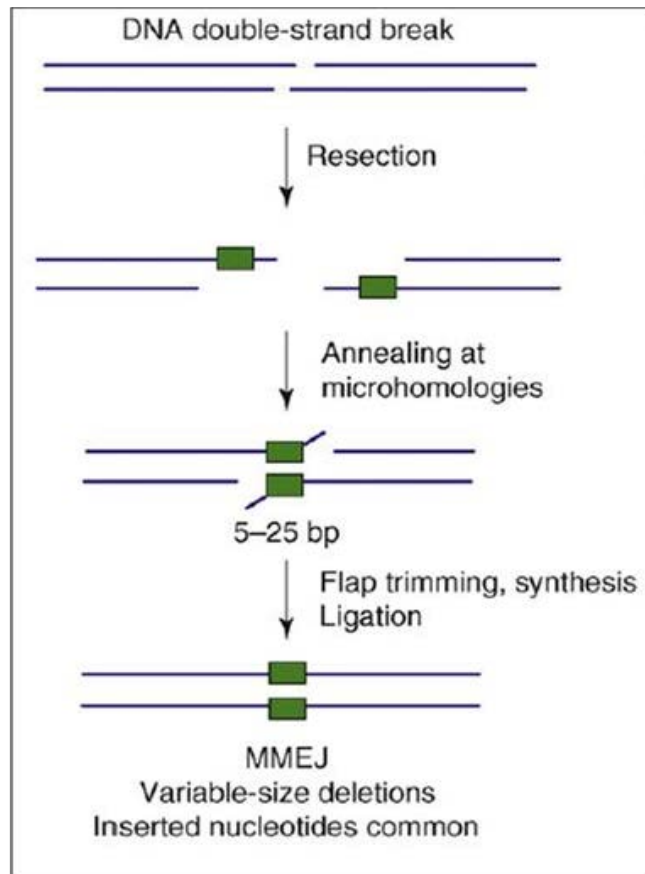


Figure 5. Model of MMEJ (reproduced from McVey, M. et al. (2008) ^[35])

This repair mechanism is very error prone due to arising deletions during sequence alignment. MMEJ is therefore not just associated with DNA repair but also with chromosome translocations, rearrangements and other abnormalities³⁵.

Homologous recombination (HR)

Homologous recombination is a high fidelity DNA repair mechanism in eukaryotic cells, using the information on an undamaged sister chromatid or homologous chromosome as a template. This pathway is composed of three main steps including strand invasion, branch migration and the formation of so called Holliday junctions^{22,23,33}. In contrast to NHEJ which mainly acts in G₁, HR plays a major role in DNA repair in S-phase due to the formation of sister chromatids in this phase of the cell cycle³³.

The MRN complex is a key component of the homologous recombination pathway in human cells comprising the proteins MRE 11, RAD 50 and NBS 1. After DNA damage resulting in a double strand break, DNA gets processed producing a single stranded segment with a 3' overhang. RPA, RAD 51 and RAD 52 can now bind to this 3' overhang generating a nucleoprotein filament which then searches for a homologous sequence in the genome. After strand invasion and binding to the homolog sequence, which additionally requires the action of RAD 54, DNA synthesis is performed by forming a so called Holliday junction. After synthesis is completed the Holliday junction is cleaved by resolvases, a structure- specific endonuclease and the duplex structure is restored again^{22,23,33}.

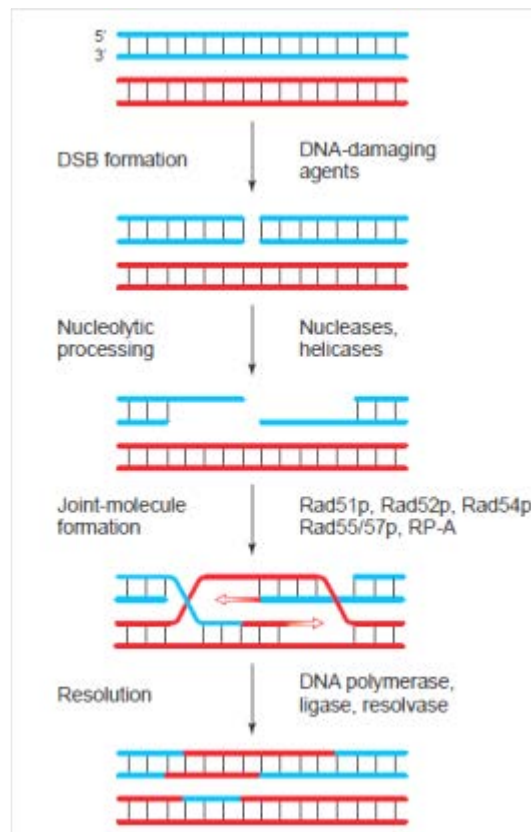


Figure 6. HR in mammalian cells (reproduced from Kanaar, R. et al (1998) ^[23])

1.3. Defective DNA repair mechanisms in human cancers

During their whole lifetime cells are exposed to various endogenous and exogenous sources, affecting DNA structure. These changes include introduction of DNA strand breaks, formation of adducts or other forms of perturbations which have an impact on DNA structure. To cope with those permanently arising lesions and maintain genomic stability, cells have evolved several DNA repair mechanisms to restore the original structure after DNA damage. These DNA repair mechanisms involve DNA damage sensors which are able to recognise perturbations in DNA structure and facilitate binding of proteins essential for DNA repair and cell cycle checkpoint activation. Defects in DNA repair mechanisms are associated with specific DNA repair related disorders and a predisposition for developing cancer^{21,22,23}.

Germ line mutations in the genes *MLH1* or *MSH2* required for DNA mismatch repair are associated with a predisposition to develop hereditary non-polyposis colorectal cancer³⁶. Defects in the nucleotide excision repair pathway are the initiator of the autosomal recessive disease Xeroderma pigmentosum²⁵. The ATR cascade also plays a major role in DNA repair and checkpoint activation. An impaired ATR signalling cascade due to mutations triggers the rare autosomal recessive disorder known as Seckel syndrome^{22,37}. The two tumour suppressor genes *BRCA1* and *BRCA2* play a major role in maintaining genomic stability. Mutations in these genes can lead to a truncated protein and thereby affect its functionality.

Germ line mutations in *BRCA1* and *BRCA2* are associated with a higher risk of developing breast cancer and ovarian cancer^{38,39,40}.

1.3.1 ATM/ATR

Phosphatidylinositol 3-kinase-related kinases (PIKKs) represent a group of kinases related to the family of phosphoinositide 3-kinases (PI3K). The family of PIKKs includes the two main transducers in DNA damage response signalling, ataxia telangiectasia mutated (ATM) and Rad3-related protein (ATR), but also mammalian target of rapamycin (mTOR) kinases, the catalytic subunit of DNA-dependent protein kinase (DNA-PKcs) and hSMG-1^{37,41,42}.

ATM and ATR play a major role in DNA damage response by phosphorylating their targets and thereby starting various phosphorylation cascades. These cascades amplify the signal of DNA damage and lead to cell cycle arrest at appropriate cell cycle checkpoints. Although they are activated by different types of DNA damage, ATM and ATR show substrate similarities and both enzymes preferentially phosphorylate serine or threonine followed by a glutamine. Their targets act as downstream mediators in DNA damage response coordinating cell cycle progression and apoptosis^{37,41,42}.

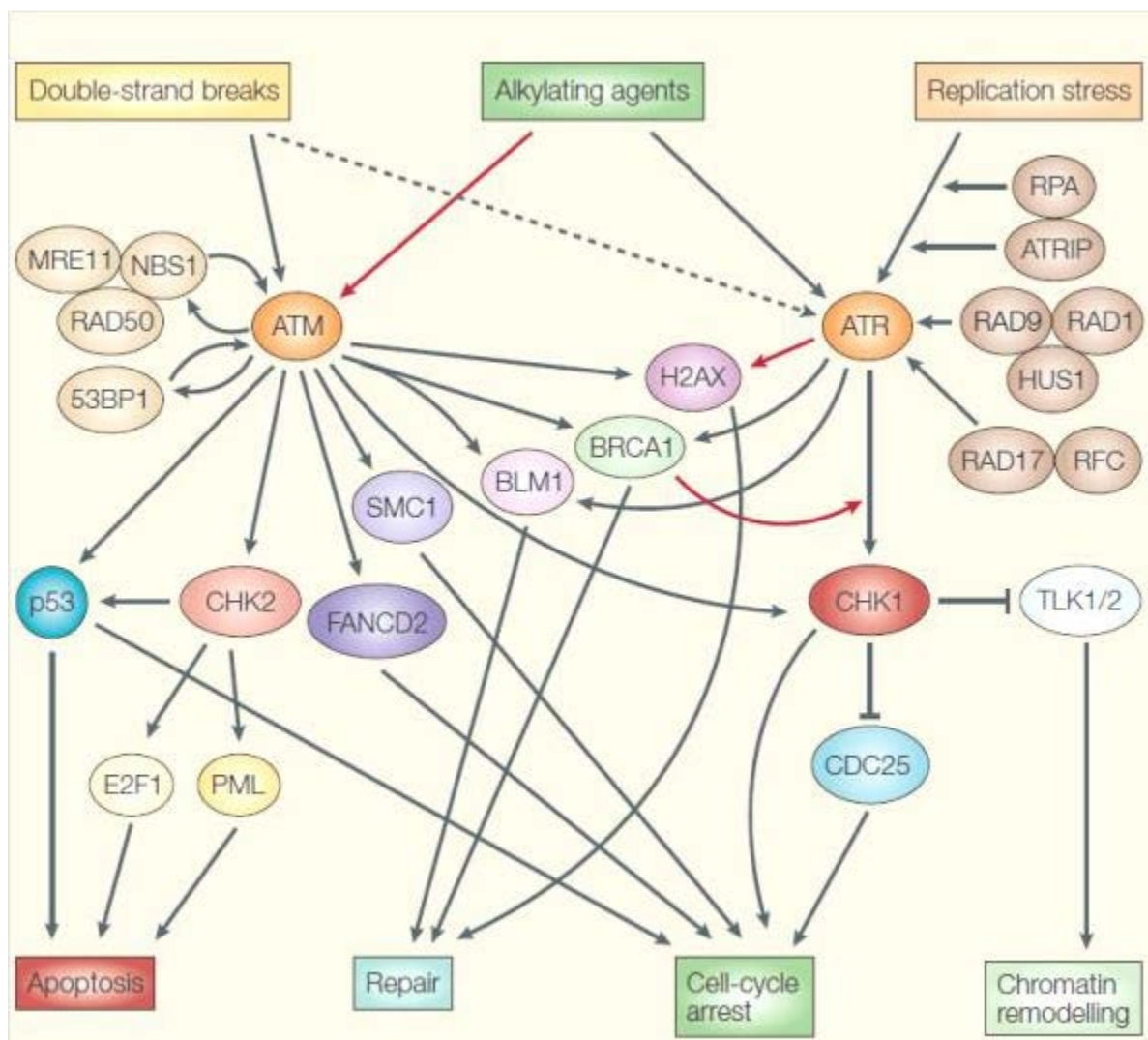


Figure 7. ATM and ATR signalling (picture reproduced from Zhou, B. et al. (2004) ^[43])

ATM signalling represents a pathway which is induced by DNA double strand breaks and shows activity during the entire cell cycle. DNA single strand breaks and DNA damage as a result of replication stress triggers activation of ATR. In contrast to ATM the ATR signalling cascade is limited to S and G₂ phase of the cell cycle^{37,43}.

Ataxia telangiectasia mutated (ATM)

ATM is a member of the serine/threonine protein kinases, phosphatidylinositol 3-kinase related kinases (PIKKs) and initiator of the rare human disease Ataxia telangiectasia⁴⁴. ATM kinase is activated by DNA damaging agents or ionizing radiation causing DNA double strand breaks. The MRN complex encompassing the proteins MRE11, RAD50 and NBS1 serves as a sensor of double strand breaks and triggers activation of ATM^{37,42,43,45}.

Similar to the other members of the PIKK family, ATM consists of a FAT domain (FRAP, ATM, TRAPP), several HEAT repeats and a PIKK regulatory domain. In addition to the FAT domain, ATM also harbours an additional C-terminal FAT domain known as FATC, which plays a major role in kinase activity. The autophosphorylation site is located in a small region between the FAT domain and the amino-terminal located HEAT repeats^{42,46}.

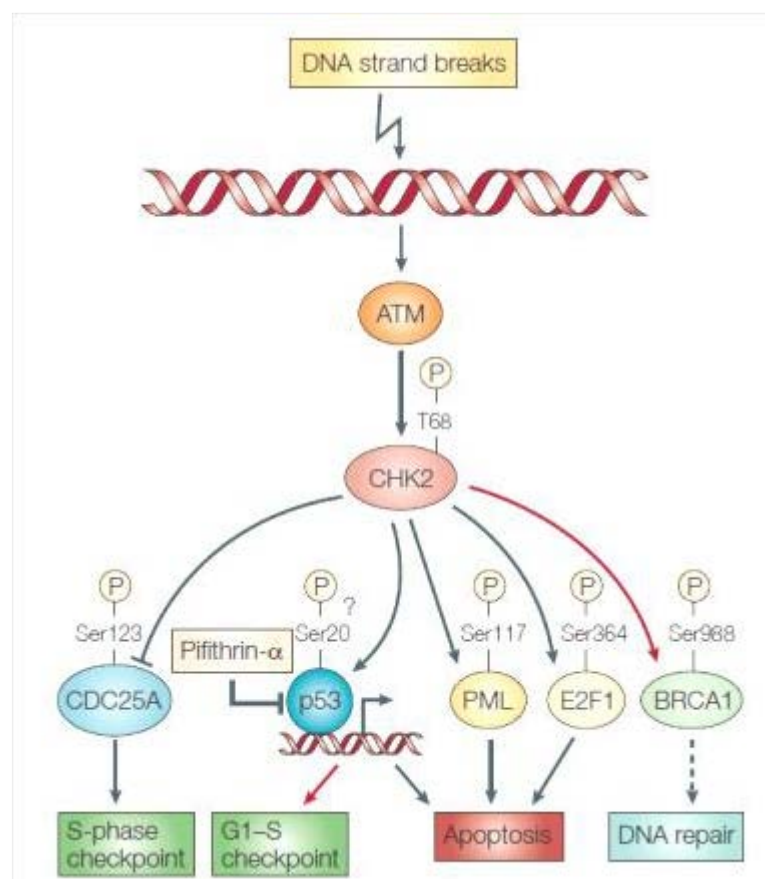


Figure 8. ATM signalling cascade (picture reproduced from Zhou, B. et al. (2004) ^[43])

As response to DNA damage, ATM interacts with several downstream proteins so called effectors. These proteins are involved in cellular processes such as transcription regulation, DNA repair, apoptosis and cell-cycle control. One of them is the protein kinase Chk2 which is

phosphorylated on Thr-68 and thereby activated, leading to induction of phosphorylation of the tumour suppressor p53 and inactivation of the CDC25 phosphatase. Proteins which also showed interaction with ATM kinase are the MRN complex component NBS1, the histone variant H2AX, the in DNA repair involved protein BRCA1 as well as BLM1 and FANCD2^{37,42,43,45}.

Ataxia telangiectasia and Rad3 related (ATR)

As a member of the PIKK family, the serine/threonine-protein kinases, ATR shows several similarities in structure and function to other members of this protein family. Although ATR exhibits several commonalities with ATM, like the affinity for certain substrates, their activations are induced by different cellular processes. ATR gets activated *via* single strand breaks as a result of replication induced stress or UV radiation induced DNA damage.

After recruitment of ATR and ATRIP (ATR interacting protein) by the DNA single-strand-binding protein replication protein A (RPA), ATR triggers phosphorylation and thereby activation of the effector kinase Chk 1. Chk1 induced phosphorylation of the CDC25 phosphatases CDC25A and CDC25C leads to their ubiquitin mediated degradation and thereby cell cycle arrest^{22,37,43}. The ATR signalling cascade also mediates phosphorylation of tousel-like kinases (TLK1/2) which are known to play an important role in chromatin remodelling processes⁴³.

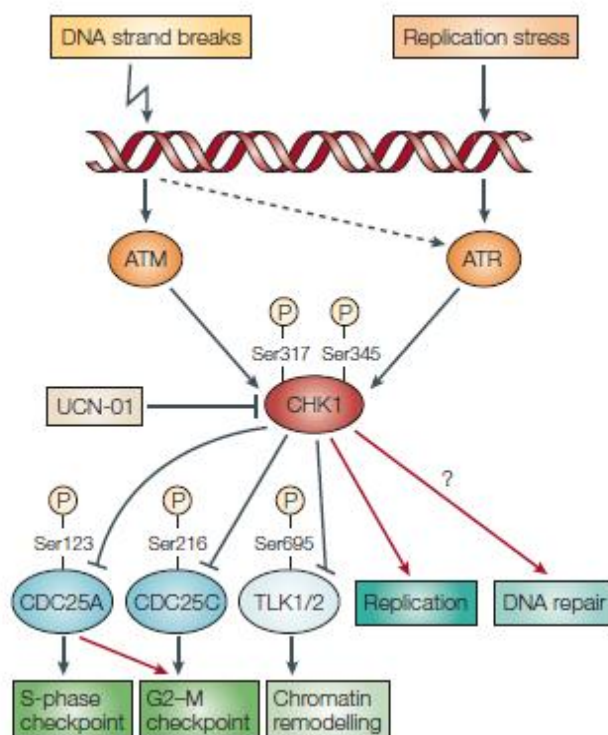


Figure 9. ATR signalling cascade (picture reproduced from Zhou, B. et al. (2004) ^[43])

Impaired ATR signalling due to mutations in the ATR encoding gene are the initiator of a rare autosomal recessive disorder known as Seckel syndrome^{22,37}.

1.3.2 BRCA1/BRCA2

BRCA1 (breast cancer type 1 susceptibility protein) and BRCA2 (breast cancer type 2 susceptibility protein) are proteins encoded by the tumour suppressor genes *BRCA1* and *BRCA2*, respectively. The two proteins play a major role in the homologous recombination DNA repair pathway during S and G₂ phase of the cell cycle. Mutations in these tumour suppressor genes are associated with an increased risk of developing breast or ovarian cancer^{22,37,38,40,47,48}.

BRCA1

BRCA1 is a large protein (over 200 kDa) involved in DNA repair and DNA damage response, the gene encoding BRCA1 is located on chromosome 17q21^{37,38}.

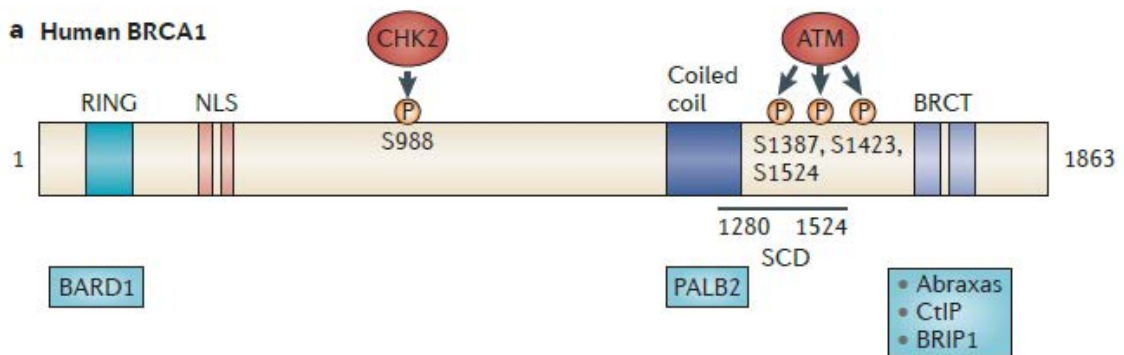


Figure 10. Human BRCA1 (picture reproduced from Roy, R. et al. (2012) ^[48])

The BRCA1 protein contains an N-terminal RING domain through which it interacts with another RING domain and BRCT domain containing protein, BARD1 (BRCA1-associated RING domain protein 1). Formation of this BRCA1-BARD1 heterodimer enhances its E3 ubiquitin ligase activity, binding of BARD1 to BRCA1 also preserves it from degradation^{37,38,47,48}. The C-terminal domain harbours a coiled-coil and a BRCT (BRCA1 C Terminus) domain. The BRCT domain is essential for phospho-protein binding and thereby interaction with other proteins involved in DNA damage response and DNA repair^{38,47,48}. BRCA1 also contains a SQ/TQ cluster domain (SCD) which harbours phosphorylation sites required for ATM interaction⁴⁸.

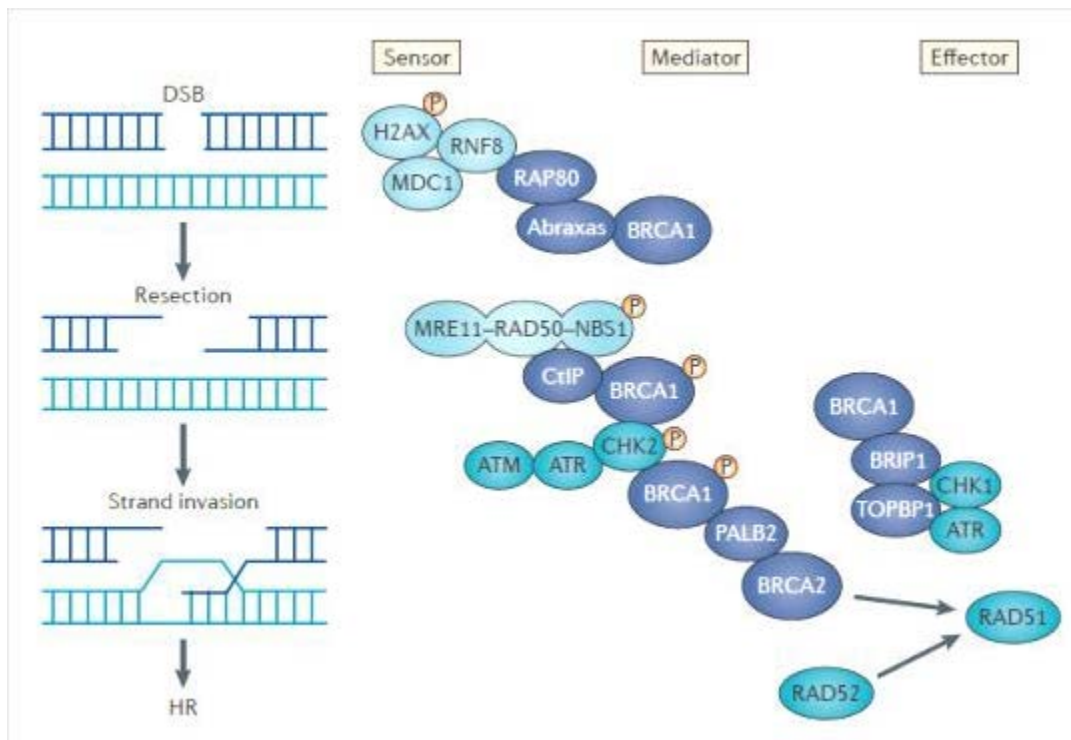


Figure 11. Involvement of BRCA1 and BRCA2 in DNA damage response (picture reproduced from Roy, R. et al. (2012) ^[48])

Phosphorylation of histone H2AX at serine 139 either *via* ATM or ATR signalling leads to recruitment and accumulation of proteins involved in DNA repair to DNA damage sites. Phosphorylated H2AX mediates the interaction of the protein Abraxas with the ubiquitin binding protein RAP80, which is supported by the DNA damage checkpoint protein 1 (MDC1) and the RING finger protein 8 (RNF8)^{38,48}. BRCA1 also plays a role in recruitment of RAD51 and accomplishes RAD51 mediated homologous recombination by forming an effector complex including BRCA1, PALB2 (Partner and localizer of BRCA2) and BRCA2^{40,48}. Phosphorylation of BRCA1 on serine 988 is carried out by the protein kinase CHK2⁴⁸.

After DNA damage occurred the components of the MRN complex, bind to the DNA double strand break and thereby promote formation of the BRCA1–CtIP complex, leading to generation of DNA single strands at DNA double strand breaks^{38,48}. DNA damage also induces the formation of a BRCA1 containing macro complex including besides BRCA1 the proteins BRIP1 (BRCA1-interacting protein C-terminal helicase 1) and TOPBP1 (DNA topoisomerase 2-binding protein 1). This complex seems to be involved in mediating the ATR signalling cascade during replication⁴⁸.

BRCA2

As the multifunctional protein BRCA1, BRCA2 also plays a major role in DNA repair acting as a tumour suppressor in cells. In contrast to BRCA1, function of BRCA2 is more limited to specific tasks especially in mediation of homologous recombination in cells. BRCA2 interacts with the recombinase RAD51, forming so called RAD51 filaments^{38,40,47,48}. BRCA2 is also involved in formation of an effector complex including BRCA1 and PALB2, which further triggers RAD51 recruitment to DNA damage sites^{38,48}. The gene encoding BRCA2 is located

on the q arm of chromosome 13. The N-terminus of BRCA2 harbours PALB2 binding site. 8 central located BRC repeats are required for binding the recombinase RAD51. To enable BRCA2 binding to either single stranded or double stranded DNA, BRCA2 possesses a DNA binding domain consisting of a helical domain three oligonucleotide binding folds and a tower domain. Besides a nuclear localization signal (NLS), the C-terminal end of BRCA2 exhibits a phosphorylation site for CDK2 at S3291⁴⁸.

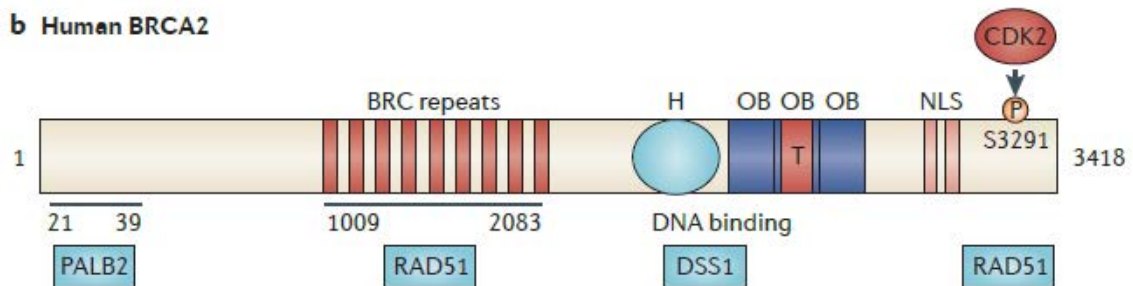


Figure 12. Human BRCA2 (picture reproduced from Roy, R. et al. (2012) ^[48])

1.3.3 Components of the MRN complex

The human MRN complex is a multifunctional complex consisting of the proteins MRE11, RAD50 and NBS1. MRN is involved in different cellular processes affecting DNA repair and cell cycle progression at cell cycle checkpoints. This makes the MRN complex to a key player in maintaining genomic stability. Impaired functionality is associated with an increased risk of developing cancer and the genetic disorder Nijmegen Breakage Syndrome. Although the MRN complex is mainly associated with DNA repair during homologous recombination and non homologous end joining, its functions are versatile^{38,49,50}. Studies showed its involvement in DNA replication by interacting with members of the E2F protein family⁵¹. The MRN complex also plays a role in telomere end processing⁵² and processes involved in meiotic recombination⁵³.

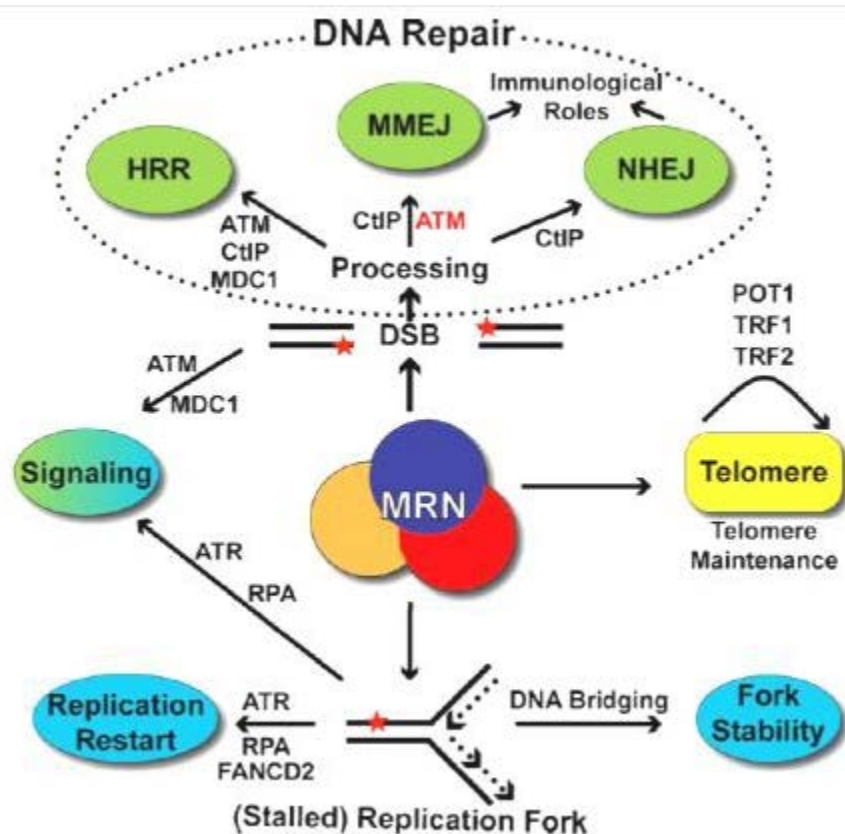


Figure 13. Involvement of the MRN complex in DNA damage response (picture reproduced from Williams, G. et al. (2010)^[50])

MRE11

MRE11 is one of three components that form a complex, involved in DNA repair and other cellular processes, the so called MRN complex. MRE11 is a protein which exhibits besides nuclease activity also single strand endonuclease and double strand 3'-5' exonuclease activity. This protein harbours binding sites for both partners, a NBS1 binding site at the N-terminal end and a RAD50 binding site at the C-terminal end^{49,50,53,54}. Two DNA binding sites, one central located and one at the C-terminal end facilitate binding of MRE11 to DNA^{50,53,55}.

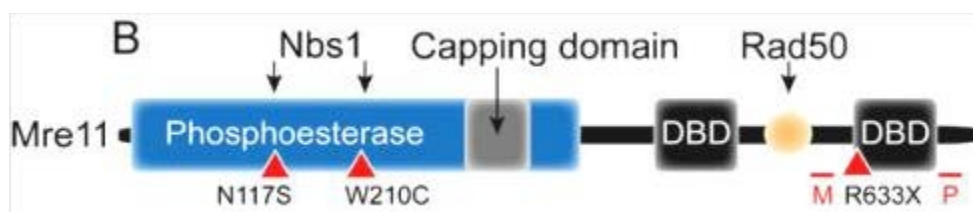


Figure 14. Structure of MRE11 (picture reproduced from Williams, G. et al. (2010)^[50])

Binding of MRE11 to DNA can be differentiated depending on the existing DNA damage. MRE11 is able to respond to different ways of DNA damage by binding to single stranded and double stranded DNA. This either leads to a symmetrical conformation of MRE11 bound

to DNA, in case of binding to double stranded DNA or promotes an asymmetrical conformation if interaction occurs at a DNA single strand. These differences in MRE11 conformation led to the assumption that binding DNA symmetrical as in presence of DNA double strand breaks activates the ATM signal cascade. Whereas MRE11 bound to single stranded DNA leads to an asymmetric conformation of MRE11 and thereby may inhibit ATM interaction but triggers ATR signalling⁵⁰.

Mutations in the *MRE11* gene are rare and cause a disorder very similar to ataxia-telangiectasia, known as ataxia-telangiectasia-like disorder (ATLD)^{55,51}.

RAD50

RAD50 is one of the three components which form the MRN complex. RAD50 possesses ATPase activity and thereby regulates endonuclease activity and nuclease activity of MRE11^{50,53,54}.

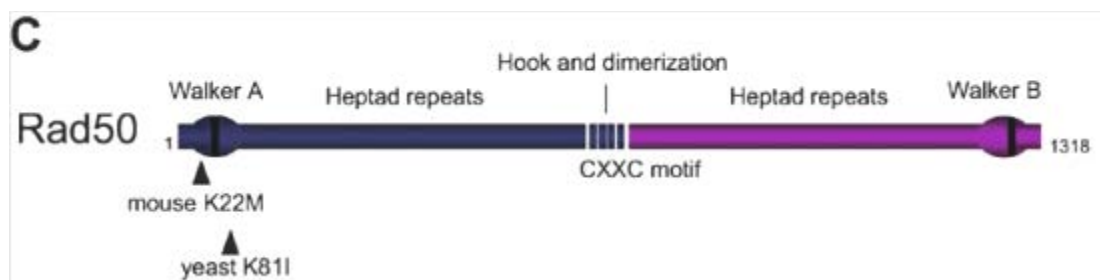


Figure 15. Structure of RAD50 (picture reproduced from Borde, V. et al. (2007) ^[53])

RAD 50 consists of two central located heptad repeats which facilitate folding into a coiled-coil structure and thereby approximate the N-and the C- terminal ATPase harbouring Walker A and Walker B motifs^{53,55}. This approximation of both Walker motifs enables binding and hydrolysis of ATP, required for binding of MRE11 to DNA^{53,54,55}. RAD50 performed ATPase activity is essential for a functional MRN complex, mutations in RAD50 which affect its ATPase activity sensitises cells to double strand causing agents^{50,53,55}.

NBS1

In contrast to MRE11 and RAD50 which both are highly conserved in eukaryotes, the third component of the MRN complex NBS1 is poorly conserved among species, showing only marginal similarity to its yeast homolog Xrs2^{49,54}.

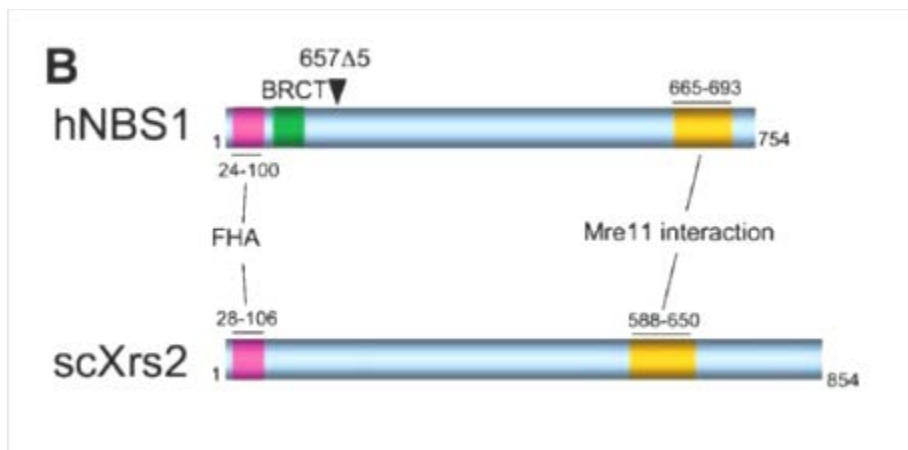


Figure 16. Structure of human NBS1 and its yeast homolog Xrs2 (picture reproduced from Borde, V. et al. (2007) ^[53])

The N-terminal end of NBS1 harbours a BRCT repeat domain and a FHA domain which are both involved in protein-protein interactions *via* phospho-protein binding⁵⁰. C-terminally located domains mediate the interaction with MRE11 and harbour a phosphorylation site required for binding of the protein kinase ATM to NBS1^{50,53}. NBS1 plays an important role in MRN signalling through its interaction with several different proteins involved in the DNA damage response including CtIP, MDC1, phosphorylated histone H2AX and ATM. NBS1 also mediates localisation of the MRN complex to DNA damage sites and induces activation of ATM signalling^{49,50}. Activation of ATM autophosphorylation through recruitment of MRN to the damage site indicates activity of the MRN complex upstream of the ATM signalling cascade⁵³. After its activation, ATM in turn phosphorylates NBS1 on Ser-343. This phosphorylation step seems to be necessary for activation of other downstream substrates of ATM like CHK2, SMC1 and FANCD2⁴⁵.

Mutations in the gene encoding *NBS1* are associated with the rare autosomal recessive disorder Nijmegen breakage syndrome (NBS). NBS is associated with an increased risk of developing cancer. The 657del5 mutation is the most common observed mutation in NBS patients. The 657del5 mutation was also found in patients who suffer from skin melanomas, breast tumours or cancer of colon and rectum as well as in non-Hodgkin lymphoma patients⁴⁹.

1.3.4 Increased sensitivity of DNA repair defective cells to inhibitors of topoisomerases

Cellular processes such as replication and transcription generate topological problems which have to be resolved by the action of DNA topoisomerases. These features of DNA topoisomerases make them essential for cellular functions like DNA synthesis, transcription and sister chromatid segregation. Inhibition of DNA topoisomerases has crucial impact on cell faith, which makes DNA topoisomerase inhibitors to a suitable target in cancer therapy^{11,12,20,56}.

Action of DNA topoisomerase targeting agents, lead to DNA damage by generating either DNA double strand breaks or DNA single strand breaks. These generated lesions accumulate if they remain unrepaired, leading to cell cycle arrest and apoptosis^{11,12,20,56}.

Cells exhibiting deficiencies in DNA repair pathways either due to mutations in PARP, BRCA1/BRCA2 or in the Fanconi anemia protein, FANCD2, showed hypersensitivity to treatment with topoisomerase targeting drugs. These findings suggest that cells exhibiting an impaired DNA repair cannot cope with topoisomerase poison induced lesions as well as those with a functional DNA repair^{5,57}. Cells carrying a mutation in the tumour suppressor genes *BRCA1* and *BRCA2* are known to have an impaired DNA damage repair due to their involvement in homologous recombination^{5,56}. Loss of functionality of BRCA1 or BRCA2 increases genomic instability and makes them hypersensitive to agents causing DNA lesions such as topoisomerase targeting drugs⁵. The anti proliferative effects of the topoisomerase II inhibitor C-1305 on cells lacking a functional *PARP1* gene have been already demonstrated¹⁸. Pharmacological inhibition of PARP-1 activity also sensitised cells to topoisomerase targeting drugs by potentiating the cytotoxic effects of topoisomerase inhibitors on cells⁵⁷. These findings suggested that deficiencies in DNA repair either due to mutations in genes essential for DNA repair pathways or synthetically induced by drugs, can potentiate cytotoxic effects generated by topoisomerase inhibitors⁵⁸.

1.4. Concept of synthetic lethality

Targeting DNA repair mechanisms in cancer therapy became an issue of interest by further inventing the concept of synthetic lethality^{5,36,59,60,61}.

The phenomenon of synthetic lethality was first described in 1946 by the geneticist Theodosius Dobzhansky based on his observations in *Drosophila Pseudoobscur*. Dobzhansky's studies on *Drosophila* are an example for inducing lethality in fruit flies due to the combination of two different mutations, which are harmless if they occur alone but are lethal when combined⁶². Tumour cells that carry a mutation affecting DNA repair got in the spotlight of interest in cancer medicine by applying the concept of synthetic lethality to those DNA repair impaired cells. Continuous exposure to DNA damage gave cells the opportunity to evolve several DNA repair pathways to remove DNA lesions and maintain genomic stability. If one pathway is defective cells are able to repair arising DNA damage, using an alternative repair pathway. Tumour cells with deficiencies in a specific DNA repair pathway are right from the start limited in their usage of alternative pathways as response to DNA damage. Treatment with agents that target one of the alternative DNA repair pathways can induce apoptosis in those cells due to accumulation of DNA lesions^{5,36,59,60,61}.

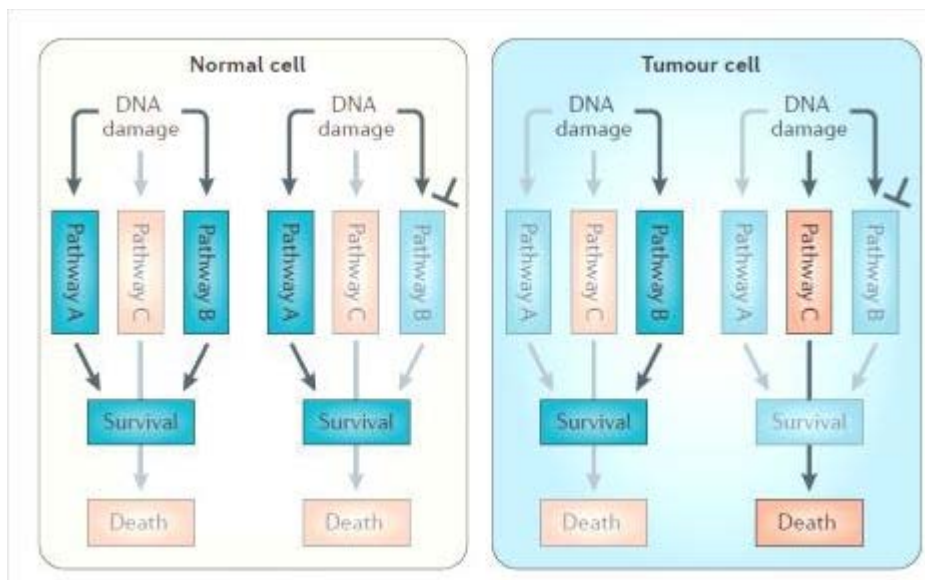


Figure 17. Concept of synthetic lethality (picture reproduced from Curtin, N. et al. (2012) ^[60])

Recent research aimed at the improvement of the synthetic lethality concept by targeting alternative repair pathways used in cells harbouring a cancer associated mutation in their DNA repair. This tumour specific therapy already showed success in treatment of tumour cells carrying a mutation in the tumour suppressor gene *BRCA1/2* with PARP inhibitors^{36,59,60,5,61}.

1.4.1 Therapeutic agents which selectively exploit DNA damage repair pathways (e.g. PARP-1)

Cells are permanently confronted with DNA lesions either due to DNA damage inducing agents or normal metabolic cellular processes. To cope with such arising lesions, cells have evolved several DNA damage repair pathways as already described in 1.2.^{21,22,23,36}.

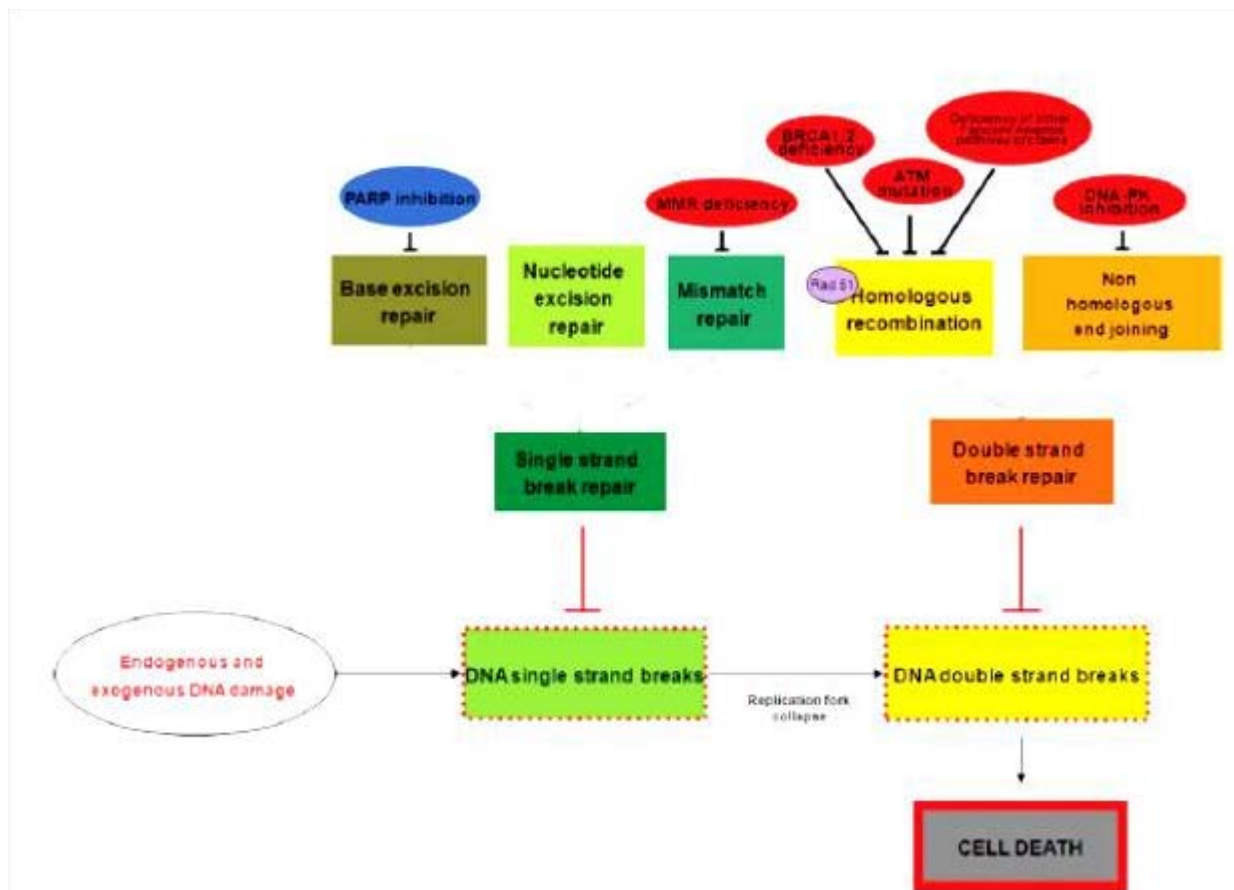


Figure 18. DNA repair mechanisms (picture reproduced from Yap, T. et al. (2011) ^[59])

PARP-1

Poly-Adenosine diphosphate (ADP)-ribosylation is a post-translational modification of proteins carried out by specific poly(ADP-ribose) polymerases so called PARPs. PARP-1 and PARP-2 are the most abundant and two best characterized members of the PARP superfamily which is assumed to consist of at least 17 members. Together with DNA repair proteins such as DNA polymerase β , DNA ligase III and X-ray repair cross-complementing protein 1 (XRCC1), PARP-1 activates the base excision pathway. Further investigations showed that PARP may facilitate DNA damage response to DNA double strand breaks by interacting with proteins involved in HR and NHEJ. Recognising DNA lesions, PARPs play an important role in DNA damage response and are therefore a suitable target in cancer therapy. Inhibition of PARP enhances the cytotoxic action of alkylating agents in cells with deficiencies in DNA damage repair. This approach of combining PARP inhibition and cell damaging agents leads to an additional therapeutic benefit in cells impaired in DNA repair^{63,64,65,66,59}.

Structure of PARP-1

PARP-1 is a highly conserved protein with a molecular weight of 113kDa, which consists of 1013 amino acids⁶⁷. The gene encoding this enzyme is located on the q arm of chromosome 1⁶⁸, its closest paralog in the PARP superfamily is the also DNA dependent enzyme PARP-2⁶⁹. PARP-1 consists of three functional units, including a DNA binding domain, an automodification domain and a catalytic domain. The DNA binding domain (DBD) is located at the amino terminal end and harbours zinc finger motifs required for detection of DNA damage and further binding to DNA single or double strand breaks^{63,65,70,69}.

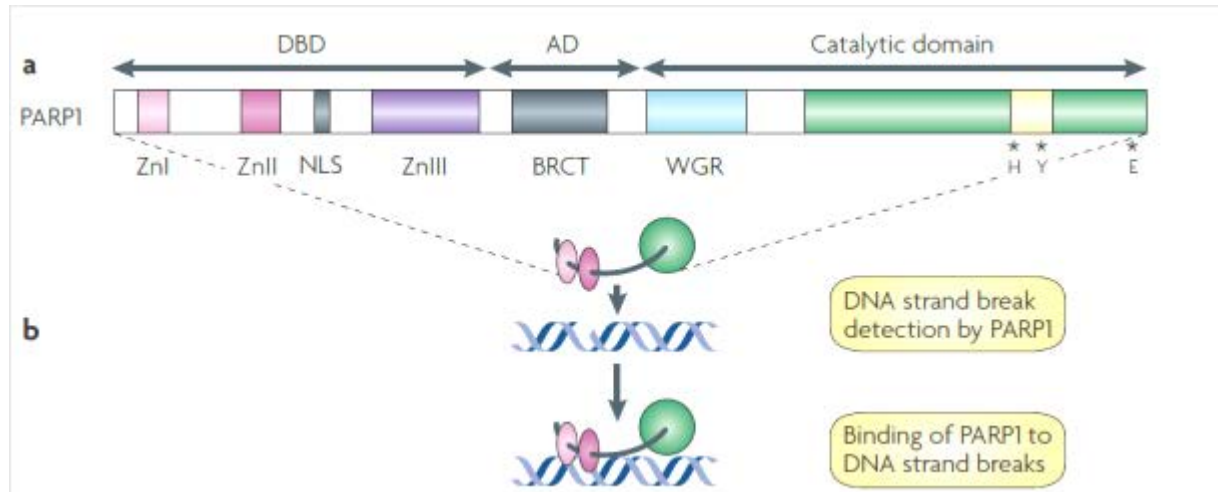


Figure 19. Structure of PARP-1 (picture reproduced from Rouleau, M. et al. (2010) ^[65])

The centrally located automodification domain is rich in glutamate and lysine residues. These specific residues serve as acceptors of (ADP) ribose moieties and facilitate the dimerisation of the protein. PARP-1 also harbours a BRCA1 carboxy-terminus (BRCT) motif which is essential for interacting with various proteins involved in DNA damage response^{63,65,69,70}. The catalytic domain of PARP-1 is located at the C-terminal end and harbours the PARP signature motif which is required for NAD⁺ binding^{63,65,69,70}. This motif consists of a β - α -loop- β - α NAD⁺ fold, and represents the most conserved structure among PARP family members^{63,69}. PARP-1 also showed to be involved in other DNA repair pathways by facilitating the recruitment of proteins required for DNA damage repair. These proteins include one of the components of the MRN complex, MRE11 and the protein kinase ATM, which both play a major role in DNA repair by homologous recombination^{65,59,69}.

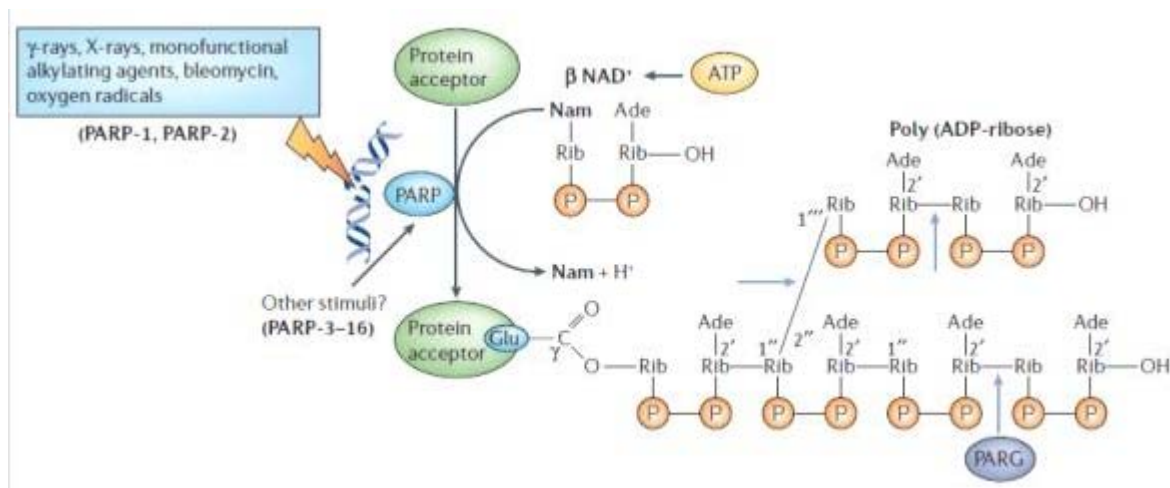


Figure 20. Action of poly (ADP-ribose)polymerase (picture reproduced from Schreiber, V. et al. (2006) ^[63])

In this reaction nicotinamide adenine dinucleotide (NAD^+) is used as a substrate. PARP hydrolyses NAD^+ , this process generates besides ADP-ribose moieties, nicotinamide (NAM) and one proton (H^+). The generated ADP moieties are attached to an acceptor protein thereby forming the poly (ADP-ribose) chain. The synthesis of poly(ADP) ribose moieties serves as a signal for proteins required for DNA repair and occurs either on PARP itself or the chain gets transferred to various acceptor proteins^{63,65,70}. Degradation of the poly (ADP-ribose) chain is performed by poly ADP-ribose) glycohydrolase (PARG). Possessing both, endo- and exoglycolytic activities PARG catalyses cleavage of the poly (ADP-ribose) chain between its ADP-ribose units generating free ADP-ribose^{63,65,70}.

Studies have shown that PARP-1 plays a major role in the base excision repair pathway as response to DNA single strand breaks. After PARP-1 binds to the DNA lesion *via* its DNA binding domain, the enzyme catalysis the transfer of ADP-ribose moieties from NAD^+ to itself, thereby facilitating interaction with XRCC1, another protein involved in base excision repair. XRCC1 further interacts with DNA ligase III and DNA polymerase β which both also participate in this DNA repair pathway^{63,65,59,70,71}. Inhibition of poly(ADP) ribose polymerase activity using PARP inhibitors, leads to persistent DNA damage due to an inactive base excision repair pathway resulting in increased genomic instability and cell death^{63,65,71}.

1.4.2 Tumours carrying mutations in *BRCA1/2*

Cancer is major health problem and affects people worldwide. Cancer studies showed that breast cancer was the most common diagnosed cancer in women in the United States with approximately 29% new incidences in 2012⁷².

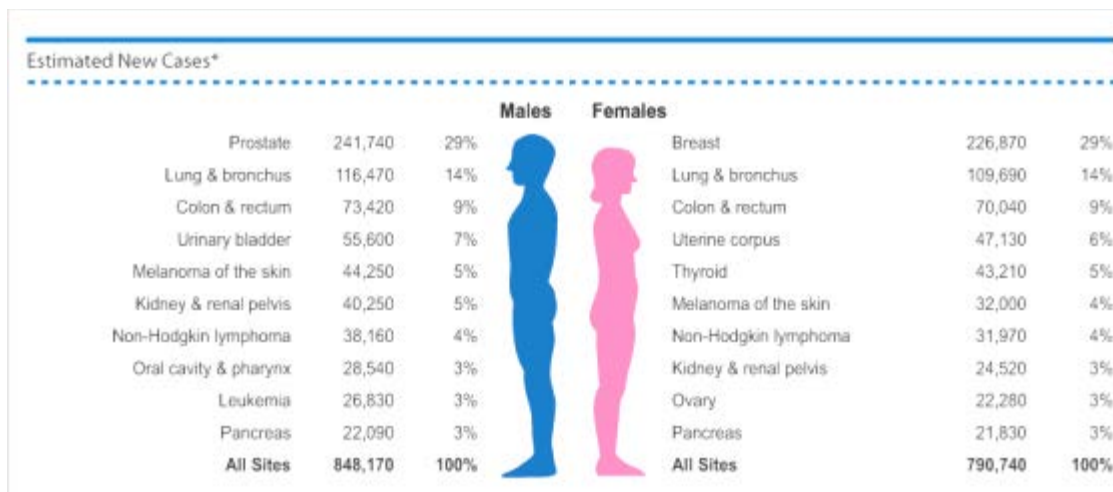


Figure 21. U.S. cancer statistic 2012 (picture reproduced from Siegel, R. et al. (2012) ^[72])

The two tumour suppressors BRCA1 and BRCA2 are known to have major functions in DNA repair and are necessary for maintaining genomic stability. Mutations in the genes coding for BRCA1 and BRCA2 often affect their functionality by generating a truncated or inactive protein. Germ line mutations in these genes account for approximately 5% in reported breast cancer cases. Carriers of a germ line mutated *BRCA1* or *BRCA2* copy are at higher risk of developing cancer during their lifetime due to a second hit which leads to loss of heterozygosity^{38,48,73,74,75}. *BRCA1* germ line mutations lead to an average cumulative risk of 59% for developing ovarian cancer by age 70, whereas the average cumulative risk of developing breast cancer was up to 60%. Carriers of germ line mutations in *BRCA2* showed an average cumulative risk of 55% for developing breast cancer by age 70, with an average cumulative risk of 16.5% the risk for ovarian cancer was diminished compared to *BRCA1* mutation carriers⁷⁵.

The hereditary breast and ovarian cancer (HBOC) syndrome is an inherited cancer syndrome which leads to a predisposition for developing breast and ovarian cancer^{48,74}. This syndrome is associated with mutations in multiple high-risk genes, including the tumour suppressor genes *BRCA1*, *BRCA2*, *TP53*, *PTEN*, *CDH1* and the gene coding for the protein kinase LKB1⁷⁴. Patients with hereditary breast and ovarian cancer syndrome also are predisposed towards other malignancies including pancreatic, laryngeal, stomach, uterine tube and prostate cancer⁴⁸.

1.4.3 Inhibition of PARP-1 in cancers carrying mutations in DNA damage repair pathways (e.g. *BRCA1/2*)

PARP-1 inhibition affects cell viability by increasing cytotoxic effects due to accumulation of DNA lesions as a result of impaired DNA repair pathways. Studies showed that enzymatic inactivation of PARP-1 increases genomic instability in cells which already carry mutations in other DNA repair pathways^{5,36,60,76,77}.

Cancer cells carrying mutations in the tumour suppressor genes *BRCA1* or *BRCA2* exhibit an impaired DNA repair pathway as a result of loss of heterozygosity. PARP-1 inhibition in *BRCA* mutation carriers provides an example for the concept of synthetic lethality. Neither PARP-1 inhibition nor dysfunctional *BRCA1* or *BRCA2* alone greatly affects cell viability. Inhibition of PARP-1 leads to accumulation of DNA lesions which are normally removed by homologous recombination using the exchange of sister chromatids. These lesions persist in cells with an impaired DNA repair and further lead to cell cycle arrest and apoptosis. In contrast, cells that possess a normal wild-type *BRCA1* or *BRCA2* gene are able to remove DNA damage arising from the inhibition of PARP-1^{5,36,60,76,77}.

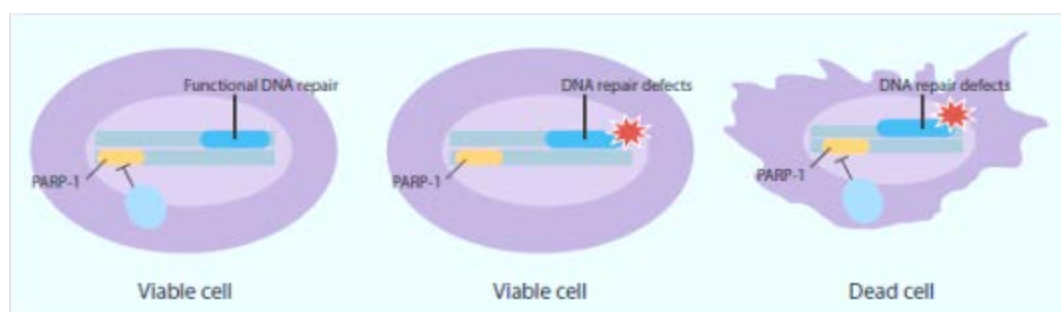


Figure 22. Synthetic lethality induced by PARP-1 inhibition (picture reproduced from Węsierska-Gądek, J. et al. (2012) ^[5])

This selective approach offers the opportunity to specifically induce apoptosis in cancer cells by exclusively targeting cells with an impaired DNA repair. Cells in normal tissues expressing at least one wild-type allele of *BRCA* are not affected which enables a more targeted and less toxic cancer treatment in *BRCA* mutation carriers^{5,36,60,76,77}.

1.4.4 PARP-1 inhibitors in clinical trials

Targeting DNA repair pathways in cancer cells which already carry mutations in DNA repair became a main issue in cancer therapy, focusing on the concept of synthetic lethality^{5,58,78}.

Several classes of PARP-1 inhibitors have been developed and used in combinatory therapies, indicating that inhibition of PARP activity potentiates existing DNA damage and thereby enhances therapeutic effects. These DNA lesions can be generated using cytotoxic agents such as topoisomerase inhibitors, alkylating agents or methylating agents^{5,58,78}. Studies that demonstrated the therapeutic effects of PARP inhibition in cancer therapy got PARP inhibitors into the limelight and further boosted their development. PARP inhibitors could be grouped into seven classes differing in their inhibitory action, including benzamide analogs, isoindolinones, phthalazines and quinazolinones, phenanthridinones and other inhibitors of diverse chemical structures. A couple of these PARP inhibitors seemed to be promising candidates for combined cancer therapy and their clinical efficacy has already been tested in clinical trials⁵.

PARP-1 inhibitors that currently participate in clinical trials include Iniparip (phase III), Olaparib, Rucaparib, Veliparib, CEP-9722 (phase II), MK 4827 and INO-1001 (phase I)^{79,80}.

Inhibition of PARP-1 or other members of the PARP family seems to be a promising target in cancer therapy using the concept of synthetic lethality to develop a more personalised and less toxic medication for patients. Recent findings also showed that PARP-1 inhibition also improved therapeutic effects in cancer cells without mutations in *BRCA1* or *BRCA2*. These findings indicate that treatment with PARP inhibitors is also an option in cells with other deficiencies in DNA repair pathways that affect HR^{5,58,77,81}.

2. Aims of the master thesis

Previous findings in our group already showed that, among five examined human breast cancer cell lines, BRCA-1 expressing BT-20 cells were most sensitive to the interference with PARP-1 activity. Furthermore, inhibition of PARP-1 activity in cells treated with the topoisomerase II inhibitor C-1305, strongly potentiated the topoisomerase inhibitor induced DNA damage in these cells. This synergistic effect upon inhibition of PARP-1 and topoisomerase II activity was only observed in the BRCA-1 expressing breast cancer cell line, BT-20. Although our results demonstrated the synergistic effect observed in combined treated cells, BT-20 cells were found to be relative resistant to the weak DNA damage generating topoisomerase II inhibitor C-1305.

These unexpected findings raised the question whether the strong potentiating effect of the inhibition of PARP-1 activity in combination with C-1305 was attributable to the weak DNA damaging effect of the latter. We further decided to investigate the effects of camptothecin (CPT), a DNA topoisomerase I inhibitor that generates DNA strand breaks, alone and in combination with PARP-1 inhibitor on human breast cancer cells differing in the capacity to repair damaged DNA.

First, we determined to check the impact of the drugs applied alone and in combination on the integrity of DNA. Consequently, we focused on the question on the type of the interaction between both tested compounds in breast cancer cells differing in their *BRCA1* status.

3. Material and methods

3.1Material

3.1.1 Cell culture

RPMI-1640 Medium
DMEM medium
DMEM medium without phenol red (white)
Heat-inactivated foetal calf serum (FCS)
Insulin
Trypsin
Cell culture dishes (10cm, 6cm, 3,5cm)
Cell culture flasks (T25, T75, T162)
Microtiter plates (96-wells)

Cell Scraper
Filter 0.2 µm
CO₂ Incubator
Cell counting chamber (Bürker-Türk)

Sigma-Aldrich®, St. Louis, MO
PAA Laboratories GmbH, Pasching, Austria
Sigma-Aldrich®, St. Louis, MO
PAA Laboratories GmbH, Pasching, Austria
Sigma-Aldrich®, St. Louis, MO
BD/Difco Laboratories, Detroit, MI
Corning Incorporated, Corning, NY
Corning Incorporated, Corning, NY
Greiner Bio-One GmbH Frickenhausen,
Germany
Sarstedt AG, Nümbrecht, Germany
Sartorius AG, Göttingen, Germany
Thermo Fisher Scientific, Waltham, MA
Karl Hecht GmbH & Co KG,
Sondheim/Rhön, Germany

3.1.2 Buffers

10x Blotting buffer – per litre

144 g glycine
30 g TRIS
2 g SDS (sodium dodecyl sulphate)
in ddH₂O
Stored at RT

Carl Roth, Karlsruhe, Germany GmbH
AppliChem, Darmstadt, Germany
Carl Roth GmbH, Karlsruhe, Germany

1x Blotting buffer (pH 8.3) – per litre

100 ml 10x blotting buffer
200 ml methanol
in ddH₂O
Stored at +4°C

Carl Roth GmbH, Karlsruhe, Germany

10x Electrophoresis buffer - per litre

144 g glycine
30 g TRIS
10 g SDS
in ddH₂O
Stored at RT

Carl Roth GmbH, Karlsruhe, Germany
AppliChem, Darmstadt, Germany
Carl Roth GmbH, Karlsruhe, Germany

1x Electrophoresis buffer

10x electrophoresis buffer diluted 1:10 with ddH₂O
Stored at RT

10x PBS

Dulbecco's phosphate buffered saline (DPBS)
diluted in 1L ddH₂O

Sigma-Aldrich®, St. Louis, MO

1x PBS

10x PBS diluted 1:10 with ddH₂O
Stored at + 4°C

KGaA, Darmstadt, Germany

**RIPA (radioimmuno precipitation assay buffer)
buffer**

50 mM TRIS/HCl (pH 7.4)
500 mM NaCl
1 % (v/v) NP-40
0.5 % (w/v) sodium deoxycolate
0.2 % (w/v) SDS
0.05 % NaN₃
Stored at + 4°C

AppliChem, Darmstadt, Germany
Merck KGaA, Darmstadt, Germany
United States Biochemical Corp.
Carl Roth GmbH, Karlsruhe, Germany
Carl Roth GmbH, Karlsruhe, Germany
Sigma-Aldrich®, St. Louis, MO

SDS Stock buffer (pH 6.8) – per 100 ml

6.006 g TRIS
0.4 g SDS
0.01 g NaN₃ in 100ml
in ddH₂O
Stored at +4°C

AppliChem, Darmstadt, Germany
Carl Roth GmbH, Karlsruhe, Germany
Sigma-Aldrich®, St. Louis, MO

2x SDS Buffer – per 100 ml

2 g SDS
10 mg EDTA
20 mg NaN₃
5 ml stock buffer
20 ml glycerol
Stored at RT

Carl Roth GmbH, Karlsruhe, Germany
Merck KGaA, Darmstadt, Germany
Sigma-Aldrich®, St. Louis, MO

Amresco Inc., Solon, OH

**2x SDS sample buffer stained/non-reduced –
per 25 ml (pH 6.8)**

0.5 g SDS
1.5 mg EDTA
5 mg NaN₃
5 mg bromphenol blue
5 ml glycerol
1.25 ml SDS stock buffer

Carl Roth GmbH, Karlsruhe, Germany
Merck KGaA, Darmstadt, Germany

Sigma-Aldrich®, St. Louis, MO
United States Biochemical Corp.
Amresco Inc., Solon, OH

2x SDS sample buffer stained/reduced

1 ml 2x SDS sample buffer stained/non-reduced
20 µl 2.6M DTT stock solution

Sigma-Aldrich®, St. Louis, MO

10x TBS – per litre

24.2 g TRIS

AppliChem, Darmstadt, Germany

84.8 g NaCl
in ddH₂O
Stored at + 4°C

Merck KGaA, Darmstadt, Germany

1x TBS-Tween 20

10x TBS diluted 1:10 with ddH₂O
0.1 % (v/v) Tween 20
Stored at RT

Sigma-Aldrich®, St. Louis, MO

3.1.3 Solutions

10 % APS (Ammonium persulphate)

1 g APS
10 ml ddH₂O
Stored at -20°C

Carl Roth GmbH, Karlsruhe, Germany

3% BSA/PBS

1.2 g BSA
in 40 ml 1xPBS

BSA/PBS-T

0.5% BSA
0.05% Tween
in 1xPBS
Stored at +4°C

3% BSA/TBS-T

1.2 g BSA
in 40 ml 1x TBS-Tween 20
Stored at +4°C

Carbonic Anhydrase I /BSA marker for protein gels

20 µl BSA [1µg/µl]

10 µg/µl carbonic anhydrase I [2µg/µl]
90 µl 2x SDS sample buffer stained/reduced
Stored at -20°C

PAA Laboratories GmbH, Pasching,
Austria

Amresco Inc., Solon, OH

DAPI stock solution (5mg/ml [14.3mM])

2.5 mg DAPI
0.5 ml DMF (Dimethylformamide)
Stored at -20°C

Invitrogen Corporation, Carlsbad, CA
Sigma-Aldrich®, St. Louis, MO

2.6M DDT stock solution

250 mg DDT
in 500 µl ddH₂O

Sigma-Aldrich®, St. Louis, MO

Stored at -20°C

Hoechst staining solution (2mg/ml)

2 mg Hoechst
in 1 ml ddH₂O
Stored at -20°C

Sigma-Aldrich®, St. Louis, MO

MeOH/Aceton (3:2)

30 ml MeOH
20 ml Aceton
Stored at -20°C

Merck KGaA, Darmstadt, Germany

20 mM Pefablock stock solution

12 mg Pefablock (protease inhibitor)
in 50 ml ddH₂O
Stored at +4°C

Merck KGaA, Darmstadt, Germany

0.1 M PMSF stock solution

0.1 M PMSF
in Isopropanol
Stored at RT

Sigma-Aldrich®, St. Louis, MO

Ponceau S

0.1 % (w/v) Ponceau S
5 % (v/v) Acetic acid
Stored at RT

Merck KGaA, Darmstadt, Germany
Fluka, Buchs, Schweiz

20 % SDS

20 g SDS
100 ml ddH₂O
Stored at RT

Carl Roth GmbH, Karlsruhe, Germany

Stock solution for flow cytometric DNA measurement (pH 7.6)

20.4 mM tri-sodium citrate x 2 H₂O
0.6 % (v/v) NP-40
9 mM spermine tetrahydrochloride
3 mM TRIS
Stored at -20°C

Merck KGaA, Darmstadt, Germany
US Biochem. Corp.
Sigma-Aldrich®, St. Louis, MO
AppliChem, Darmstadt, Germany

Solution A

9 mg trypsin 250
in 50 ml stock solution (pH 7.6)
Stored at -20°C

Becton Dickinson, Franklin Lakes, NJ

Solution B

150 mg chicken egg white

Sigma-Aldrich®, St. Louis, MO

30 mg ribonuclease A (boiled before use for 3 minutes)
in 50 ml stock solution (pH 7.6)
Stored at -20°C

Sigma-Aldrich®, St. Louis, MO

Solution C

4.9 mg propidium iodide
69.6 mg spermine tetrahydrochloride
in 10 ml stock solution (pH 7.6)
Stored at +4°C

Sigma-Aldrich®, St. Louis, MO

Sigma-Aldrich®, St. Louis, MO

3.1.4 Chemicals

acetone
acrylamide/bis-acrylamide (29:1) 30%
APS
BSA (bovine serum albumin)

Caspase-Glo® 3/7 Assay
CellTiterGlo™ Assay
DMSO (Dimethyl sulfoxide)
DDT
ECL blot detection system reagent A

ECL+ blot detection system reagent B

ECL Select

EDTA
ethanol
formaldehyde 37%
glycerol
HCl
HOECHST 33342
Methanol
Mounting Medium, DAKO® Fluorescent
Mounting Medium
Na-Doc
NaF
NaOH

Nonidet P-40
Paraformaldehyde 37%
PBS Dulbecco's phosphate buffered saline
(4-(2-Aminoethyl) benzenesulfonyl fluoride
hydrochloride) commercial name: Pefablock
PMSF

Merck KGaA, Darmstadt, Germany
Sigma-Aldrich®, St. Louis, MO
Carl Roth GmbH, Karlsruhe, Germany
PAA Laboratories GmbH, Pasching,
Austria
Promega Corporation, Madison, WI
Promega Corporation, Madison, WI
Sigma-Aldrich®, St. Louis, MO
Roche, Basel, Switzerland
Amersham International, Little Chalfont,
Buckinghamshire, England
Amersham International, Little Chalfont,
Buckinghamshire, England
Amersham International, Little Chalfont,
Buckinghamshire, England
Merck KGaA, Darmstadt, Germany
Australco, Spillern, Austria
Merck KGaA, Darmstadt, Germany
Amresco Inc., Solon, OH
Carl Roth GmbH, Karlsruhe, Germany
Sigma-Aldrich®, St. Louis, MO
Carl Roth GmbH, Karlsruhe, Germany
DAKO AS, Glostrup, Denmark

Carl Roth GmbH, Karlsruhe, Germany
Merck KGaA, Darmstadt, Germany
Merck KGaA, Darmstadt, Germany / Carl
Roth GmbH, Karlsruhe, Germany
United States Biochemical Corp
Merck KGaA, Darmstadt, Germany
Sigma-Aldrich®, St. Louis, MO
Merck KGaA, Darmstadt, Germany

Sigma-Aldrich®, St. Louis, MO

Ponceau S	Sigma-Aldrich®, St. Louis, MO
DC Protein Assay solution A	Bio-Rad Laboratories, Inc., Hercules, CA
DC Protein Assay solution B	Bio-Rad Laboratories, Inc., Hercules, CA
RNAse A (20 mg/ml)	Sigma-Aldrich®, St. Louis, MO
SDS	Carl Roth GmbH, Karlsruhe, Germany
Spermine tetrahydrochloride	Sigma-Aldrich®, St. Louis, MO
Sodium acid (NaN ₃)	Sigma-Aldrich®, St. Louis, MO
Sodium orthovanadate	Sigma-Aldrich®, St. Louis, MO
TEMED (Tetramethylethylenediamin)	Carl Roth GmbH, Karlsruhe, Germany
TRIS	AppliChem, Darmstadt, Germany
TWEEN 20	Sigma-Aldrich®, St. Louis, MO
Vybrant assay (Membrane Permeability/ Dead Cell Apoptosis Kit)	Invitrogen Corporation, Carlsbad, CA

3.1.5 Chemotherapeutics

NU1025	Axon Medchem BV Groningen, Netherlands
Camptothecin (CPT)	Sigma-Aldrich®, St. Louis, MO

3.1.6 Technical equipment and softwares

CalcuSyn software (Version 2.0)	Biosoft, Cambridge, UK
Centrifuge 3K30	Sigma-Aldrich®, St. Louis, MO
Centrifuge 5417C	Eppendorf AG, Germany
Chemi-SmartTM 5100	PEQLAB Biotechnology GmbH, Erlangen, Germany
Comet Assay IV	Perceptive Instruments, UK
Confocal Laser Scanning Microscope LSM700	Carl Zeiss GmbH Jena, Germany
Eclipse TE300 inverse microscope	Nikon Corporation, Tokyo
Electroblotting Cell	Bio-Rad Laboratories, Inc., Hercules, CA
Electrophoresis chamber	Invitrogen Corporation, Carlsbad, CA
Electrophoresis comb (10 well / 12 well)	Invitrogen Corporation, Carlsbad, CA
Eppendorf tubes 0.6 ml, 1.5 ml, 2 ml	Eppendorf AG, Germany
Falcons 15 ml, 50 ml (sterile)	Greiner Bio-One GmbH Frickenhausen, Germany
FACScan cytometer	Becton Dickinson, Franklin Lakes, NJ
Gel Cassettes 1.5 mm	Invitrogen Corporation, Carlsbad, CA
GraphPad Prism software	GraphPad Software, Inc., La Jolla, CA
Hybond-P PVDF Membrane	Amersham International, Little Chalfont, Buckinghamshire, England
Nikon EFD-3	Tokyo, Japan
Power supply, PowerPac 200	Bio-Rad Laboratories, Inc., Hercules, CA
Round-bottom tubes 5 ml for flow cytometry	Becton Dickinson, Franklin Lakes, NJ
Sonificator, Sonoplus GM60	Bandelin, Berlin, Germany
Multilabel-Multitask Plate Counter Tecan Photometer (Infinite® M200 PRO)	Tecan, Männedorf, Switzerland

3.1.7 Primary antibodies

antibody	company
Anti-Actin	ICN Biochemicals, Aurora, OH
Caspase-3	DAKO, Glostrup, Denmark
Anti-H2Ax phospho-Serine 139	Cell Signaling Technology Inc., Danvers, MA
Anti-H2Ax	BioLegend, San Diego, CA
Anti MCM-7 Ab-1	Oncogene Science, Cambridge MA
Anti-MDM2	Sigma-Aldrich®, St. Louis, MO
Anti-MRE11 phospho-Serine 676	Cell Signaling Technology Inc., Danvers, MA
Anti-MRE11	Cell Signaling Technology Inc., Danvers, MA
Anti-NPM (B-23)	Santa Cruz Biotechnology, Santa Cruz, CA
Anti-NBS1 phospho-Serine 343	Cell Signaling Technology Inc., Danvers, MA
Anti-NBS1	Cell Signaling Technology Inc., Danvers, MA
Anti-p21waf1/cip1	Cell Signaling Technology Inc., Danvers, MA
Anti-p53 phospho-Serine 15	Cell Signaling Technology Inc., Danvers, MA
Anti-p-53 (DO-1)	BioLegend, San Diego, CA
Anti-PARP [poly(ADP-ribose) polymerase-1]	Santa Cruz Biotechnology, Santa Cruz, CA
Anti-RAD 50	Cell Signaling Technology Inc., Danvers, MA

3.1.8 Secondary antibodies

antibody	company
Anti-rabbit, peroxidase conjugated	Sigma-Aldrich®, St. Louis, MO
Anti-mouse, peroxidase conjugated	Sigma-Aldrich®, St. Louis, MO
Anti-rabbit, Dyelight, Alexa Fluor 488 conjugated	Vector Laboratories, Inc. Burlingame, CA
Anti-mouse, Dyelight, Alexa Fluor 488 conjugated	BioLegend, San Diego, CA

3.1.9 Cell lines

Table 2. Characteristics of breast cancer cell lines data summarised from^{82,83}

Cell line	Medium and culturing conditions	Genotype
BT-20	RPMI + 10% FCS, grown at 37°C and 5 % CO ₂ ; splitting ratio: 1:6 to 1:8	<ul style="list-style-type: none"> • mutated p53 (Lys132Gln) • estrogen receptor negative • BRCA1^{+/+}
SKBr-3	DMEM + 10% FCS, grown at 37°C and 8 % CO ₂ ; splitting ratio: 1:3	<ul style="list-style-type: none"> • mutated p53 (Arg175His) • estrogen receptor negative • overexpression of the HER2/c-erb-2 gene product • BRCA1^{-/-}
T47D	DMEM + 10% FCS, grown at 37°C and 8 % CO ₂ ; splitting ratio: 1:5	<ul style="list-style-type: none"> • mutated p53 (Leu194Phe) • estrogen receptor negative • BRCA1^{+/+}

3.1.10 Drugs

Drug	Stock solution	Dissolved in	Storage
NU 1025	200 mM	DMSO	-20°C
CPT	15 mM	DMSO	-20°C

3.1.11 Cell cultivation

Cells were grown at 37°C and 5% CO₂ (BT-20) and 8% CO₂ (SKBr-3) until they reached about 70% confluence. For further preparation cells were trypsinized and centrifuged at 200 g, 4°C for 3'. resuspended in fresh medium containing 10% FCS. Cells were then either transferred to a 75 cm² Falcon flask for further cultivation (BT-20: splitting ratio 1:6 to 1:8; SKBr-3: splitting ratio 1:3), or counted and seeded (8x10⁴ cells/ml) in Petri dishes or microtiterplates for drug treatment. After a recovery period of 24 h cells were treated with distinct drugs.

3.1.12 Treatment of cells with drugs

Cells were treated with drugs 24 h after seeding at indicated concentrations and periods of time. For further treatment, stock solutions were diluted with appropriate medium for the cell line used, to the required working solutions. The working solutions were then sterile filtered using filters with a pore size of 0.2 µm. After medication cells were incubated for a given period of time at 37°C with a CO₂ amount of either 5% (BT-20) or 8% (SKBr-3).

3.2.Methods

3.2.1 Fixation of cells

Cells were seeded out in PDs of 3.5 cm Ø and treated with the drug of interest for an indicated period of time. Afterwards the medium was discarded and cells were washed three times with 1x PBS-T and either fixed with methanol or paraformaldehyd.

Methanol fixation

This organic fixation method dehydrates cells and leads to precipitation of proteins but also distorts the micro-anatomy of the cell.

Cells were covered with ice- cold (-20°C) 100 % methanol for 30' at -20°C and then washed three times with PBS-T.

Alternatively in some cases cells were fixed with an ice-cold methanol-acetone mixture (1:3) for 30' at -20°C followed by three washing steps with PBS-T.

Paraformaldehyde fixation

Paraformaldehyd fixation cross-links proteins, thereby affecting immunohistochemical stainings.

Cells were covered with 4% paraformaldehyd in 1x PBS for 30' at RT and then washed three times with PBS-T.

3.2.2 Visualisation of nuclei after Hoechst staining

Cells grown in 3.5 cm PDs were treated with the drugs of interest. Medium was removed, the attached cells were carefully washed twice with 1x PBS and then fixed with paraformaldehyde for 30' at RT. After three washing steps with 1x PBS-T cells were stained with 2 ml of the Hoechst dye ($c_E = 2 \mu\text{g/ml}$) for 30' in the dark at 4°C. Then cells were washed three times with ddH₂O, air dried and inspected under the fluorescence microscope (Eclipse TE300 inverted microscope, Nikon Corporation, Tokyo, Japan).

3.2.3 Visualisation of nuclei after DAPI staining

2 µl of the stock solution were diluted 1:100 in PBS in a following dilution step this solution was diluted 1:50 in DAKO® Fluorescent Mounting Medium (DAKO AS, Glostrup, Denmark). 15-20 µl were then placed in the middle of the sample and covered with a clean cover slip.

3.2.4 Detection of apoptotic cells *in situ* using the M30 CytoDeath antibody

Blocking-solution (3% BSA in PBS-T):

1.2 g BSA in 40 ml TBS-Tween-20 solution

Stored at +4°C

Solution for antibody dilution (1% BSA in 1xPBS + 0.1% NaN₃):

0.5 g BSA in 50 ml PBS Tween-20 solution, 0.1% NaN₃

Stored at +4°C

0.2 % Triton X-100ml:

200 µl Triton X 100 in 99.8 ml ddH₂O

Stored at RT

M30 CytoDEATH fluoresceine-coupled antibody (Roche Applied Science)

Diluted in 1 % BSA in 1xPBS+ 0.1% NaN₃

Stored at +4°C in the dark

In already early events of apoptosis, cytokeratin 18 was reported to be cleaved by activated caspase-3, recognising a special tetrapeptide motif. Monoclonal M30 CytoDEATH antibody was designed to detect only cytokeratin 18 cleaved by caspase-3. In its intact form the antigen is not recognized by the M30 CytoDEATH antibody resulting in no fluorescence signal. The M30 CytoDEATH antibody is a tool to determine events of apoptosis in single cells and tissue sections.

Cells were seeded out in 3.5 cm PD's and treated with the drug of interest. After an indicated period of time the medium was removed and the still to the PD attached cells were washed three times with 1x PBS-T and immediately fixed in ice-cold methanol for 30' at -20°C. After fixation, methanol was discarded and cells were again washed three times with PBS-T. For permeabilisation cells were covered with 0.2 % Triton X-100 for another 20' at RT. For further preparation the cells were again washed twice with PBS-T. To avoid unspecific antibody binding, cells were blocked with 3 % BSA in PBS for 1 h and washed twice with PBS-T before the M30 CytoDEATH fluorescein antibody was added. Cells were incubated with the fluorescein-conjugated antibody, diluted 1:300 in PBS containing 1 % BSA for at least 1 h at RT. After incubation the antibody was removed, cells were washed twice with PBS-T and air-dried over night. The dried preparations were additionally stained with DAPI (Sigma-Aldrich®, St. Louis, MO) in mounting medium to visualize chromatin structure in all cells. Unlike normal interphase cells, apoptotic cells show condensed and/or fragmented chromatin and thereby strongly accumulate the dye resulting in bright fluorescence.

3.2.5 Determination of numbers of living cells

Proliferation of cells and their sensitivity to various drugs in context to increasing treatment concentrations was determined by the CellTiter-Glo[®] assay. The CellTiter-Glo[®] assay detects the numbers of viable cells by measuring their amount of cellular ATP that is produced in metabolically active cells. The ATP concentration directly correlates with the numbers of viable cells. Luminescence signals were measured using a multilabel-multitask plate counter Tecan Photometer (Infinite[®] M200 PRO).

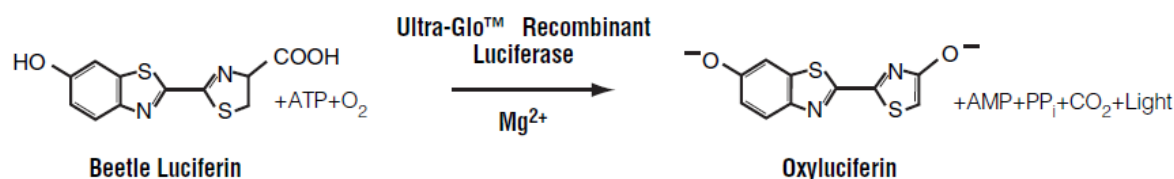


Figure 23. The luciferase reaction (picture reproduced from the Promega manufacturers protocol^[84])

CellTiterGlo[®] assay kit (Promega):

CellTiterGlo[®] Buffer

CellTiterGlo[®] Substrate

Stored at -20°C

Multilabel-Multitask Plate Counter (Tecan Photometer (Infinite[®] M200 PRO))

Cells were grown in 96-wells microtiter plates (5x10⁴) and treated with the drug of interest. The microtiter plates were centrifuged for 3' at 200 g at 4°C to make sure cells are attached to the bottom of the plate. The supernatant was reduced to 50 µl in each well an equal amount of the assay buffer+ substrate was added to each well. The cells were then incubated at 37°C for 30'. Next step was the transfer of the cell suspension to a white microtiter plate for further measurement. Measurement was performed using the Multilabel-Multitask Plate Counter (Tecan Photometer (Infinite[®] M200 PRO)).

3.2.6 Determination of Caspase-3/7 Activity

Caspase-Glo[®] 3/7 Assay kit(Promega):

Caspase-Glo[®] 3/7 Buffer

Caspase-Glo[®] 3/7 Substrate (lyophilized)

Stored at -20°C

The principle of Caspase-Glo[®] Assays provides a proluminescent caspase-3/7 DEVD-aminoluciferin substrate, which contains the tetrapeptide sequence DEVD. Following caspase cleavage, a substrate for luciferase (aminoluciferin) is released, resulting in the

luciferase reaction and the generation of light. Luminescence is directly proportional to the amount of the activated caspases.

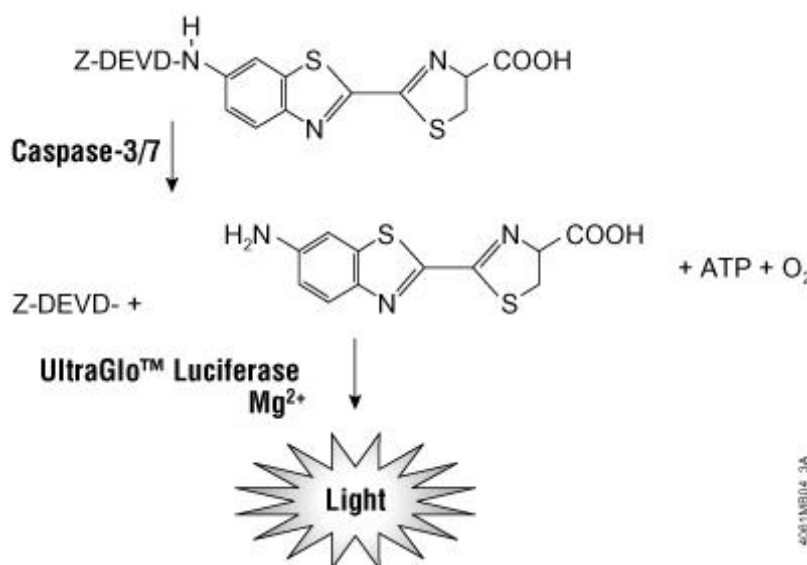


Figure 24. The luciferase reaction to determine caspases 3/7 activity (picture reproduced from the Promega manufacturers protocol^[184])

Cells were grown in 96-wells microtiter plates (5×10^4) and treated with the drug of interest. The microtiter plates were centrifuged for 3' at 200 g at 4°C to make sure cells are attached to the bottom of the plate. The supernatant was reduced to 50 μ l in each well an equal amount of the assay buffer+ substrate was added to each well. Either caspase levels in the cells or in the supernatant were measured. The cells were then incubated at 37°C for different periods of time to assess the best signal-to-background ratio. Next step was the transfer of the cell suspension to a white microtiter plate for further measurement. Measurement was performed using the Multilabel-Multitask Plate Counter (Tecan Photometer (Infinite® M200 PRO)).

3.2.7 Measurement of the DNA content in single cells using flow cytometry

Staining single cells with propidium iodide, gives us the opportunity to determine in which phase of the cell cycle cells reside. Harvested cells get permeabilized by a limited proteolysis (a short incubation with trypsin): this reaction was stopped by adding chicken egg white. To avoid propidium iodide binding to RNA, it was destroyed by incubation with RNase. Propidium iodide enters the permeabilized cells and intercalates into the DNA strands. When bound to DNA, propidium iodide has a fluorescence excitation maximum of 535 nm and an emission maximum of 617 nm. DNA content of cells can then be determined using flow cytometry.

For measuring the DNA content, cells were seeded out in 6 cm PDs (8×10^4 cells/ml; 4 ml per PD). After treatment cells were harvested by trypsinisation. Trypsinisation occurred in the incubator (5% or 8% CO₂ depending on the cell line) until the adherent cells had come off.

The process was stopped by adding the same volume medium to the cells as trypsin was used. The cell suspension was then transferred to a falcon tube and centrifuged. The originated cell pellet was washed three times with ice-cold 1xPBS. All centrifugation steps occurred at 900 g for 3' at 4°C. After the last washing and centrifugation step the supernatant was discharged and the pellet was resuspended in 100 µl ice-cold 1xPBS and transferred into a FACS tube. The suspension was then incubated for 10' with 75 µl of Solution A at RT, followed by 10' incubation with 63.5 µl of Solution B at RT. The last incubation step with 63.5 µl Solution C lasted 30' and was done at 4°C under dark conditions. The cells were then ready for measurement by a FACScan cytometer (Becton Dickinson). DNA concentration was evaluated using ModFit LT™ software (Verity Software House, Topsham, ME) DNA histograms were generated by CellQuest software.

3.2.8 Determination of DNA damage by single-cell gel electrophoresis (SCGE)

To detect ds DNA breaks as a result of treatment with cytotoxic agents, a single cell gel electrophoresis (SCGE) also known as Comet assay was performed.

Samples of interest are embedded in low-melting-point agarose on a microscope slide. Cells are lysed using a lysis solution that contains a detergent and a highly concentrated aqueous salt to destroy cellular membranes and disrupt their proteins and RNA. After washing the cells to remove the salt, an electric field is applied. The small fragments generated as a result of cell damage are able to migrate due to their negative charge to the positively charged anode, forming the characteristic comet tails. After DNA staining the comets are inspected under a fluorescence microscope. The intensity of the comet tail gives information about the amount of DNA breaks.

Cells were seeded out in 10 cm PD's (12×10^4 cells/ ml; 8 ml per PD). After treatment with the drugs of interest and an appropriate incubation time cells were harvested in PBS.

Cell viability was determined using the Trypan blue exclusion test, vitality was more than 80% in all tested samples.

For each treatment 150 cells were analysed for Comet formation. Cells in suspension (1×10^5 cells) were embedded in low-melting-point agarose (0.5% LMA) and transferred to agarose coated slides (1.5% NMA). Cells were soaked in a lysis solution (1% Triton X-100, 10% DMSO, 2.5 M NaCl, 100 mM EDTA, 10 mM Trizma base) and lysed at a pH value of 10.0. After electrophoresis (30', 300 mA, 1.0 V/1 cm corresponding to 25V, at 4°C, pH > 13), gels were stained with ethidium bromide (20 µg/ml).

Slides were inspected under a fluorescence microscope (Nikon EFD-3, Tokyo, Japan), computer analysis of Comet tail intensity was done using a computer-aided Comet assay image analysis system (Comet Assay IV, Perceptive Instruments, UK).

3.2.9 Preparation of whole cell extracts (WCLs)

RIPA Lyses Buffer (modified):

50 mM TRIS/ HCl (pH 7.4)

500 mM NaCl

1 % (v/v) NP- 40 (Sigma-Aldrich®, St. Louis, MO)

0.5 % (w/v) Na-Doc

0.2 % (w/v) SDS

0.05 % (v/v) NaN₃

Stored at +4°C

1 x SDS Buffer:

1 g SDS

5 mg EDTA

10 mg NaN₃

5 ml stock buffer (6.006 g TRIS, 0.4 g SDS, 0.01 g NaN₃ in 100 ml ddH₂O, pH 6.8)

Stored at RT

Solutions added immediately before use:

1 mM phenylmethylsulfonyl fluoride (PMSF), stored at +4°C,

(added 1:100 to lysis buffer; C_E=10 µM)

50 µM Pefabloc, stored at RT (added 5:100 to lysis buffer; C_E=2.5µM)

200 mM sodium fluoride (NaF), stored at -20°C, (added 1:1000 to lysis buffer; C_E=200µM)

200 mM sodium orthovanadate (Na₃VO₄), solution, stored at -20°C, (added 1:1000 to lysis buffer; C_E=200µM)

Cells were seeded out in 10 cm PD's (12x10⁴ cells/ml; 8 ml per PD) and harvested by scraping followed by two washing steps with ice-cold 1xPBS and centrifugation for 5' with 900 g at 4°C. Lysis was done either with RIPA lysis buffer or SDS-non-stained/non-reduced sample buffer using 5-fold volumes of the cellular pellet. After 30' on ice, the lysates were sonicated (Sonoplus GM60, Bandelin), three times for 10'', and centrifugated (Sigma 3K30) at 1500 g for 3' at +4°C. This step was necessary to clear the cell extracts from cell debris. The whole cell lysates were stored at -20°C until use.

3.2.10 Determination of protein concentration

DC Protein Assay (Bio-Rad Laboratories, Inc., Hercules, CA):

Reagent A (alkalic Copper Tartat solution), stored at RT

Reagent B (Folin Reagent), stored at RT

Determination of protein concentration was done using the Bio-Rad DC Protein Assay following the manufacturer's instructions. The DC protein assay is based on a chemical reaction of proteins with alkine copper ttrate solution and Folin reagent resulting in blue colour development^{85,86}. Absorption was measured at 700 nm with the Tecan Photometer (Infinite® M200 PRO), a multilabel, multitask plate counter using a BSA standard calibration curve.

3.2.11 Separation of proteins by SDS-polyacrylamide gel electrophoresis

Gels were cast using 8, 10, 12 or 15 wells Novex cassettes generating 1.5 mm thick slab gels. Preparation of resolving and stacking gel was done as described in Table 3.

Table 3. Composition of the resolving and stacking gels

Resolving gel					Stacking gel	
Agents	8%	10%	12%	15%	Agents	
30 % Acrylamide	2300 µl	2900 µl	3480 µl	4350 µl	30 % Acrylamide	320 µl
2M TRIS/HCL pH 8.7	1650 µl	1650 µl	1650 µl	1650 µl	1M TRIS/HCL pH 6.8	300 µl
SDS 20 %	44 µl	44 µl	44 µl	44 µl	SDS 20 %	12 µl
APS 10 %	39.6 µl	39.6 µl	39.6 µl	39.6 µl	APS 10 %	12 µl
TEMED	6.6 µl	6.6 µl	6.6 µl	6.6 µl	TEMED	2.4 µl
ddH ₂ O	4759.8 µl	4160 µl	3579.8 µl	2710 µl	ddH ₂ O	1753.6 µl
Total	8.8 ml	8.8 ml	8.8 ml	8.8 ml	Total	2.4 ml

For further preparation of the samples 30 µg dissolved protein was mixed with equal volume of 2x SDS sample buffer, filled up to a final volume of 15-20 µl with 1x SDS buffer. The samples were boiled at 95°C for 3' and after denaturation placed on ice for 3', followed by a final centrifugation step at 1300 g for 3' (Centrifuge 5417C, Eppendorf AG, Germany). Samples were loaded on the gel and separation occurred in 1x electrophoresis buffer for 90' at 126 V.

3.2.12 Transfer of separated proteins on the PVDF membrane by electroblotting

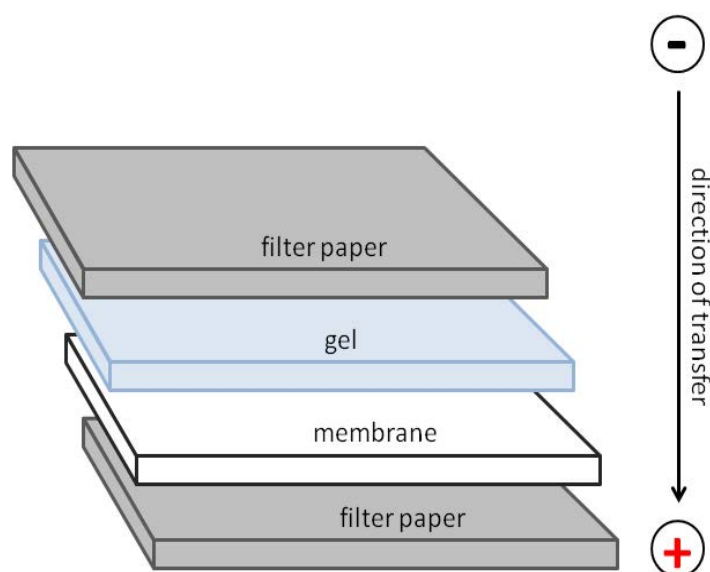


Figure 25. Assembly of the transblot Western sandwich

The transblot Western sandwich was assembled according to the scheme in Figure 25, starting from anode site: sponge, one Whatman paper sheet (soaked in 1x blotting buffer), gel, membrane (Hybond PVDF, Amersham International, Little Chalfont, Buckinghamshire, England) which was previously activated in MeOH and rinsed with 1x blotting buffer), again one Whatman paper sheet and finally a second sponge to complete the sandwich.

Blotting was done using a Bio-Rad Trans-blot Cell in 1x blotting buffer overnight at +4°C applying a constant voltage of 30 V.

3.2.13 Detection of proteins on the PVDF membrane by Ponceau S staining

Ponceau S working solution:

0.1 % (w/v) Ponceau S

5 % (v/v) Acetic acid

Stored at RT

To confirm an equal protein loading as well as the quality of protein transfer the PVDF membrane was stained with Ponceau S. After disassembly of the transblot sandwich the membrane was activated in methanol for 30'' and then incubated in Ponceau S working solution for approximately 10' on an orbital shaker at RT. Excess dye was removed from the membrane by washing in water and 1x TBS-T.

3.2.14 Immunoblotting

Solution for antibody dilution:

1.2 g BSA in 40 ml TBS Tween- solution, stored at +4°C

0.1% NaN₃ (used only by primary antibodies)

To avoid unspecific binding of antibodies, the membrane was blocked in 3% BSA in TBS-T for 1 h. After blocking, the membrane was washed for 10' in TBS-T and incubated with the primary antibody in adequate dilution over night at 4°C or at least 4 h at RT on an orbital shaker. Primary antibodies were diluted usually (1:1000) in 3% BSA in TBS-T. Non-bound primary antibodies were removed by washing the membrane three times for 10' with TBS-T at RT. After the washing steps the membrane was incubated with the secondary antibody for at least 1 h at RT. Secondary antibodies were labelled with a horseradish peroxidase (HRP) to detect immune complexes. Excess secondary antibodies were removed by washing three times for 10' with TBS-T on an orbital shaker at RT.

Detection of the HRP linked secondary antibodies was performed using the ECL+ or the ECL select detection kit (Amersham). We followed the manufacturer's recommendations.

The signal was detected using a ChemiSmart5100 apparatus (PEQLAB, Biotechnologie GmbH, Erlangen, Germany).

3.2.15 Stripping of membranes for reprobing

Stripping buffer:

100 mM DTT

2 % SDS

62.5 mM TRIS- HCl (pH 6.7)

Stored at +4°C

The membrane was activated with MeOH, submerged in stripping buffer and incubated at 50°C for 30' with occasional agitation.

Afterwards the membrane was washed 2 times for 10' with TBS-T at RT. After blocking the membrane again in 3 % BSA in TBS-T it was ready for reprobing with new primary antibodies.

3.2.16 Statistical analysis

Statistical analyses were performed using GraphPad Prism 5 Software (GraphPad Inc., La Jolla, CA). Analysis was done using One-way ANOVA with Bonferroni's multiple comparison tests. A P-value 5% to 1% is considered statistically significant (*), 1% to 0.1% statistically very significant (**), and <0.1% statistically extremely significant (***). Before analysis data was proved for normal distribution, and if necessary, logarithmized.

3.2.17 Multiple drug doses-effect calculations using CalcuSyn

For analysing combined drug effects on different cells, the CalcuSyn 2.0 (Version 2.0, Biosoft, Cambridge, UK) software was used.

This software calculates the combination index (CI) of treatments according to the method of Chou and Talalay and provides an evaluation of the kind of interaction between two treatments⁸⁷. Specifically, the analysis gives an indication whether two drugs show antagonistic, synergistic or additive effects. For calculating the CI value, potency [median dose (Dm) or IC₅₀] and the shape of the curve are necessary to determine multiple dose effects. Both tested agents should have a dose effect; otherwise the CI value cannot be calculated. Data of single and combined treatments obtained from repeated cell viability assays were used. The suggested interpretation of CI values is listed in Table 4.

Table 4. Description of CI values.

CI value	Interpretation
<0.1	Very strong synergism
0.1 – 0.3	Strong synergism
0.3 – 0.9	Synergism
0.9 – 1.1	Nearly additive
1.1 – 3.3	Antagonism
3.3 – 10	Strong antagonism
>10	Very strong antagonism

4. Results

4.1. Effect of TOPO1 inhibition on the number of living human breast cancer cells

Experiments were performed using three different human breast cancer cell lines: BT-20, SKBr-3 and T47D cells. BT-20 and SKBr-3 cells both are estrogen receptor negative and have a mutated p53, SKBr-3 cells additionally show an increased expression of the *HER2/c-erb-2* gene product. T47D cells also carry a mutation in the *TP53* gene, but contrary to BT-20 and SKBr-3, this cell line is estrogen receptor positive. We first compared the immediate and long-lasting effects of the TOPO1 inhibitor CPT on the number of living cells. For this purpose the CellTiterGLO viability assay was used.

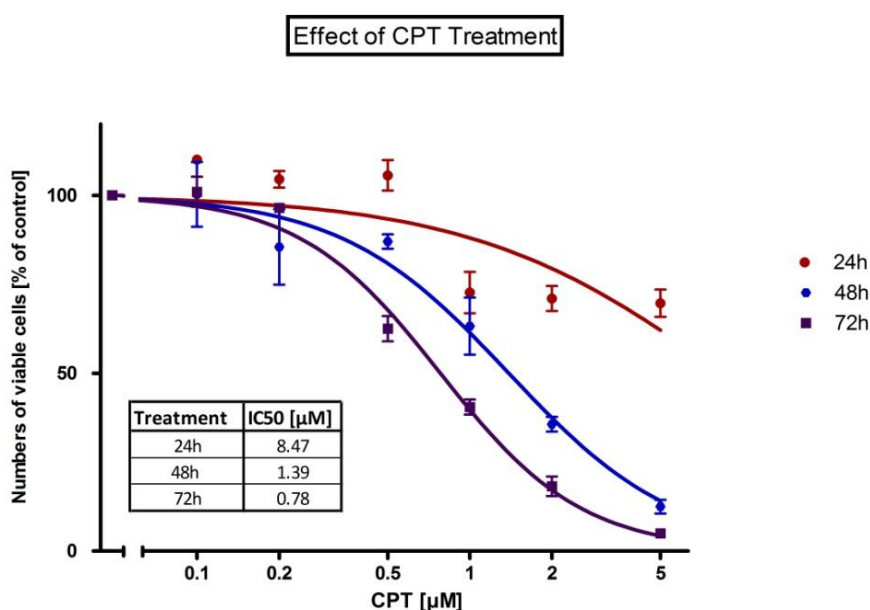


Figure 26. Reduction of numbers of viable cells after TOPO1 inhibition in BT-20 cells

Cells plated in 96-wells microtiter plates were treated for 24 h, 48 h and 72 h with CPT at indicated concentrations. The number of viable cells was measured immediately after the treatment using the CellTiterGLO viability assay. The data represent the mean \pm SD from at least three independent experiments, each performed in quadruplicates. The statistical analysis was performed with GraphPad Prism software.

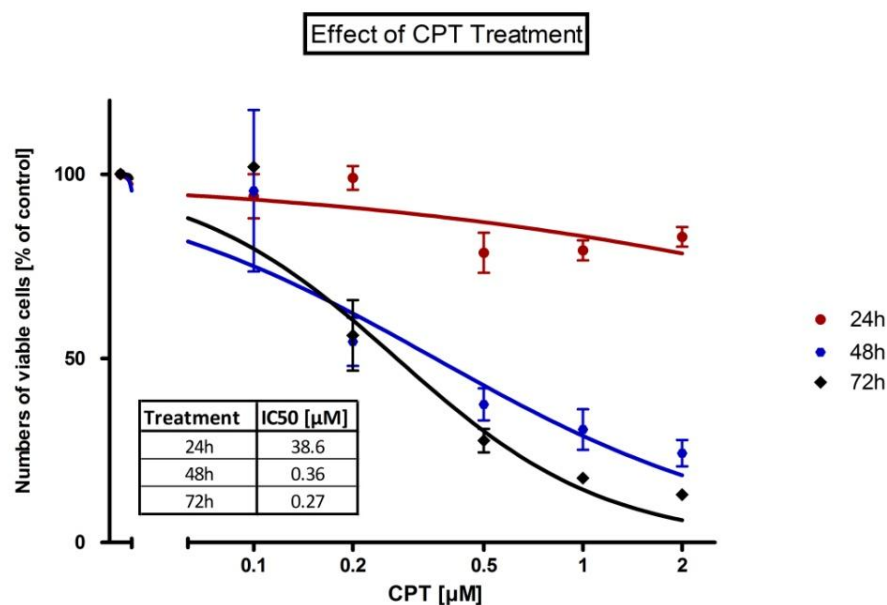


Figure 27. Reduction of numbers of viable cells after TOPO1 inhibition in SKBr-3 cells

Cells plated in 96-wells microtiter plates were treated for 24 h, 48 h and 72 h with CPT at indicated concentrations. The number of *viable* cells was measured immediately after the treatment using the CellTiterGLO viability assay. The data represent the mean \pm SD from at least three independent experiments, each performed in quadruplicates. The statistical analysis was performed with GraphPad Prism software.

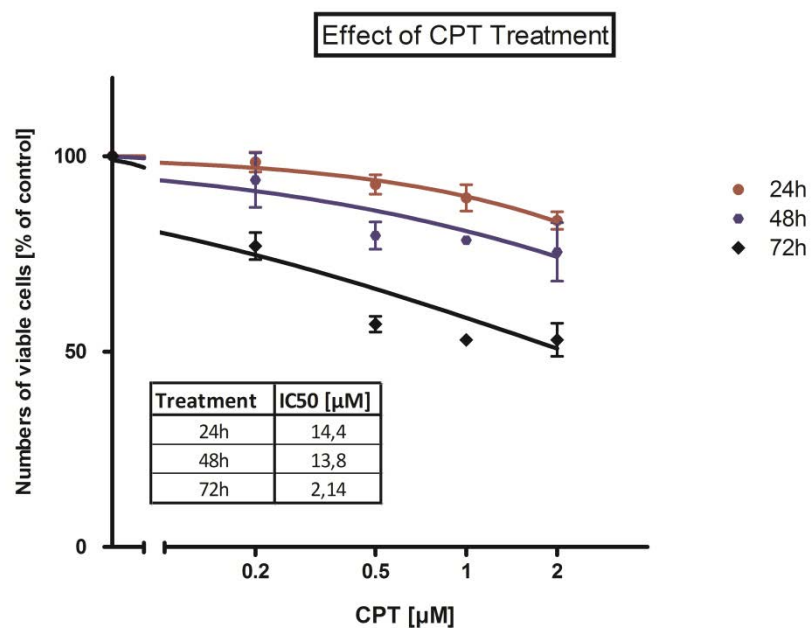


Figure 28. Reduction of numbers of viable cells after TOPO1 inhibition in T47D cells

Cells plated in 96-wells microtiter plates were treated for 24 h, 48 h and 72 h with CPT at indicated concentrations. The number of *viable* cells was measured immediately after the treatment using the CellTiterGLO viability assay. The data represent the mean \pm SD from at least three independent experiments, each performed in quadruplicates. The statistical analysis was performed with GraphPad Prism software.

Table 5. Effect of CPT treatment on the number of living breast cancer cells

The IC₅₀ values calculated for all cell lines were compared and for a better overview summarized in a table.

Cell line	IC ₅₀ [μM] duration of treatment		
	24 h	48 h	72 h
BT-20	8.47	1.39	0.78
SKBr-3	38.6	0.36	0.27
T47D	14.4	13.8	2.14

Both, BT-20 and SKBr-3 are estrogen receptor-negative breast cancer cells whereas T47D cells are estrogen receptor-positive. All three cell lines have a mutation in the *TP53* gene. Unlike SKBr-3 cells, BT-20 and T47D cells express the *BRCA1* gene. The comparison of the IC₅₀ values between BT-20, SKBr-3 and T47D cells showed that the anti-proliferative effect of TOPO1 inhibitor CPT after a short treatment (24 h) was much weaker in SKBr-3 than in BT-20. However after long-term treatment the viability of SKBr-3 cells markedly decreased and IC₅₀ values were within the same magnitude as in BT-20 cells. Both cell lines displayed a continuous reduction in cell viability after 48 h and 72 h. The T47D breast cancer cells were the most resistant cell line towards TOPO1 inhibition. Although they showed higher sensitivity compared to SKBr-3 cells after 24 h treatment, this anti-proliferative effect did not increase markedly after 48 h. After 72 h the T47D cell line showed a 6.7 fold decrease in cell viability, however this effect was less pronounced compared to the other two tested breast cancer cell lines. In SKBr-3 the decrease after 48 h was much greater than in BT-20. SKBr-3 showed a 107.2 fold reduction of cell viability after 48 h whereas the amount of reduction in BT-20 was “only” 6.1 fold.

4.2. Impact of the inhibition of PARP-1 activity in breast cancer cells

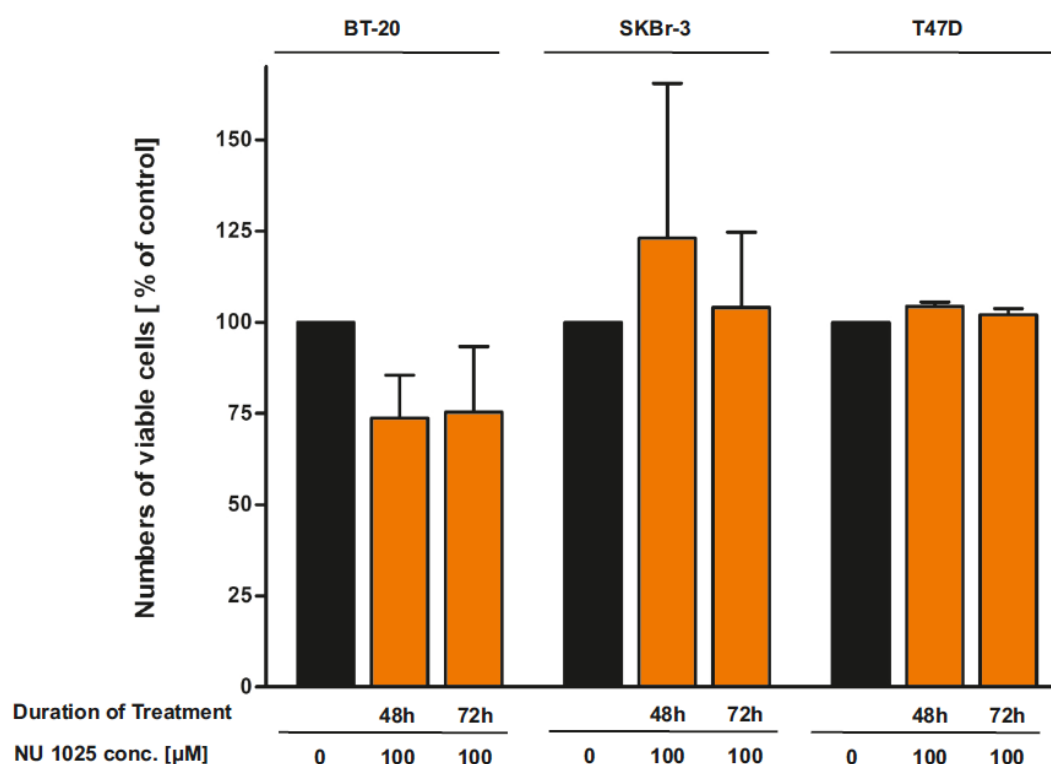


Figure 29. Effects of PARP-1 inhibition on cell viability in different breast cancer cell lines

Cells plated in 96-wells microtiter plates were treated for 48 h and 72 h with PARP-1 inhibitor NU1025 at a final concentration of 100 μ M. The number of *viable* cells was measured immediately after the treatment using the CellTiterGLO viability assay. The data represent the mean \pm SD from at least three independent experiments, each performed in quadruplicates. The statistical analysis was performed with GraphPad Prism software.

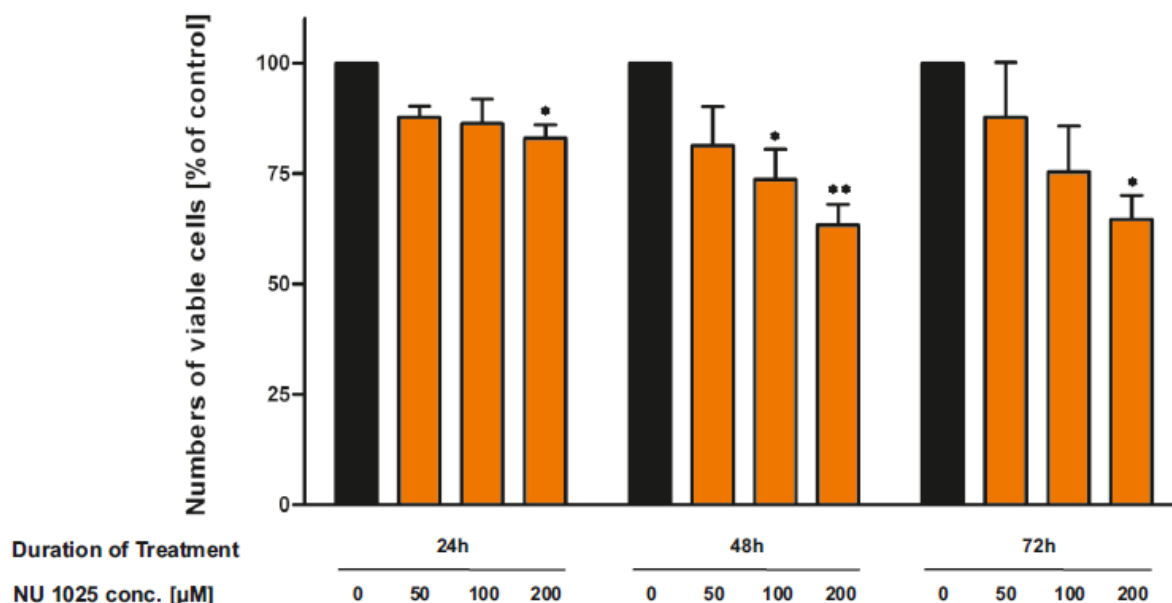


Figure 30. Inhibition of PARP-1 activity affects cell viability in BT-20 cells in a time- and dose-dependent manner

Cells plated in 96-wells microtiter plates were treated for 24 h, 48 h and 72 h with PARP-1 inhibitor NU1025 at indicated concentrations. The number of viable cells was measured immediately at the appropriate time using the CellTiterGLO viability assay. The data represent the mean \pm SD from at least three independent experiments, each performed in quadruplicates. The statistical analysis was performed with GraphPad Prism software using One-way ANOVA and Dunnett's multiple comparison test.

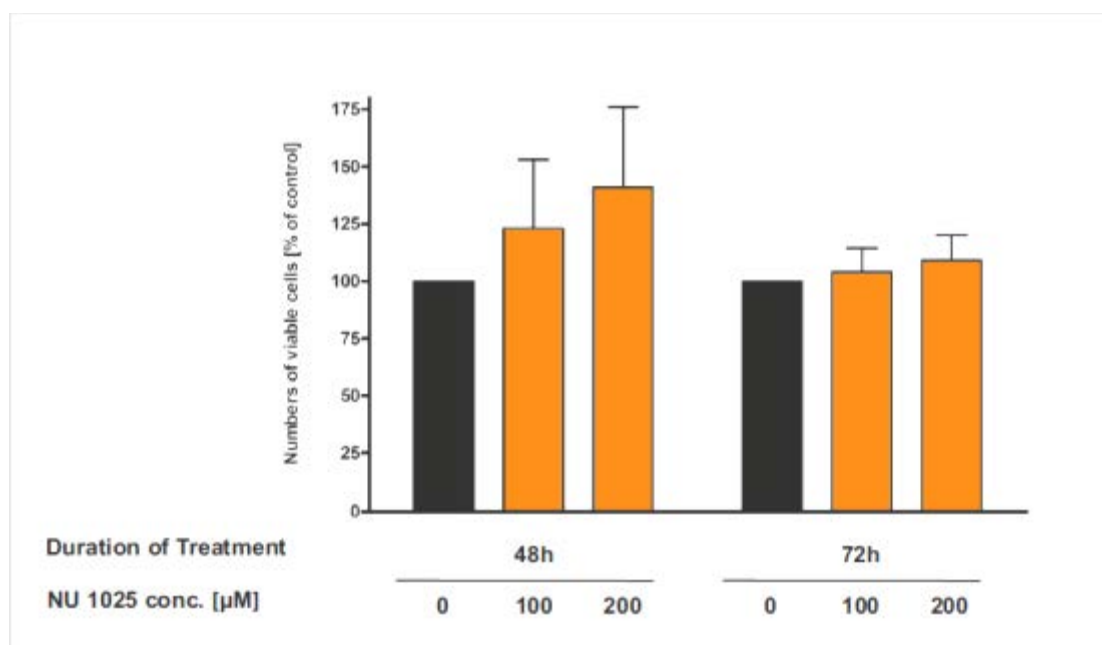


Figure 31. Effects of PARP-1 inhibition on the number of viable cells in SKBr-3 breast cancer cells

Cells plated in 96-wells microtiter plates were treated for 48 h and 72 h with PARP-1 inhibitor NU1025. The number of viable cells was measured immediately at the appropriate time using the CellTiterGLO viability assay. The data represent the mean \pm SD from at least three independent experiments, each performed in quadruplicates. The statistical analysis was performed with GraphPad Prism software using One-way ANOVA and Dunnett's multiple comparison test.

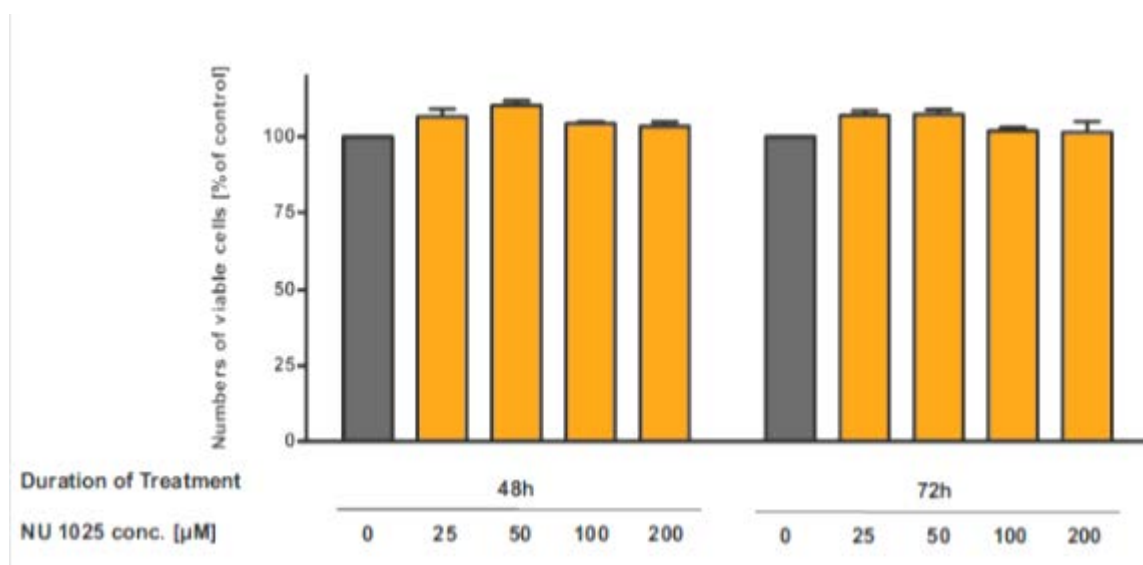


Figure 32. Effects of PARP-1 inhibition on the number of viable cells in T47D breast cancer cells

Cells plated in 96-wells microtiter plates were treated for 48 h and 72 h with PARP-1 inhibitor NU1025 at concentrations as indicated. The number of *viable* cells was measured immediately at the appropriate time using the CellTiterGLO *viability* assay. The data represent the mean \pm SD from at least three independent experiments, each performed in quadruplicates. The statistical analysis was performed with GraphPad Prism software using One-way ANOVA and Dunnett's multiple comparison test.

Figure 30, Figure 31 and Figure 32 show the effects of the pharmacological interference with the activity of PARP-1 on the number of viable cells in three different breast cancer cell lines. As shown in Figure 30 inhibition of PARP-1 activity in BT-20 cells significantly decreased the number of *viable* cells compared to the untreated controls. The cytotoxic effect was time- and concentration-dependent. The strongest reduction of the number of *viable* cells occurred after treatment of BT-20 cells with NU1025 at a final concentration of 200 μ M for 48 h. Extension of the treatment for the next 24 h did not decrease the number of living cells. In contrast to these findings, inhibition of PARP-1 activity in SKBr-3 as well as in T47D cells neither affected the rate of cell proliferation nor the cell *viability*. These results are concordant with previous results from the group published recently by Węsierska-Gądek, J. *et al.*(2012)⁵⁶.

4.3. Inhibition of PARP-1 potentiates the anti-proliferative action of CPT in BT-20 cells

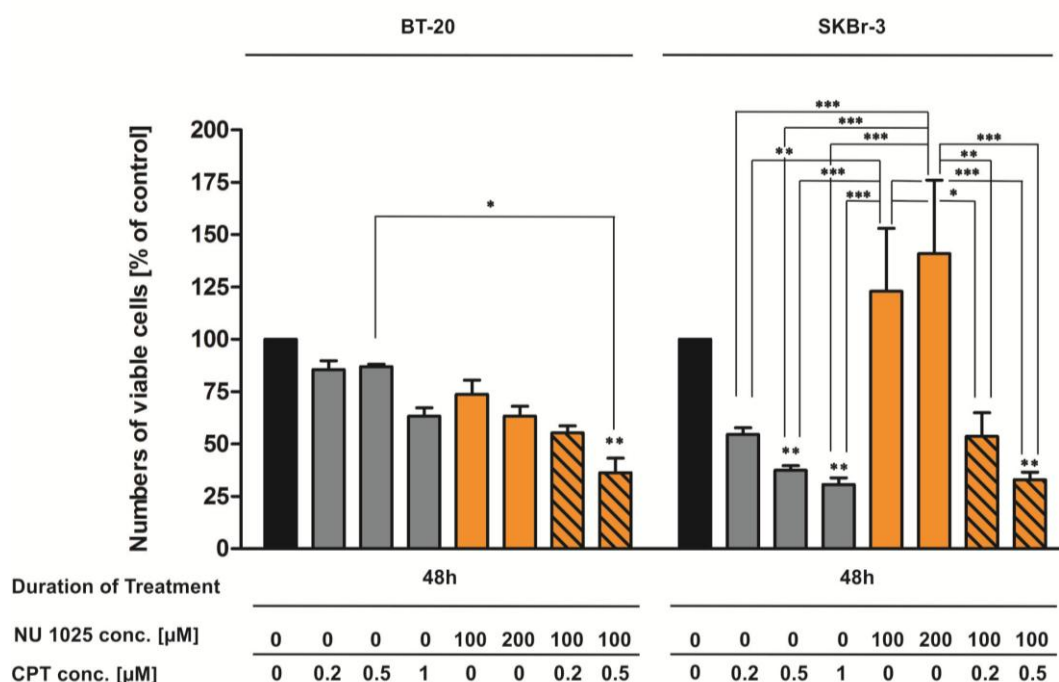


Figure 33. Inhibition of PARP-1 reduces numbers of viable BT-20 cells and potentiates the anti-proliferative action of CPT (48 h)

Cells plated in 96-wells microtiter plates were treated for 48 h with TOPO1 inhibitor CPT and PARP-1 inhibitor NU1025 alone or their combinations at indicated concentrations. The number of viable cells was measured immediately at the appropriate time using the CellTiterGLO viability assay. The data represent the mean \pm SD from at least three independent experiments, each performed in quadruplicates. The statistical analysis was performed with GraphPad Prism software using One-way ANOVA and Bonferroni's multiple comparison test.

Single treatment with CPT at final concentrations up to 1 μ M or with NU1025 at a final concentration of 100 μ M for 48 h did not considerably reduced the number of viable BT-20 cells compared to the controls. However, after exposure of BT-20 to a combination of both agents the number of viable BT-20 cells markedly decreased indicating that the interference with the activity of PARP-1 enhanced the anti-proliferative action of CPT Figure 33. Compared to the controls, the numbers of living cells after the combined treatment was highly significantly reduced. A substantial reduction of cell viability was also observed upon double medication compared to single medication with CPT. These results clearly show an amplifying effect of PARP inhibition in conjunction with CPT and substantiate the relevance of the functional status of PARP-1 to the cytotoxicity of the inhibitors of topoisomerase I e.g. CPT.

A quite different effect was observed in SKBr-3 cells. In compliance with our previous results this cell line was completely insensitive to PARP-1 inhibition⁵⁶. After single medication with PARP-1 inhibitor NU1025 for 48 h the number of living cells even slightly increased (Figure 33). Moreover, SKBr-3 cells were much more sensitive to the inhibition of TOPO1 than BT-20

cells. Single medication with CPT already reduced significantly the number of living cells compared to the controls. The combined therapy also showed a highly significant reduction in cell viability, but it became apparent that PARP-1 inhibitor NU1025 did not enhance the cytotoxic effect of CPT on SKBr-3 cells (Figure 33).

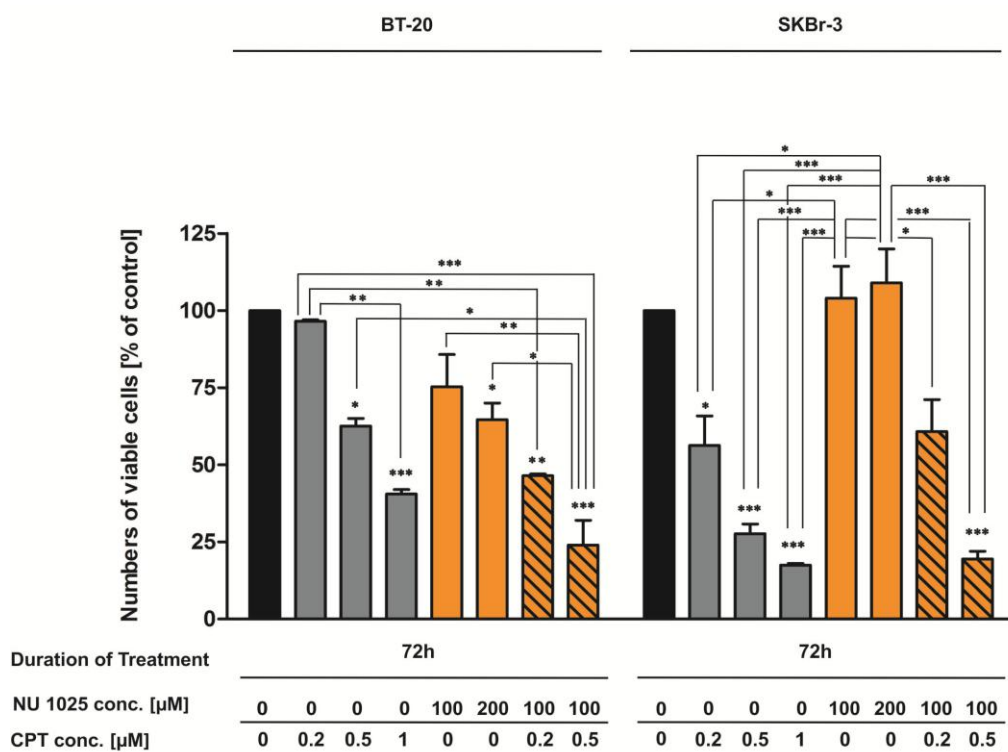


Figure 34. Inhibition of PARP-1 reduces numbers of viable and potentiates anti-proliferative action of CPT exclusively in BT-20 cells (72 h)

Cells plated in 96-wells microtiter plates were treated for 72 h with TOPO1 inhibitor CPT and PARP-1 inhibitor NU1025 at indicated concentrations. The number of viable cells was measured immediately at the appropriate time using the CellTiterGLO viability assay. The data represent the mean \pm SD from at least three independent experiments, each performed in quadruplicates. The statistical analysis was performed with GraphPad Prism software using One-way ANOVA and Bonferroni's multiple comparison test.

After 72 h treatment of BT-20 cells with CPT or NU1025 alone a significant decrease in numbers of *viable* cells was observed. The already after 48 h detected effect of NU1025 cytotoxic enhancing cytotoxicity of CPT was also observed after 72 h. As shown in Figure 34, combined treatment at lower doses of CPT significantly reduced cells' *viability* compared to the controls but also compared to single treatment with CPT.

Unlike BT-20 cells, SKBr-3 cells remained insensitive to the inhibition of PARP-1 activity. The combining of the pharmacologic PARP-1 inhibitor with CPT did not sensitize SKBr-3 cells. These results indicate that the interference with PARP-1 activity is successful in BT-20 cells for two reasons: their relative low sensitivity to CPT and high susceptibility to the inhibition of PARP-1.

4.4. Interference with the PARP-1 activity potentiates the distribution changes in the cell cycle phases of BT-20 cells

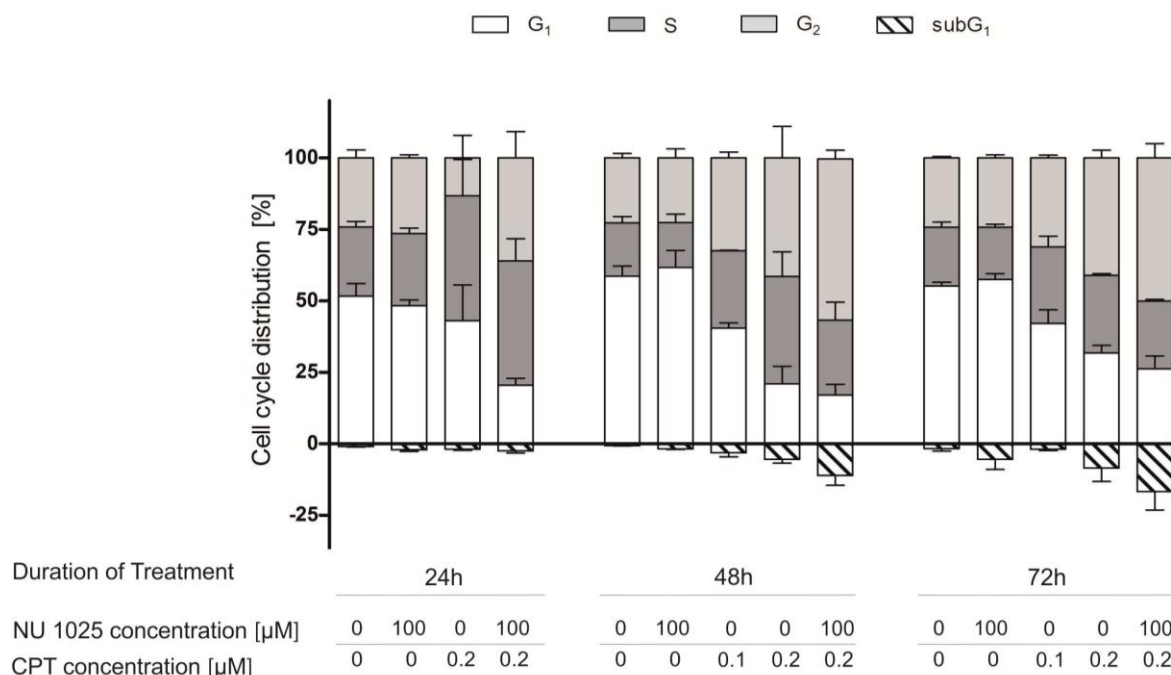


Figure 35. PARP-1 inhibition induces apoptosis in CPT-treated BT-20 cells arrested in G₂/M phase

BT-20 cells were treated for 24 h, 48 h and 72 h with CPT and NU1025 at indicated concentrations. Cells were harvested and stained with propidium iodide. DNA concentrations were determined using ModFit LT™ software (Verity Software House, Topsham, ME).

Inhibition of PARP-1 had no effect on the distribution of BT-20 cells in the cell cycle phases (Figure 35). However, interference with the TOPO1 activity strongly affected the cell cycle progression of BT-20 cells. As shown in Figure 35 TOPO1 inhibitor CPT increased the fraction of BT-20 cells in S-phase after treatment for 24 h. Long-term treatment (48 h and 72 h) with CPT led to G₂ arrest associated with the reduction of G₁-phase cells. Furthermore, after combined treatment the rate of hypoploid cells increased, indicating that simultaneous interference with PARP-1 and TOPO1 activity promotes induction of apoptosis.

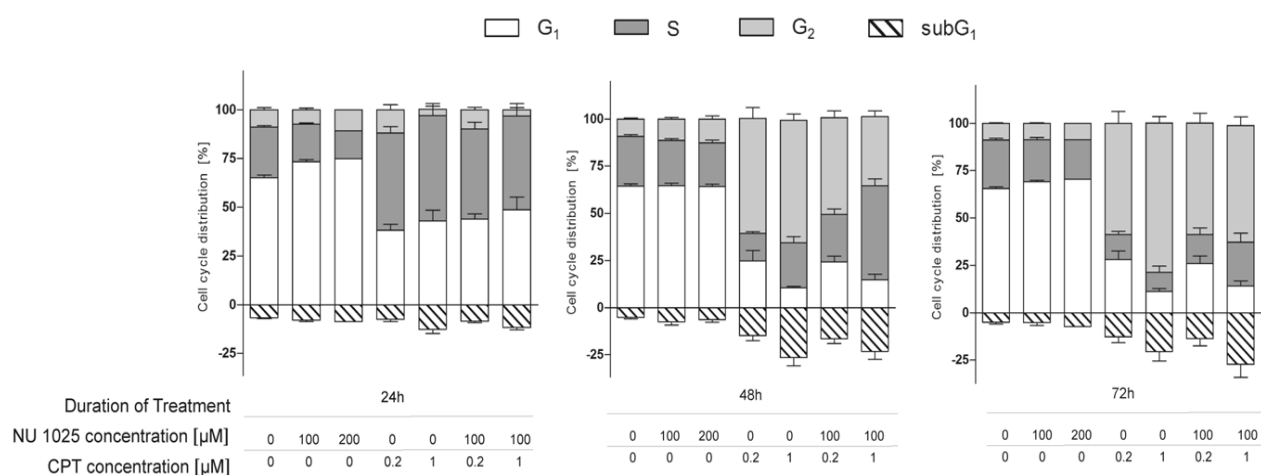


Figure 36. PARP-1 inhibitor has a weak or no effect on cell cycle distribution in CPT treated SKBr-3 cells

SKBr-3 cells were treated for 24 h, 48 h and 72 h with CPT and NU1025 at indicated concentrations. Cells were harvested and stained with propidium iodide. DNA concentrations were evaluated using ModFit LT™ software (Verity Software House, Topsham, ME).

Comparison of changes in the cell cycle distribution of SKBr-3 cells after single treatment with CPT and NU1025 or their combination revealed that single medication with CPT was more effective. After longer exposure (for 48 h and 72 h), CPT arrested SKBr-3 cells mainly in G₂ phase and also induced apoptosis. In contrast, NU1025 alone or in combination with CPT neither affected the distribution of cells in cell cycle phases nor promoted apoptosis in SKBr-3 cells.

4.5. Simultaneous inhibition of TOPO1 and PARP-1 showed synergistic effects exclusively in BT-20 cells

Hitherto collected results showed that the interference with PARP-1 activity enhances the anti-proliferative action of CPT solely in BT-20 cells. Therefore, the question appeared about the kind of interaction between both drugs.

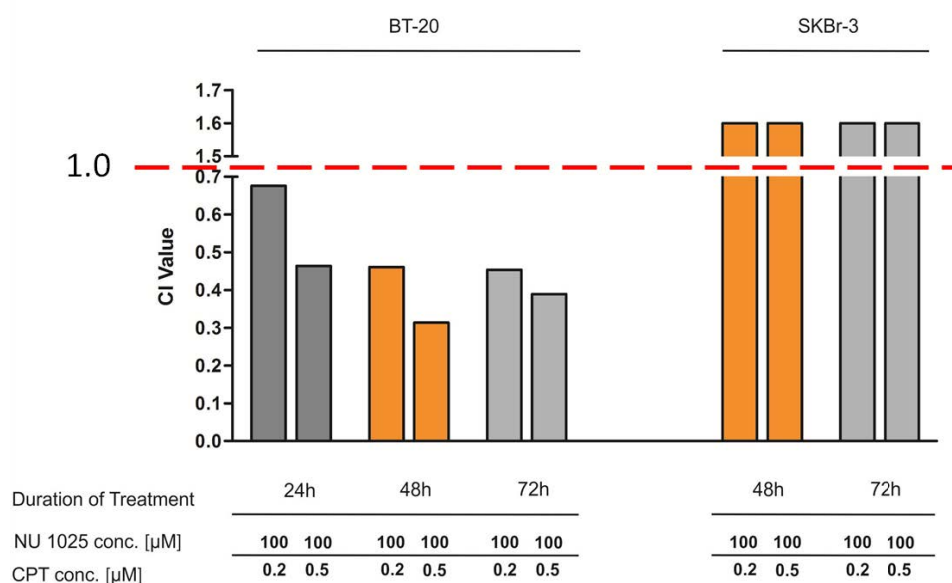


Figure 37. Synergistic interaction between PARP-1-inhibitor and CPT solely in BT-20 cells

Cells were plated in 96-wells microtiter plates treated for 24 h, 48 h and 72 h with CPT and NU1025 at indicated concentrations. The number of viable cells was measured immediately at the appropriate time using the CellTiterGLO viability assay. The data represent the mean \pm SD from at least three independent experiments, each performed in quadruplicates. The statistical analysis was performed with GraphPad Prism software. For the additional analysis of the synergistic cooperation between NU1025 and CPT CalcuSyn 2.0 software was used. The CalcuSyn 2.0 software calculates the combination index (CI) of treatments and shows if two drugs act antagonistically, synergistically or show additive effects.

Table 6. Table of CI values of BT-20 cells

BT-20	24 h	48 h	72 h
0.2 μM CPT+ 100 μM NU1025	0.676	0.461	0.454
0.5 μM CPT+ 100 μM NU1025	0.464	0.314	0.389

Table 7. Table of CI values of SKBr-3 cells

SKBr-3	48 h	72 h
0.2 μM CPT+ 100 μM NU1025	>10	>10
0.5 μM CPT+ 100 μM NU1025	>10	>10

To calculate the combination index of CPT and NU1025, data obtained from repeated cell viability assays were analysed with CalcuSyn 2.0 software. According to the description of CI values in Table 4 analysis with CalcuSyn 2.0 indicated a synergistic effect if BT-20 cells were treated with a combination of CPT and NU1025.

Observed synergistic effects in BT-20 cells increased in a dose- and time dependent manner. Synergistic effects with the lower CPT concentration treatment increased after 24 h, but did not change markedly after 72 h. A dose-dependent gain in synergy was observed at all given times. In SKBr-3 cells, the obtained CI values suggested that CPT and NU1025 act antagonistically in this cell line.

4.6. Inhibition of PARP-1 induces apoptosis and mitotic aberrations in BT-20 cells

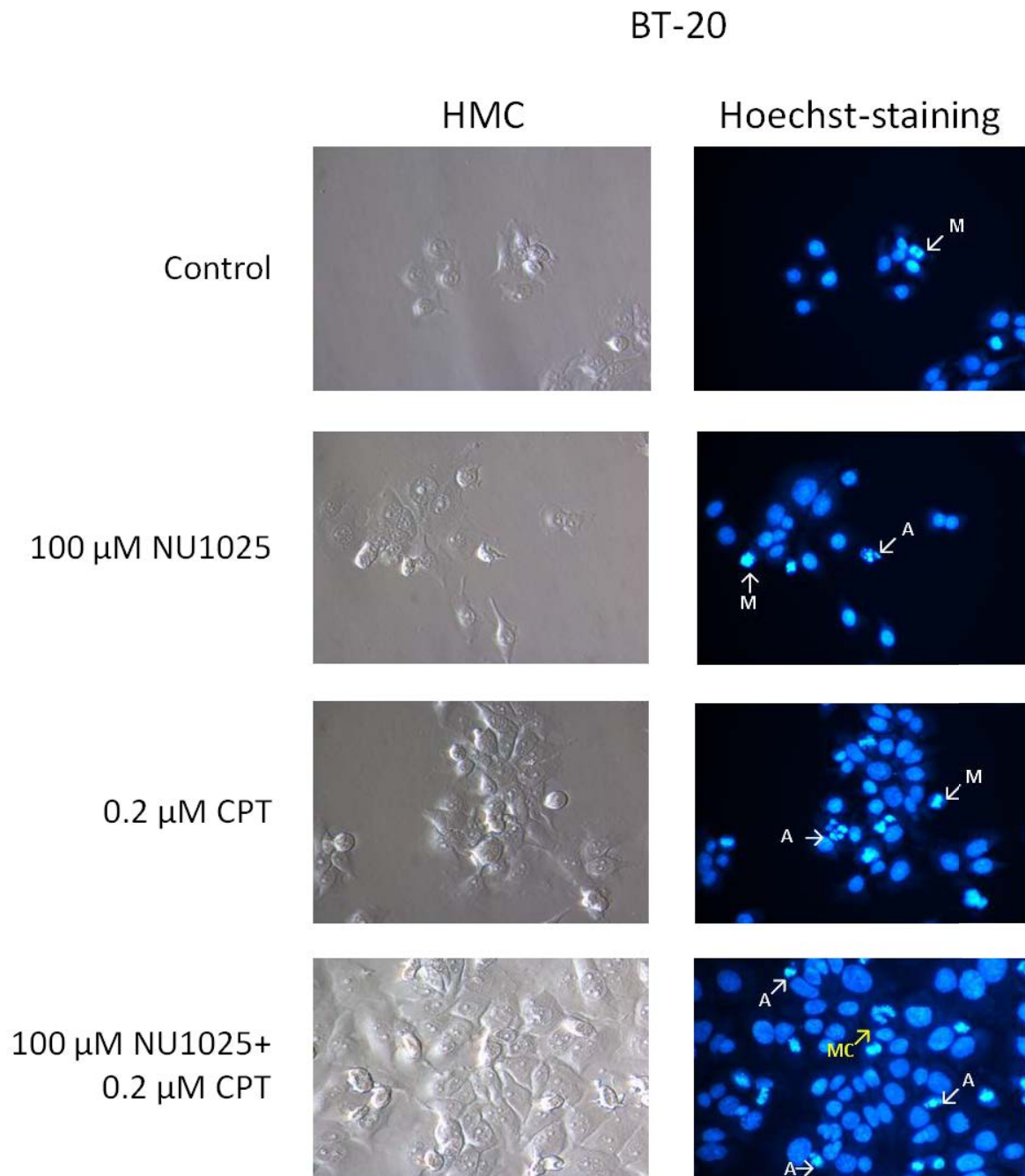


Figure 38. PARP-1 inhibition induces apoptosis and leads to mitotic catastrophe in BT-20 cells.

BT-20 cells were incubated either with 0.2 μ M CPT and 100 μ M NU1025 alone or with a combination of both agents for 72 h. Untreated controls and drug-treated cells were fixed and stained with Hoechst 33258. Phenotype and morphology of the air dried samples were inspected under the light microscope using Hoffmann Modulation Contrast (HMC) (left panel). Chromatin structure was visualized by Hoechst-staining and monitored by fluorescence microscopy (right panel). A, apoptosis; M, mitosis; MC, mitotic catastrophe;

Visualization of chromatin structure using Hoechst staining facilitated monitoring of the changes in the nuclear morphology in BT-20 cells occurring after inhibition of TOPO1 and PARP-1 either alone or their combination. After 72 h of treatment, dividing cells as well as cells undergoing apoptosis were detected in samples of cells upon administration of drugs as a monotherapy. The number of apoptotic cells but also mitotic aberrations resulting in mitotic catastrophe increased when cells were treated with both, CPT and NU1025.

4.7. PARP-1 inhibition induces caspase-3 activity in BT-20 cells

Considering the fact that the interference with PARP-1 triggered chromatin changes characteristic for apoptosis such as chromatin condensation and nuclear fragmentation we checked the effect of PARP-1 inhibition on the activity of caspase-3, the major effector caspase.

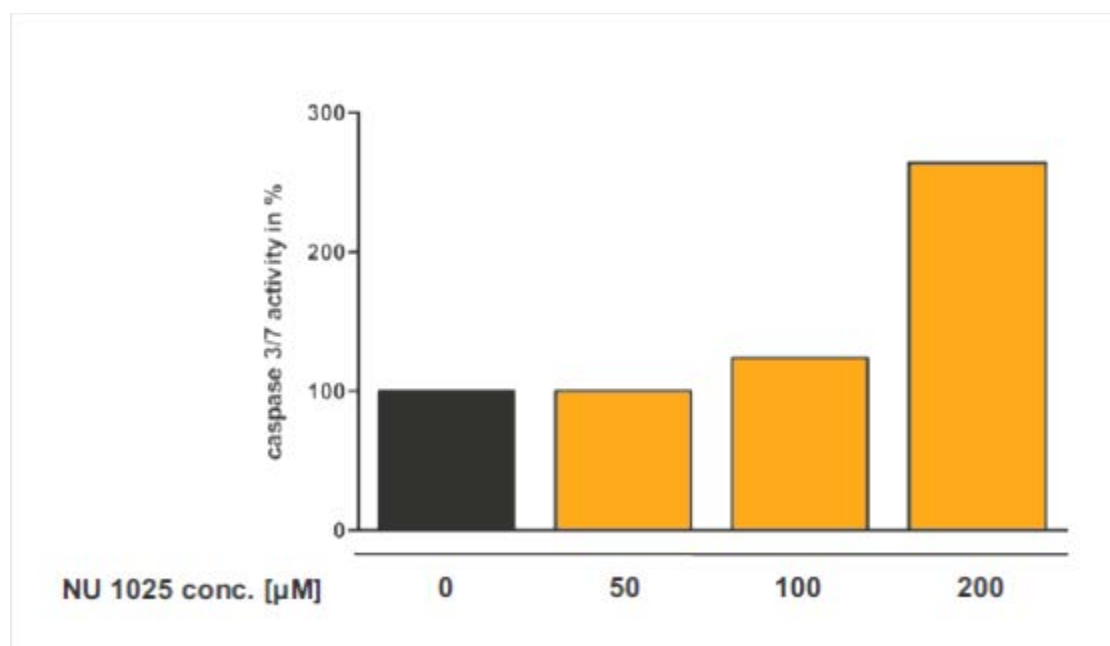


Figure 39. Inhibition of PARP-1 in BT-20 cells induces caspase-3 activity in a dose dependent manner

Cells were plated in 96-wells microtiter plates and treated for 72 h at indicated concentrations with PARP-1 inhibitor NU1025. The activity of caspase-3 activity was measured using the Caspase3/7GLO assay.

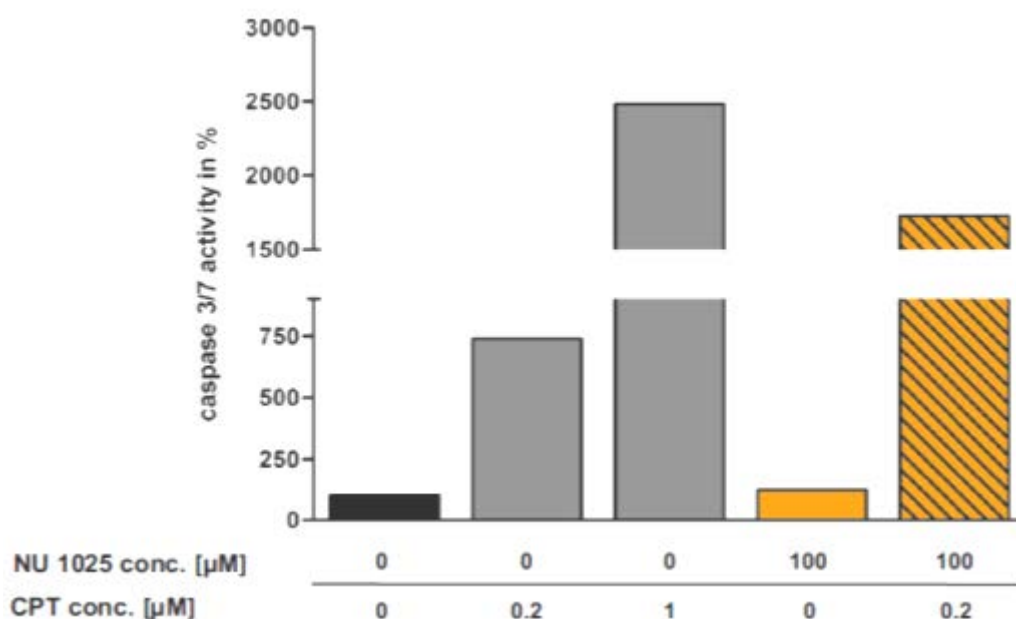


Figure 40. PARP-1 inhibition potentiates CPT-induced caspase-3 activity in BT-20 cells

Cells were plated in 96-wells microtiter plates and treated 72 h at indicated concentrations either with NU1025 and CPT alone or both combined. The caspase-3 activity was measured using the Caspase3/7 GLO assay.

Determination of the caspase-3 activity revealed that cells treated with NU1025 displayed a caspase-dependent apoptotic response to PARP-1 inhibition resulting in a strong activation of caspase-3 (Figure 39). The pharmacological interference with the PARP-1 activity stimulated caspase-3 activity in BT-20 cells in a dose-dependent manner (Figure 39). Exposure of BT-20 cells to 0.2 µM CPT increased caspase-3 activity. Interestingly, this effect was clearly enhanced by a combined medication with NU1025 (Figure 40, Figure 41 and Figure 42). Inhibition of both, TOPO1 and PARP-1, strongly raised caspase-3 activity in this cell line. To substantiate these results we performed additional tests to search for the outcome of the caspase-3 activation. We stained untreated control BT-20 cells and cells treated with CPT and NU1025 alone or their combination with CytoDEATH antibody detecting caspase-3 cleaved cytokeratin 18. As shown in Figure 41 and Figure 42 no CytoDEATH-positive staining was detected in untreated control cells. However, in BT-20 cells treated with CPT and NU1025 alone or their combination a characteristic CytoDEATH reactivity associated with chromatin fragmentation was detected thereby substantiating assumption that activated caspase-3 after PARP-1 inhibition participated in the execution of apoptosis in BT-20 cells. Summing up, this evidences that concomitant inhibition of PARP-1 in CPT-treated BT-20 cells potentiates apoptosis by strong induction of caspase-3 already at low doses of CPT.

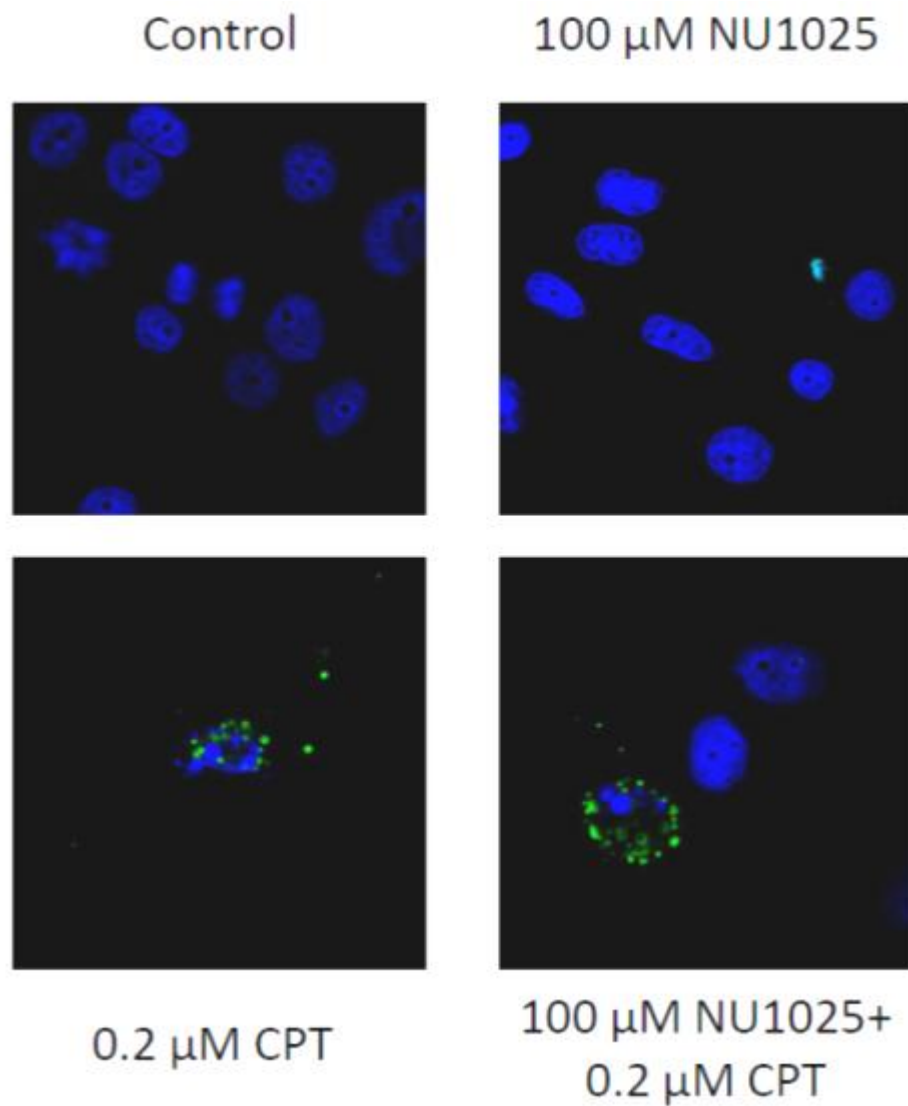


Figure 41. Caspase-3 activation and distribution in BT-20 cells visualized by M30-CytoDEATH antibody using confocal microscopy

BT-20 cells were incubated either with 0.2 μ M CPT and 100 μ M NU1025 alone or in combination for 48 h. Untreated controls and treated cells were fixed and incubated with the M30-CytoDEATH antibody for 1 h. Cells were then stained with DAPI to additionally visualise chromatin structure, staining was monitored by confocal microscopy.

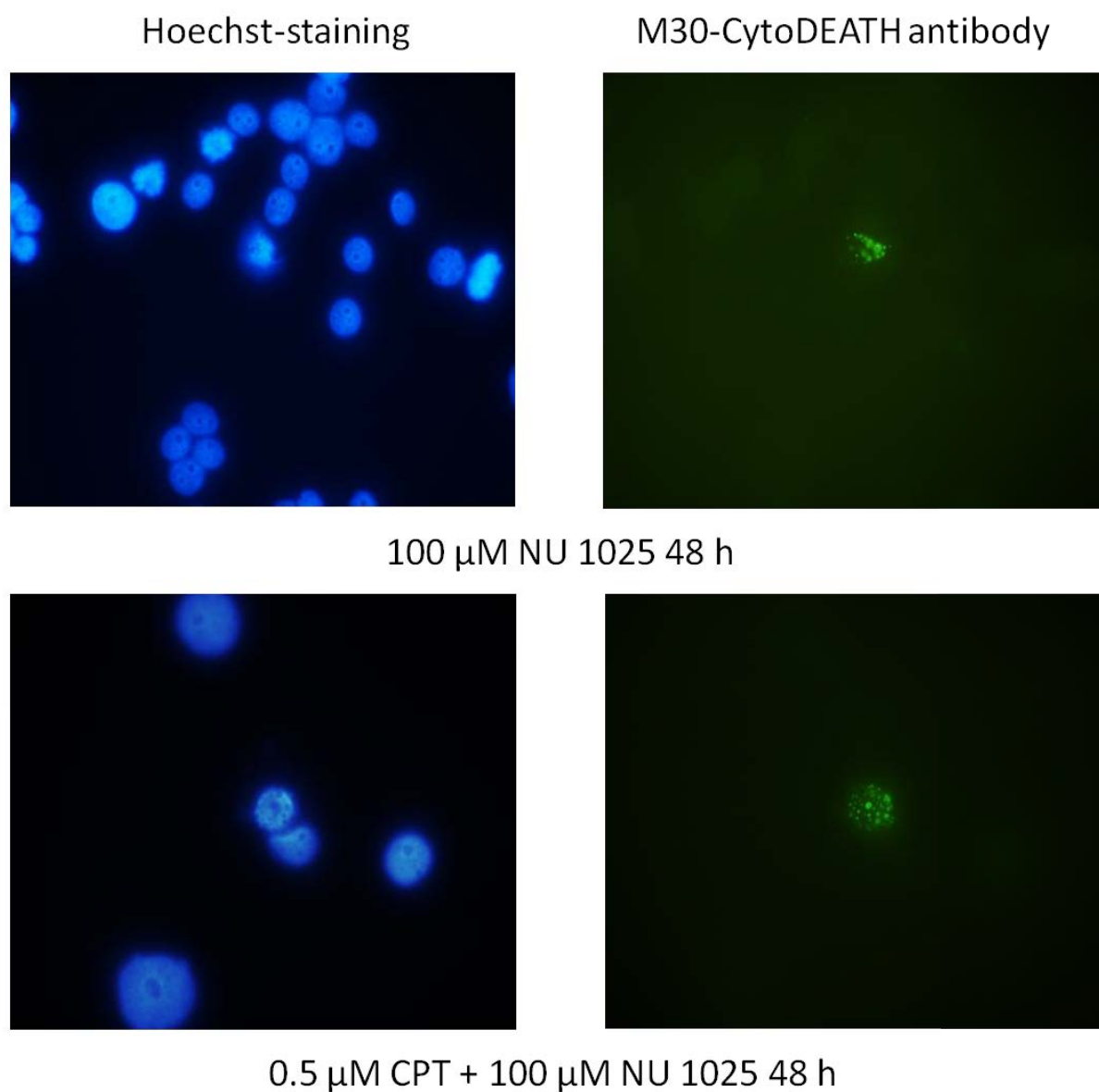


Figure 42. Caspase-3 activation and distribution in BT-20 cells visualized by M30-CytoDEATH antibody using fluorescence microscopy

BT-20 cells were incubated either with 0.5 μ M CPT and 100 μ M NU1025 in combination or with 100 μ M NU1025 alone for 48 h. Samples were fixed and incubated with the M30-CytoDEATH antibody for at least 1 h. Cells were then stained with Hoechst to additionally visualise chromatin structure, staining was monitored by fluorescence microscopy.

4.8. Inactivation of PARP-1 leads to accumulation of DNA damage in BT-20 cells

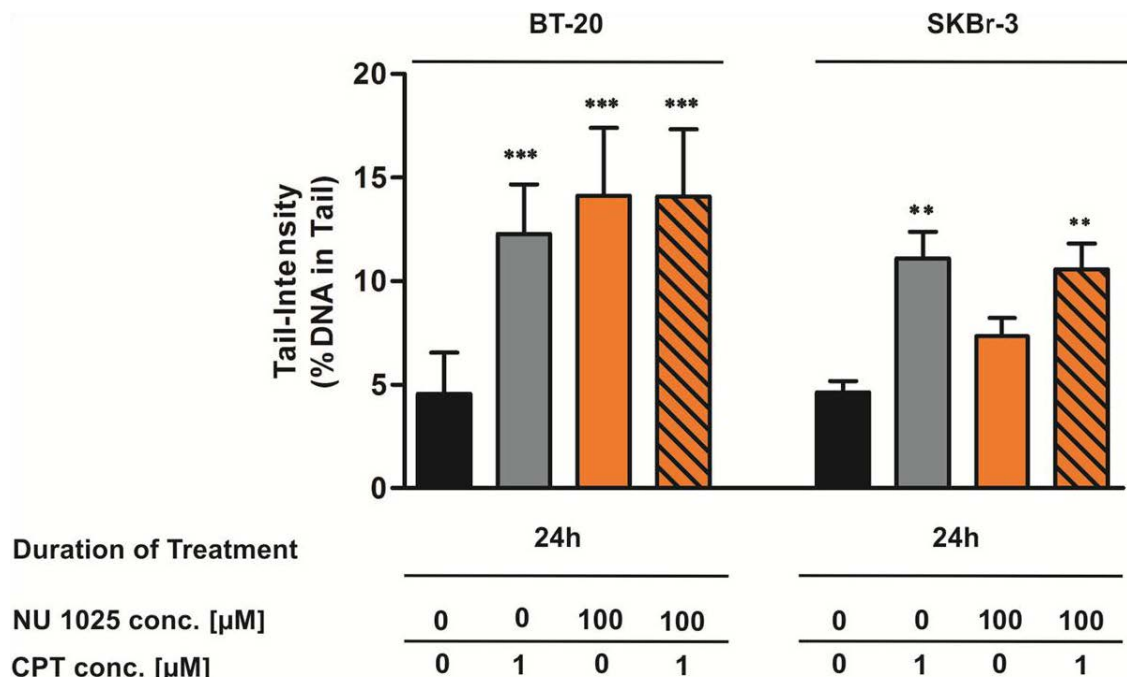


Figure 43. PARP-1 inhibition induces high levels of dsDNA breaks in BT-20 cells

Cells of both cell lines were treated for 24 h either with CPT and NU1025 alone or in combination at indicated concentrations. Samples were resolved by electrophoresis and stained with ethidium bromide. Slides were inspected under a fluorescence microscope and DNA migration was determined based on tail intensity (% DNA in tail). Data were analysed using a computer aided Comet assay image analysis system (Comet Assay IV, Perceptive Instruments, UK). The statistical analysis was performed with GraphPad Prism software using One-way ANOVA and Bonferroni's multiple comparison test.

Finally, to monitor the DNA damaging action of CPT and NU1025 either in single or in combinatory treatment, single cell electrophoresis (SCGE) was performed. As shown in Figure 43, PARP-1 inhibition and TOPO1 inhibition severely injured DNA. These agents significantly induced high levels of dsDNA breaks in BT-20 cells. Moreover, the cellular level of dsDNA breaks after the inhibition of PARP-1 activity exceeded that generated by CPT (Figure 43). In contrast in SKBr-3 cells this DNA damaging effect was observed only upon inhibition of TOPO1 (Figure 43).



Figure 44. CPT induces site-specific phosphorylation of p33 protein in BT-20 cells

BT-20 cells were incubated for 24 h either with CPT and NU1025 alone or their combination. Protein samples from the untreated controls and drug-treated cells were prepared in SDS sample buffer. Samples were electrophoretically separated on 12 % SDS slab gels, proteins immobilized on the PVDF membrane were incubated with primary antibodies as indicated. Appropriate secondary antibodies coupled to HRP were used to detect immune complexes on the PVDF membrane by chemiluminescence using luminol (ECL+) as a substrate. To ensure equal protein loading, membranes were stained with Ponceau S.

Figure 44 shows the site-specific phosphorylation of p33 at Ser15 as a response to DNA damage. This DNA damage specific phosphorylation was only observed in BT-20 cells treated either with CPT alone or in combination with PARP-1 inhibitor NU1025. These findings demonstrated the cytotoxic effect, topoisomerase I inhibitor CPT has on BT-20 cells. In contrast to CPT no phosphorylation of p33 was found in BT-20 cells treated with topoisomerase II inhibitor C-1305. This indicates that neither treatment with C-1305 alone nor the combination therapy with NU1025 stimulated DNA damage induced phosphorylation of p33 at Ser15.

5. Discussion

Cancer is one of the most common causes of death worldwide. On the strength of the recent report of the American Cancer Society the cancer incidence continues to rise. It has been evidenced in the annual cancer statistics that with estimated 1.6 million new cases in the U.S. in 2012, cancer is a major health problem not only in the U.S but also in other parts of the world.⁷²

Interestingly, in 2008 approximately 70% of cancer deaths occurred in low-income and middle-income countries although there is a lower cancer incidence than in industrialised countries. Low survival rates of cancer patients in developing countries is attributable to lack or low access of cancer patients to treatment facilities.⁸⁸ This clearly indicates that therapeutic strategies developed and implemented in industrialised countries are effective. DNA damaging agents but also agents that target cell signalling pathways in tumours involved in cell cycle checkpoint control, cell cycle progression, DNA repair or apoptosis got in the light of interest and seemed to be suitable targets for treatment and personalised therapy became a main issue.

Inhibitors of DNA topoisomerases represent an example of those promising agents in anti-cancer therapy. During its lifetime the cell is confronted with several topological problems arising as a result of the DNAs double helical nature. Both, DNA topoisomerase I and II are enzymes specialized in different aspects of spatial DNA manipulation and therefore are involved in the regulation of basal cellular processes such as replication, transcription, recombination and higher ordered chromatin structure. During replication and transcription, the DNA has to be unwound to gain access to the DNA so it can be duplicated or copied. Topoisomerase I can introduce single-stranded breaks that allow these processes to proceed. In contrast topoisomerase II is involved in the control of the DNA supercoiling; it generates double-stranded breaks, and as needed causes chromatin condensation or relaxation.

Agents that target DNA topoisomerases and stabilise the so called cleavable complex prevent the resealing of the DNA strands. This trapping of the DNA-enzyme intermediate further leads to DNA breakage; primarily double strand DNA breaks during replication and transcription. If this damage is not removed by the cell's DNA repair pathways, it accumulates and triggers apoptosis^{11,12,20}. Cells exhibiting deficiencies in their DNA repair pathways were shown to be very sensitive to topoisomerase inhibition due to their impairment to cope with topoisomerase inhibitor induced DNA damage^{5,59,60,61,89,57}.

Treatment of tumours carrying mutations in the tumour suppressor genes *BRCA1* and *BRCA2* with inhibitors of poly (ADP -ribose) polymerase has been proposed as a promising option for treating cancer patients harbouring germline *BRCA1/2* mutations by applying the concept of synthetic lethality. PARP-1 is an extremely tetchy sensor of DNA breakage and is stimulated already after appearance of a few free DNA ends during physiological processes

such as DNA replication or transcription. In response to DNA breakage PARP-1 is rapidly and strongly activated, binds to DNA at breakage sites and facilitates recruiting of proteins specialized in the repair of single-stranded DNA breaks. Inhibition of PARP-1 activity hampers the base-excision repair (BER) of single-stranded DNA breaks appearing during replication or transcription that by and by are converted into double-stranded DNA breaks. In cells with functioning homology recombination (HR) pathway these breaks are repaired. In contrast, in *BRCA1/2*-deficient cells the inhibition of PARP-1 activity causes strongly cytotoxic effects as a result of both, an impaired BER and a defective DNA double strand repair pathway^{5,36,60,76,77}. The present work focuses on the effects of DNA topoisomerase I inhibition in combination with PARP-1 inactivation on different breast cancer cell lines.

In this study three breast cancer cell lines differing in their hormone receptor (estrogen and progesterone) and *BRCA1* status, were either treated with camptothecin, an inhibitor of DNA topoisomerase I or PARP-1 inhibitor NU1025 alone or their combination. Camptothecin (CPT), a cytotoxic plant alkaloid specifically targets DNA topoisomerase I and stabilises the cleavable complex by intercalating into the DNA- enzyme intermediate thereby forming a ternary complex. This formation is crucial for the effectiveness of CPT as a DNA damaging agent. DNA topoisomerase I-induced single strand breaks persist and become double strand breaks during replication. Simultaneously inhibition of PARP-1 activity in CPT treated cells increases the DNA damaging effect of the topoisomerase I inhibitor. DNA lesions remain unrepaired, accumulate and induce apoptosis^{3,8,10,11,12,90}. Treatment with CPT leads to cell cycle arrest, blocks cell proliferation and/or induces programmed cell death in all three breast cancer cell lines that have been examined. However, the sensitivity of the tested breast cancer cells strongly varied. BT-20 cells displayed the highest sensitivity to CPT after short term (24 h) treatment compared to the other two tested cell lines SKBr-3 and T47D. The decline of number of viable cells proceeded after 48 h and 72 h in BT-20 cells, in SKBr-3 cells cell viability remarkably decreased after 48 h showing a 107.2 fold reduction of the IC₅₀ value. This reduction of cell viability in SKBr-3 cells after 48 h treatment with CPT seem to be attributable to a much slower kinetics of cell proliferation compared to BT-20 cells. CPT traps the DNA enzyme intermediate thereby targeting cells in S-phase, this specific cell cycle dependent mode of action of CPT may explain the delayed inhibition of the proliferation in SKBr-3 cells. In all three examined breast cancer cell lines a continuous, time-dependent decline in cell viability was reported. After long term treatment (48 h and 72 h) SKBr-3 cells showed the highest sensitivity upon topoisomerase I inhibition. BT-20 cells displayed the highest sensitivity after short time treatment among the tested cell lines. In T47D cells topoisomerase I inhibition also resulted in a continuous decrease in cell viability, however this observed effect was less pronounced compared to those in BT-20 and SKBr-3 cells.

Previous studies already indicated that simultaneously inhibition of DNA topoisomerase and PARP-1 enhances topoisomerase-induced cytotoxicity^{89,57,91}. According to the concept of synthetic lethality, *BRCA1*-negative SKBr-3 cells were assumed to be the most sensitive cell line upon PARP-1 inhibition, compared to the *BRCA1*-positive breast cancer cell lines BT-20

and T47D. Surprisingly, this wasn't the case. Treatment of SKBr-3 cells with PARP-1 inhibitor NU1025 did not affect their proliferation and viability, displaying a similar effect as it appeared in PARP-1-inhibited T47D cells. In contrast to these observations blocking PARP-1 activity in BRCA1-expressing BT-20 cells significantly reduced their proliferation.

DNA damaging effects upon CPT treatment in BT-20 cells were also proved by monitoring the site-specific phosphorylation of p53 protein at Ser15 in CPT- and NU1025-treated cells and untreated controls. Only interference with topoisomerase I activity in BT-20 induced phosphorylation of p53 at Ser 15. This site-specific phosphorylation at Ser15 catalyzed by ATM kinase is a cellular response to DNA damage, reducing p53 affinity for its regulatory protein MDM2 and thereby promoting activation of p53. Considering the fact that p53 in BT-20 cells is mutated and highly stable, the impact of its specific modification is not clear. However, the very fact that p53 was phosphorylated upon DNA injury indicates that DNA damage signalling pathway in BT-20 is not impaired. Simultaneously inhibition of both, topoisomerase I and PARP-1 activity potentiated the CPT-induced DNA damage exclusively in BT-20 cells. This enhancing effect of cytotoxicity as a result of PARP-1 inhibition combined with topoisomerase inhibition was highly significant compared to untreated controls but also to single treatment with either CPT or NU1025.

Inhibition of DNA topoisomerase I led to an increase in the S-phase fraction after short term treatment and triggered G₂ arrest after long term treatment. Additional inhibition of PARP-1 activity in BT-20 cells amplified CPT induced effects and was accompanied by an augmented induction of apoptosis. Hoechst-staining enabled us to visualise expected cellular aberrations, like mitotic catastrophe and an increased apoptosis rate. PARP-1 inhibition in BT-20 cells increased caspase-3 activity resulting in caspase-3-mediated apoptosis. Experiments also indicated that CPT-induced caspase-3 activity is enhanced after co-treatment of cells with NU1025. These results are not only concordant with previous findings by Węsierska-Gądek, J. *et al.* (2012)⁵⁶ but bring also new insights. In the recent paper Węsierska-Gądek, J. *et al.* already demonstrated that human BT-20 breast cancer cells were relative resistant to C-1305, a unique inhibitor of topoisomerase II. C-1305 was not directly cytotoxic and PARP-1 inhibition enhanced its cytotoxic effects by promoting caspase-dependent apoptosis. In this context the question came up whether the synergizing effect of PARP-1 inhibition in BT-20 cells was attributable to the low DNA damaging effect of C-1305 and whether the interference with PARP-1 activity would also synergize with topoisomerase inhibitors that strongly damage DNA. This issue was addressed in this master thesis. Results collected in this study show that the pharmacological interference with PARP-1 activity strongly synergizes with CPT, a topoisomerase I inhibitor resulting in extensive DNA damage in BRCA1 expressing BT-20 cells but not in BRCA1-negative SKBr-3 cells. In SKBr-3 cells the interaction between PARP-1 inhibitor and CPT was strongly antagonistic.

These findings lead to the assumption that human breast cancer BT-20 cells harbour so far unknown deficiencies in DNA repair pathways which make them sensitive to PARP-1

inhibition. The exploited PARP-1 sensitivity was reflected in decreased cell viability, accumulation of DNA strand breaks and chromosomal aberrations like mitotic catastrophe. These observations are important for further development and improvement of the concept of synthetic lethality and personalised therapy, indicating that treatment with PARP inhibitors is not exclusively restricted to patients carrying mutations in *BRCA1* and *BRCA2*. Breast cancer is not a homogeneous disease, in fact there are many different tumour subgroups exhibiting different properties which affect disease progression and response to treatment⁹². Only about 5-7% of all breast cancer cases account for familial breast cancer carrying inherited germ line mutations in the tumour suppressor genes *BRCA1* and *BRCA2*⁴⁰.

If cancer therapy based on the concept of synthetic lethality is not limited to the small subgroup of cancer patients with *BRCA1* and *BRCA2* mutations, a larger group of patients could benefit from this targeted therapy. Deficiencies in DNA repair pathways that sensitises cells to PARP inhibition are versatile and could also arise as a result of an impaired ATM/ATR signalling, deficiencies in the phosphoinositide 3-kinase (PI3K) signalling pathway or loss of function of proteins involved in cell cycle checkpoint control like Chk1 and Chk2^{93,76,78,94,95}.

These patients could also show great response to PARP inhibition either in single treatment or combined with radiation, platinum-containing therapy or treatment with cytotoxic agents^{96,4,40,77,93}. During the last years the application of PARP inhibitors in anti-cancer therapy displayed promising results in anti-tumour activity. Various studies already demonstrated the synergistic effects of PARP inhibition in combination with blockage of specific cell signalling pathways among them the phosphoinositide 3-kinase (PI3K) signalling pathway^{94,95}. These findings indicate that the potential of application of PARP inhibitors in anti-cancer therapy is not fully exploited yet. Consequently, further scientific approaches should be directed towards the targeting of defects in DNA repair mechanisms without committing to one specific gene defect.

6. Appendix

6.1. Abbreviations

ADP	adenosine diphosphate
AP site	apurinic/apyrimidinic site
APE1	human AP endonuclease
APS	ammonium persulphate
ATLD	ataxia-telangiectasia-like disorder
ATM	ataxia-telangiectasia mutated
ATP	adenosine triphosphate
ATR	ataxia telangiectasia and Rad3-related protein
ATRIP	ATR interacting protein
BARD1	BRCA1-associated RING domain protein 1
BCR	breakpoint cluster region (Ser/Thr kinase)
BER	base excision repair
BLM1	Bloom syndrome protein
BRCA1/2	breast cancer 1/2, early-onset tumorsuppressor gene
BRCT	BRCA1 C Terminus domain
BRIP1	BRCA1-interacting protein C-terminal helicase 1
BSA	bovine serum albumin
CDC25	cell division cycle phosphatase 25 (phosphatases CDC25A-C)
CDH1	cadherin-1
Chk1	checkpoint kinase 1
Chk2	checkpoint kinase 2
Co	control
CPT	Camptothecin
C-terminal	carboxy-terminal
DAPI	4',6-diamidino-2-phenylindole
DBD	DNA binding domain
DMEM	Dulbecco's Modified Eagle's Medium
DMF	dimethylformamide
DMSO	dimethyl sulfoxide
DNA	deoxyribonucleic acid
DNA -Pkcs	DNA-dependent protein kinase, catalytic subunit,
DSB	double strand break

DTT	dithiothreitol
E2F	elongation factor 2F
ECL	enhanced chemiluminescence
EDTA	ethylenediaminetetraacetic acid
ER	estrogen receptor
EXO1	exonuclease 1
FANCD2	Fanconi anemia group D2 protein
FAT domain	FRAP, ATM, TRAPP domain
FATC	C-terminal FAT domain
FCS	foetal calf serum
FHA domain	forkhead-associated domain
H2AX	H2A histone family, member X
HBCO	hereditary breast and ovarian cancer
HEAT repeats	Huntingtin, elongation factor 3 (EF3), protein phosphatase 2A (PP2A), and the yeast kinase TOR1
Her2	human epidermal growth factor receptor 2
HR	homologous recombination
HRP	horseradish peroxidase
kDa	kiloDalton
Ku	protein that binds to DNA double-strand break ends during DNA repair
LKB1	liver kinase B1
MDC1	mediator of DNA damage checkpoint protein 1
MDM-2	mouse double minute-2
MeOH	methanol
ml	millilitre
MLH1	MutL homolog 1
MMEJ	microhomology-mediated end joining
MMR	mismatch repair
MRE11	DNA repair protein
MRN	multifunctional complex consisting of the proteins MRE11, RAD50 and NBS1
MSH2	MutS homolog 2
mTOR	mammalian target of rapamycin
MutH	protein involved in mismatch repair
MutL	protein involved in mismatch repair
MutS	protein involved in mismatch repair

MutSα	heterodimer formed by MSH2/MSH6
MutSβ	heterodimer formed by MSH2/MSH3
NAD⁺	nicotinamide adenine dinucleotide
NaF	sodium fluoride
NAM	nicotinamide
NBS1	Nijmegen breakage syndrome 1 protein (nibrin)
NER	nucleotide excision repair
NHEJ	non-homologous end joining
NLS	nuclear localization signal
NP-40	nonidet-P 40
N-terminal	amino-terminal
p53	tumor suppressor protein
PALB2	partner and localizer of BRCA2
PARG	poly (ADP-ribose) glycohydrolase
PARP	poly (ADP-ribose) polymerase
PBS	phosphate buffered saline
PD	Petri dish
PI	propidium iodide
PI3K	phosphatidylinositide 3-kinases
PIKKs	phosphatidylinositol 3-kinase-related kinases
PMSF	phenylmethylsulfonyl fluoride
PTEN	phosphatase and tensin homolog
PVDF	polyvinylidene fluoride
RAD50	DNA repair protein
RFC	replication factor C
RING	really interesting new gene
RIPA	radioimmuno precipitation assay buffer
RNF8	RING finger protein 8
RPA	replication protein A
RPM	Revolutions per minute
RPMI1640	medium used in cell culture, name derived from Roswell Park Memorial Institute
RT	room temperature
SCD	SQ/TQ cluster domain
SDS	sodium dodecyl sulphate
SSB	single strand break

TBS	Tris-buffered saline
TEMED	tetramethylethylenediamine
TLK1	tousled-like kinase 1
TLK2	tousled-like kinase 2
TOPBP1	DNA topoisomerase 2-binding protein 1
TOPO1	topoisomerase 1
TP53	gene that encodes the tumor suppressor protein p53
UV	ultraviolet
V	volt
wt	wild type
XRCC1	X-ray repair cross-complementing protein 1
XRCC4	X-ray repair cross-complementing protein 4

6.2.List of figures

Figure 1. Problems in DNA topology arising during replication (picture reproduced from Wang, J. C et al. (2002)^[1])

Figure 2. Problems in DNA topology arising during transcription (picture reproduced from Wang, J. C et al. (2002)^[1])

Figure 3. Binding of camptothecin to the cleavable complex (picture reproduced from Leppard, J. B et al. (2005)^[3])

Figure 4. Non homologous end joining in mammalian cells (reproduced from Downs, J. et al. (2007)^[32])

Figure 5. Model of MMEJ (reproduced from McVey, M. et al. (2008)^[34])

Figure 6. HR in mammalian cells (reproduced from Kanaar, R. et al (1998)^[22])

Figure 7. ATM and ATR signalling (picture reproduced from Zhou, B. et al. (2004)^[42])

Figure 8. ATM signalling cascade (picture reproduced from Zhou, B. et al. (2004)^[42])

Figure 9. ATR signalling cascade (picture reproduced from Zhou, B. et al. (2004)^[42])

Figure 10. Human BRCA1 (picture reproduced from Roy, R. et al. (2012)^[47])

Figure 11. Involvement of BRCA1 and BRCA2 in DNA damage response (picture reproduced from Roy, R. et al. (2012)^[47])

Figure 12. Human BRCA2 (picture reproduced from Roy, R. et al. (2012)^[47])

Figure 13. Involvement of the MRN complex in DNA damage response (picture reproduced from Williams, G. et al. (2010)^[49])

Figure 14. Structure of MRE11 (picture reproduced from Williams, G. et al. (2010)^[49])

Figure 15. Structure of RAD50 (picture reproduced from Borde, V. et al. (2007)^[52])

Figure 16. Structure of human NBS1 and its yeast homolog Xrs2

Figure 17. Concept of synthetic lethality (picture reproduced from Curtin, N. et al. (2012)^[59])

Figure 18. DNA repair mechanisms (picture reproduced from Yap, T. et al. (2011)^[58])

Figure 19. Structure of PARP-1 (picture reproduced from Rouleau, M. et al. (2010)^[64])

Figure 20. Action of poly (ADP-ribose)polymerase (picture reproduced from Schreiber, V. et al. (2006)^[62])

Figure 21. U.S. cancer statistic 2012 (picture reproduced from Siegel, R. et al. (2012)^[71])

Figure 22. Synthetic lethality induced by PARP-1 inhibition (picture reproduced from Węsierska-Gądek, J. et al. (2012)^[5])

Figure 23. The luciferase reaction

Figure 24. The luciferase reaction to determine caspases 3/7 activity

Figure 25. Assembly of the transblot Western sandwich

Figure 26. Reduction of numbers of viable cells after TOPO1 inhibition in BT-20 cells

Figure 27. Reduction of numbers of viable cells after TOPO1 inhibition in SKBr-3 cells

Figure 28. Reduction of numbers of viable cells after TOPO1 inhibition in T47D cells

Figure 29. Effects of PARP-1 inhibition on cell viability in different breast cancer cell lines

Figure 30. Inhibition of PARP-1 activity affects cell viability in BT-20 cells in a time- and dose-dependent manner

Figure 31. Effects of PARP-1 inhibition on the number of viable cells in SKBr-3 breast cancer cells

Figure 32. Effects of PARP-1 inhibition on the number of viable cells in T47D breast cancer cells

Figure 33. Inhibition of PARP-1 reduces numbers of viable BT-20 cells and potentiates the anti-proliferative action

Figure 34. Inhibition of PARP-1 reduces numbers of viable and potentiates anti-proliferative action of CPT exclusively in BT-20 cells (72 h)

Figure 35. PARP-1 inhibition induces apoptosis in CPT-treated BT-20 cells arrested in G₂/M phase

Figure 36. PARP-1 inhibitor has a weak or no effect on cell cycle distribution in CPT treated SKBr-3 cells

Figure 37. Synergistic interaction between PARP-1-inhibitor and CPT solely in BT-20 cells

Figure 38. PARP-1 inhibition induces apoptosis and leads to mitotic catastrophe in BT-20 cells.

Figure 39. Inhibition of PARP-1 in BT-20 cells induces caspase-3 activity in a dose dependent manner

Figure 40. PARP-1 inhibition potentiates CPT-induced caspase-3 activity in BT-20 cells

Figure 41. Caspase-3 activation and distribution in BT-20 cells visualized by M30-CytoDEATH antibody using confocal microscopy

Figure 42. Caspase-3 activation and distribution in BT-20 cells visualized by M30-CytoDEATH antibody using fluorescence microscopy

Figure 43. PARP-1 inhibition induces high levels of dsDNA breaks in BT-20 cells

Figure 44. CPT induces site-specific phosphorylation of p53 protein in BT-20 cells

6.3.List of tables

Table 1. Human topoisomerases data summarized from ^{1,2,3,4}

Table 2. Composition of the resolving and stacking gels

Table 3. Description of CI values

Table 4. Effect of CPT treatment on the number of living breast cancer cells

Table 5. Table of CI values of BT-20 cells

Table 6. Table of CI values of SKBr-3 cells

7. Acknowledgement

First of all I want to thank A.o. Univ. Prof. Dr. Wesierska-Gadek for giving me the possibility to work in her group and supervising my master thesis. She always supported me during the learning process of this master thesis by giving useful comments, remarks and of course helping me gaining scientific experience and knowledge.

I also want to thank Ao.Univ.-Prof. Mag. Dr. Rotheneder for supervising my master thesis.

This thesis would not have been possible without the help and support of many people. I want to thank the people working at the Cancer Research Institute especially Dr. Irene Herbacek for performing the FACS analysis and Paul Breit for his unfailing efforts to answer all my questions about confocal microscopy.

I also want to thank my lab colleagues Doris and Maria who turned into good friends after a short period of time.

Last but not least I would like to thank my family. Thanks for giving me the possibility to study and your ongoing support through all the years of learning.

8. References

1. Wang, J. C. Cellular roles of DNA topoisomerases: a molecular perspective. *Nature reviews. Molecular cell biology* **3**, 430–40 (2002).
2. Champoux, J. J. DNA topoisomerases: structure, function, and mechanism. *Annual review of biochemistry* **70**, 369–413 (2001).
3. Leppard, J. B. & Champoux, J. J. Human DNA topoisomerase I: relaxation, roles, and damage control. *Chromosoma* **114**, 75–85 (2005).
4. Nitiss, J. L. DNA topoisomerase II and its growing repertoire of biological functions. *Nature reviews. Cancer* **9**, 327–37 (2009).
5. Węsierska-Gądek, J. & Składanowski, A. Therapeutic intervention by the simultaneous inhibition of DNA repair and type I or type II DNA topoisomerases: one strategy, many outcomes. *Future medicinal chemistry* **4**, 51–72 (2012).
6. Wall, M., Wani, M. & Cook, C. Plant antitumor agents. I. The isolation and structure of camptothecin, a novel alkaloidal leukemia and tumor inhibitor from camptotheca acuminata1, 2. *Journal of the American Chemical Society* 3888–3890 (1966). doi:10.1021/ja00968a057
7. Pommier, Y. Topoisomerase I inhibitors: camptothecins and beyond. *Nature reviews. Cancer* **6**, 789–802 (2006).
8. Hsiang, Y. H., Lihou, M. G. & Liu, L. F. Arrest of replication forks by drug-stabilized topoisomerase I-DNA cleavable complexes as a mechanism of cell killing by camptothecin. *Cancer research* **49**, 5077–82 (1989).
9. Nitiss, J. L. Targeting DNA topoisomerase II in cancer chemotherapy. *Nature reviews. Cancer* **9**, 338–50 (2009).
10. Staker, B. L. *et al.* The mechanism of topoisomerase I poisoning by a camptothecin analog. *Proceedings of the National Academy of Sciences of the United States of America* **99**, 15387–92 (2002).
11. Li, T. K. & Liu, L. F. Tumor cell death induced by topoisomerase-targeting drugs. *Annual review of pharmacology and toxicology* **41**, 53–77 (2001).
12. Strumberg, D. *et al.* Conversion of topoisomerase I cleavage complexes on the leading strand of ribosomal DNA into 5'-phosphorylated DNA double-strand breaks by replication runoff. *Molecular and cellular biology* **20**, 3977–87 (2000).
13. Hande, K. R. Etoposide: four decades of development of a topoisomerase II inhibitor. *European journal of cancer (Oxford, England : 1990)* **34**, 1514–21 (1998).

14. Hande, K. R. Topoisomerase II inhibitors. *Update on Cancer Therapeutics* **1**, 3–15 (2006).
15. Kagan, V. E. *et al.* Mechanism-based chemopreventive strategies against etoposide-induced acute myeloid leukemia: free radical/antioxidant approach. *Molecular pharmacology* **56**, 494–506 (1999).
16. Felix, C. A., Lange, B. J., Hosler, M. R., Fertala, J. & Bjornsti, M. A. Chromosome band 11q23 translocation breakpoints are DNA topoisomerase II cleavage sites. *Cancer research* **55**, 4287–92 (1995).
17. Lemke, K., Poindessous, V., Skladanowski, A. & Larsen, A. K. The antitumor triazoloacridone C-1305 is a topoisomerase II poison with unusual properties. *Molecular pharmacology* **66**, 1035–42 (2004).
18. Wesierska-Gadek, J., Schloffer, D., Gueorguieva, M., Uhl, M. & Skladanowski, A. Increased susceptibility of poly(ADP-ribose) polymerase-1 knockout cells to antitumor triazoloacridone C-1305 is associated with permanent G2 cell cycle arrest. *Cancer research* **64**, 4487–97 (2004).
19. Lemke, K. *et al.* Induction of unique structural changes in guanine-rich DNA regions by the triazoloacridone C-1305, a topoisomerase II inhibitor with antitumor activities. *Nucleic acids research* **33**, 6034–47 (2005).
20. Zhao, H., Rybak, P., Dobrucki, J., Traganos, F. & Darzynkiewicz, Z. Relationship of DNA damage signaling to DNA replication following treatment with DNA topoisomerase inhibitors camptothecin/topotecan, mitoxantrone, or etoposide. *Cytometry. Part A : the journal of the International Society for Analytical Cytology* **81**, 45–51 (2012).
21. Hefferin, M. L. & Tomkinson, A. E. Mechanism of DNA double-strand break repair by non-homologous end joining. *DNA repair* **4**, 639–48 (2005).
22. Sancar, A., Lindsey-Boltz, L. a, Unsal-Kaçmaz, K. & Linn, S. Molecular mechanisms of mammalian DNA repair and the DNA damage checkpoints. *Annual review of biochemistry* **73**, 39–85 (2004).
23. Kanaar, R., Hoeijmakers, J. H. & van Gent, D. C. Molecular mechanisms of DNA double strand break repair. *Trends in cell biology* **8**, 483–9 (1998).
24. Dip, R., Camenisch, U. & Naegeli, H. Mechanisms of DNA damage recognition and strand discrimination in human nucleotide excision repair. *DNA repair* **3**, 1409–23 (2004).
25. Kraemer, K. H., Lee, M. M. & Scotto, J. DNA repair protects against cutaneous and internal neoplasia: evidence from xeroderma pigmentosum. *Carcinogenesis* **5**, 511–4 (1984).

26. Fortini, P. & Dogliotti, E. Base damage and single-strand break repair: mechanisms and functional significance of short- and long-patch repair subpathways. *DNA repair* **6**, 398–409 (2007).
27. Frosina, G. *et al.* Two pathways for base excision repair in mammalian cells. *The Journal of biological chemistry* **271**, 9573–8 (1996).
28. Liu, Y. *et al.* Coordination of steps in single-nucleotide base excision repair mediated by apurinic/apyrimidinic endonuclease 1 and DNA polymerase beta. *The Journal of biological chemistry* **282**, 13532–41 (2007).
29. Geng, H. *et al.* Biochemical analysis of the human mismatch repair proteins hMutS α MSH2(G674A)-MSH6 and MSH2-MSH6(T1219D). *The Journal of biological chemistry* **287**, 9777–91 (2012).
30. Iyer, R. R., Pluciennik, A., Burdett, V. & Modrich, P. L. DNA mismatch repair: functions and mechanisms. *Chemical reviews* **106**, 302–23 (2006).
31. Yang, W. Structure and function of mismatch repair proteins. *Mutation research* **460**, 245–56 (2000).
32. Fukui, K. DNA mismatch repair in eukaryotes and bacteria. *Journal of nucleic acids* **2010**, (2010).
33. Downs, J. a, Nussenzweig, M. C. & Nussenzweig, A. Chromatin dynamics and the preservation of genetic information. *Nature* **447**, 951–8 (2007).
34. Muller, C., Calsou, P., Frit, P. & Salles, B. Regulation of the DNA-dependent protein kinase (DNA-PK) activity in eukaryotic cells. *Biochimie* **81**, 117–25 (1999).
35. McVey, M. & Lee, S. E. MMEJ repair of double-strand breaks (director's cut): deleted sequences and alternative endings. *Trends in genetics : TIG* **24**, 529–38 (2008).
36. Furgason, J. M. & Bahassi, E. M. Targeting DNA repair mechanisms in cancer. *Pharmacology & therapeutics* **137**, 298–308 (2013).
37. Lopez-Contreras, A. & Fernandez-Capetillo, O. *Signalling DNA Damage*. (2012). doi:10.5772/50863
38. O'Donovan, P. J. & Livingston, D. M. BRCA1 and BRCA2: breast/ovarian cancer susceptibility gene products and participants in DNA double-strand break repair. *Carcinogenesis* **31**, 961–7 (2010).
39. Narod, S. a & Foulkes, W. D. BRCA1 and BRCA2: 1994 and beyond. *Nature reviews. Cancer* **4**, 665–76 (2004).
40. Melchor, L. & Benítez, J. The complex genetic landscape of familial breast cancer. *Human genetics* **1**, (2013).

41. Bensimon, A., Aebersold, R. & Shiloh, Y. Beyond ATM: the protein kinase landscape of the DNA damage response. *FEBS letters* **585**, 1625–39 (2011).
42. Kurz, E. U. & Lees-Miller, S. P. DNA damage-induced activation of ATM and ATM-dependent signaling pathways. *DNA repair* **3**, 889–900 (2004).
43. Zhou, B.-B. S. & Bartek, J. Targeting the checkpoint kinases: chemosensitization versus chemoprotection. *Nature reviews. Cancer* **4**, 216–25 (2004).
44. Lavin, M. F. & Shiloh, Y. The genetic defect in ataxia-telangiectasia. *Annual review of immunology* **15**, 177–202 (1997).
45. Lee, J.-H. & Paull, T. T. Direct activation of the ATM protein kinase by the Mre11/Rad50/Nbs1 complex. *Science (New York, N.Y.)* **304**, 93–6 (2004).
46. Ahmed, M. & Rahman, N. ATM and breast cancer susceptibility. *Oncogene* **25**, 5906–11 (2006).
47. Liu, Y. & West, S. C. Distinct functions of BRCA1 and BRCA2 in double-strand break repair. *Breast cancer research : BCR* **4**, 9–13 (2002).
48. Roy, R., Chun, J. & Powell, S. N. BRCA1 and BRCA2: different roles in a common pathway of genome protection. *Nature reviews. Cancer* **12**, 68–78 (2012).
49. Dzikiewicz-Krawczyk, A. The importance of making ends meet: mutations in genes and altered expression of proteins of the MRN complex and cancer. *Mutation research* **659**, 262–73 (2008).
50. Williams, G. J., Lees-Miller, S. P. & Tainer, J. a. Mre11-Rad50-Nbs1 conformations and the control of sensing, signaling, and effector responses at DNA double-strand breaks. *DNA repair* **9**, 1299–306 (2010).
51. Maser, R. S. *et al.* Mre11 complex and DNA replication: linkage to E2F and sites of DNA synthesis. *Molecular and cellular biology* **21**, 6006–16 (2001).
52. Chai, W., Sfeir, A. J., Hoshiyama, H., Shay, J. W. & Wright, W. E. The involvement of the Mre11/Rad50/Nbs1 complex in the generation of G-overhangs at human telomeres. *EMBO reports* **7**, 225–30 (2006).
53. Borde, V. The multiple roles of the Mre11 complex for meiotic recombination. *Chromosome research : an international journal on the molecular, supramolecular and evolutionary aspects of chromosome biology* **15**, 551–63 (2007).
54. Lim, H. S., Kim, J. S., Park, Y. B., Gwon, G. H. & Cho, Y. Crystal structure of the Mre11-Rad50-ATPyS complex: understanding the interplay between Mre11 and Rad50. *Genes & development* **25**, 1091–104 (2011).

55. Van der Linden, E., Sanchez, H., Kinoshita, E., Kanaar, R. & Wyman, C. RAD50 and NBS1 form a stable complex functional in DNA binding and tethering. *Nucleic acids research* **37**, 1580–8 (2009).
56. Węsierska-Gądek, J. *et al.* PARP inhibition potentiates the cytotoxic activity of C-1305, a selective inhibitor of topoisomerase II, in human BRCA1-positive breast cancer cells. *Biochemical pharmacology* **84**, 1318–31 (2012).
57. Patel, A. G. *et al.* Enhanced killing of cancer cells by poly(ADP-ribose) polymerase inhibitors and topoisomerase I inhibitors reflects poisoning of both enzymes. *The Journal of biological chemistry* **287**, 4198–210 (2012).
58. Sabisz, M., Wesierska-Gadek, J. & Skladanowski, A. Increased cytotoxicity of an unusual DNA topoisomerase II inhibitor compound C-1305 toward HeLa cells with downregulated PARP-1 activity results from re-activation of the p53 pathway and modulation of mitotic checkpoints. *Biochemical pharmacology* **79**, 1387–97 (2010).
59. Yap, T. A., Sandhu, S. K., Carden, C. P. & de Bono, J. S. Poly(ADP-ribose) polymerase (PARP) inhibitors: Exploiting a synthetic lethal strategy in the clinic. *CA: a cancer journal for clinicians* **61**, 31–49 (2011).
60. Curtin, N. J. DNA repair dysregulation from cancer driver to therapeutic target. *Nature Reviews Cancer* **12**, 801–817 (2012).
61. Kaelin, W. G. The concept of synthetic lethality in the context of anticancer therapy. *Nature reviews. Cancer* **5**, 689–98 (2005).
62. Dobzhansky, T. Genetics of Natural Populations. Xiii. Recombination and Variability in Populations of *Drosophila Pseudoobscura*. *Genetics* **31**, 269–90 (1946).
63. Schreiber, V., Dantzer, F., Ame, J.-C. & de Murcia, G. Poly(ADP-ribose): novel functions for an old molecule. *Nature reviews. Molecular cell biology* **7**, 517–28 (2006).
64. Do, K. & Chen, A. P. Molecular Pathways: Targeting PARP in Cancer Treatment. *Clinical cancer research : an official journal of the American Association for Cancer Research* 977–984 (2013). doi:10.1158/1078-0432.CCR-12-0163
65. Rouleau, M., Patel, A., Hendzel, M. J., Kaufmann, S. H. & Poirier, G. G. PARP inhibition: PARP1 and beyond. *Nature reviews. Cancer* **10**, 293–301 (2010).
66. Claybon, A., Karia, B., Bruce, C. & Bishop, A. J. R. PARP1 suppresses homologous recombination events in mice in vivo. *Nucleic acids research* **38**, 7538–45 (2010).
67. Kurosaki, T. *et al.* Primary structure of human poly(ADP-ribose) synthetase as deduced from cDNA sequence. *The Journal of biological chemistry* **262**, 15990–7 (1987).
68. Cherney, B. W. *et al.* cDNA sequence, protein structure, and chromosomal location of the human gene for poly(ADP-ribose) polymerase. *Proceedings of the National Academy of Sciences of the United States of America* **84**, 8370–4 (1987).

69. Sousa, F. G. *et al.* PARPs and the DNA damage response. *Carcinogenesis* **33**, 1433–40 (2012).
70. Bouchard, V. J., Rouleau, M. & Poirier, G. G. PARP-1, a determinant of cell survival in response to DNA damage. *Experimental hematology* **31**, 446–54 (2003).
71. Masson, M. *et al.* XRCC1 is specifically associated with poly(ADP-ribose) polymerase and negatively regulates its activity following DNA damage. *Molecular and cellular biology* **18**, 3563–71 (1998).
72. Siegel, R., Naishadham, D. & Jemal, A. Cancer statistics, 2012. *CA: a cancer journal for clinicians* **62**, 10–29 (2012).
73. Xu, C. F. & Solomon, E. Mutations of the BRCA1 gene in human cancer. *Seminars in cancer biology* **7**, 33–40 (1996).
74. Oluwabemiga, L. A., Oluwole, A. & Kayode, A. A. Seventeen years after BRCA1: what is the BRCA mutation status of the breast cancer patients in Africa? - a systematic review. *SpringerPlus* **1**, 83 (2012).
75. Mavaddat, N. *et al.* Cancer Risks for BRCA1 and BRCA2 Mutation Carriers: Results From Prospective Analysis of EMBRACE. *Journal of the National Cancer Institute* 1–11 (2013). doi:10.1093/jnci/djt095
76. Fong, P. C. *et al.* Inhibition of poly(ADP-ribose) polymerase in tumors from BRCA mutation carriers. *The New England journal of medicine* **361**, 123–34 (2009).
77. Farmer, H. *et al.* Targeting the DNA repair defect in BRCA mutant cells as a therapeutic strategy. *Nature* **434**, 917–21 (2005).
78. Sessa, C. Update on PARP1 inhibitors in ovarian cancer. *Annals of oncology : official journal of the European Society for Medical Oncology / ESMO* **22 Suppl 8**, viii72–viii76 (2011).
79. ClinicalTrials.gov A service of the U.S. National Institutes of Health
<<http://www.clinicaltrials.gov>>
80. Sandhu, S. K. *et al.* The poly(ADP-ribose) polymerase inhibitor niraparib (MK4827) in BRCA mutation carriers and patients with sporadic cancer: a phase 1 dose-escalation trial. *The Lancet Oncology* **14**, 882–892 (2013).
81. Underhill, C., Toulmonde, M. & Bonnefoi, H. A review of PARP inhibitors: from bench to bedside. *Annals of oncology : official journal of the European Society for Medical Oncology / ESMO* **22**, 268–79 (2011).
82. Elstrodt, F. *et al.* BRCA1 mutation analysis of 41 human breast cancer cell lines reveals three new deleterious mutants. *Cancer research* **66**, 41–5 (2006).

83. Lacroix, M., Toillon, R.-A. & Leclercq, G. P53 and Breast Cancer, an Update. *Endocrine-related cancer* **13**, 293–325 (2006).
84. Promega <<http://at.promega.com/products/cell-health-assays/>>
85. Lowry, O. H., Rosebrough, N. J., Farr, A. L. & Randall, R. J. Protein measurement with the Folin phenol reagent. *The Journal of biological chemistry* **193**, 265–75 (1951).
86. Peterson, G. L. Review of the Folin phenol protein quantitation method of Lowry, Rosebrough, Farr and Randall. *Analytical biochemistry* **100**, 201–220 (1979).
87. Chou, T. C. & Talalay, P. Quantitative analysis of dose-effect relationships: the combined effects of multiple drugs or enzyme inhibitors. *Advances in enzyme regulation* **22**, 27–55 (1984).
88. André, N., Banavali, S., Snihur, Y. & Pasquier, E. Has the time come for metronomics in low-income and middle-income countries? *The lancet oncology* **14**, e239–48 (2013).
89. Bowman, K. J., Newell, D. R., Calvert, a H. & Curtin, N. J. Differential effects of the poly (ADP-ribose) polymerase (PARP) inhibitor NU1025 on topoisomerase I and II inhibitor cytotoxicity in L1210 cells in vitro. *British journal of cancer* **84**, 106–12 (2001).
90. Ray Chaudhuri, A. *et al.* Topoisomerase I poisoning results in PARP-mediated replication fork reversal. *Nature structural & molecular biology* **19**, 417–23 (2012).
91. Delaney, C. A. *et al.* Potentiation of temozolomide and topotecan growth inhibition and cytotoxicity by novel poly(adenosine diphosphoribose) polymerase inhibitors in a panel of human tumor cell lines. *Clinical cancer research : an official journal of the American Association for Cancer Research* **6**, 2860–7 (2000).
92. Kelly, C. M. & Buzdar, A. U. Using Multiple Targeted Therapies in Oncology: Considerations for Use, and Progress to Date in Breast Cancer. *Drugs* 505–515 (2013). doi:10.1007/s40265-013-0044-0
93. Imyanitov, E. N. & Byrski, T. Systemic treatment for hereditary cancers: a 2012 update. *Hereditary cancer in clinical practice* **11**, 2 (2013).
94. Ibrahim, Y. H. *et al.* PI3K inhibition impairs BRCA1/2 expression and sensitizes BRCA-proficient triple-negative breast cancer to PARP inhibition. *Cancer discovery* **2**, 1036–47 (2012).
95. Juvekar, A. *et al.* Combining a PI3K inhibitor with a PARP inhibitor provides an effective therapy for BRCA1-related breast cancer. *Cancer discovery* **2**, 1048–63 (2012).
96. Calabrese, C. R. *et al.* Anticancer Chemosensitization and Radiosensitization by the Novel Poly(ADP-ribose) Polymerase-1 Inhibitor AG14361. *JNCI Journal of the National Cancer Institute* **96**, 56–67 (2004).

9. Curriculum vitae

Personal data	
Name	Marlene Chladek
Education	<p>2010 - currently</p> <p>University of Vienna, master programme: molecular biology, focus on molecular medicine</p> <p>Master thesis at the Institute of Cancer Research, Univ. Clinic for Internal Medicine I, Medical University of Vienna</p> <p>Thesis: "PARP inhibition potentiates the cytotoxic activity of camptothecin, a topoisomerase I inhibitor in human BRCA1-positive breast cancer cells"</p> <p>2006 - 2010</p> <p>University of Vienna, bachelor programme: biology, focus on anthropology</p> <p>1998 -2006</p> <p>BG/ BRG Neunkirchen</p> <p>1994 - 1998</p> <p>Dr. Adolf Schärf Volksschule Pottschach</p>
Lab-specific Education	<p>January 2013- March 2013</p> <p>Institute of Cancer Research, Medical University of Vienna</p> <p>Practical course in microbiology</p> <p>January 2012- December 2012</p> <p>Institute of Cancer Research, Medical University of Vienna</p> <p>Practical course in course of the master thesis</p>